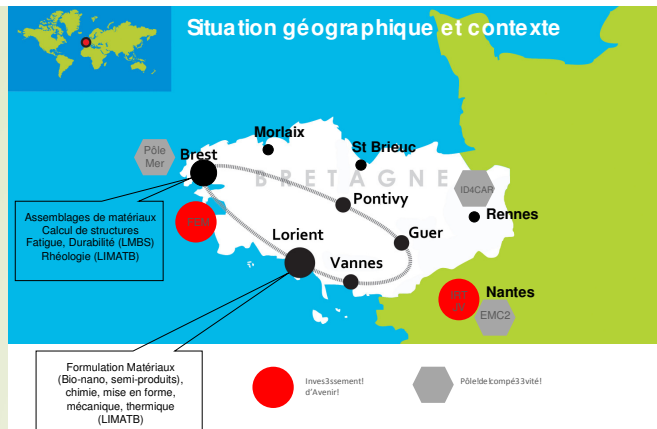


From the measurements with thermocouples to the estimation of heat source terms with inverse methods

Philippe Le Masson – IRDL – UBS.



My Team in our laboratory IRDL (21 permanent research professors – 2 engineers – 15 phd students and 2 post doc)

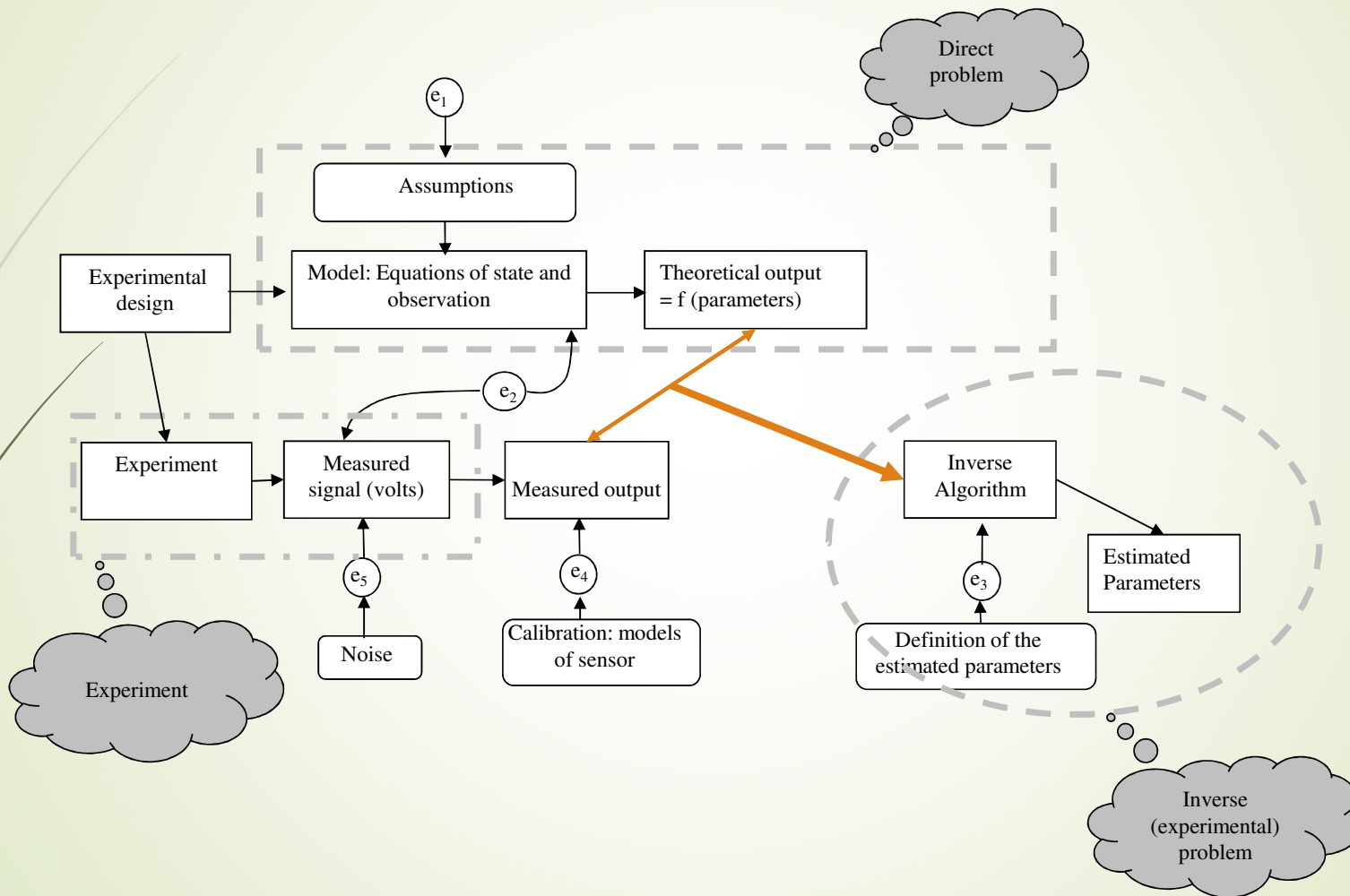
The assemblies

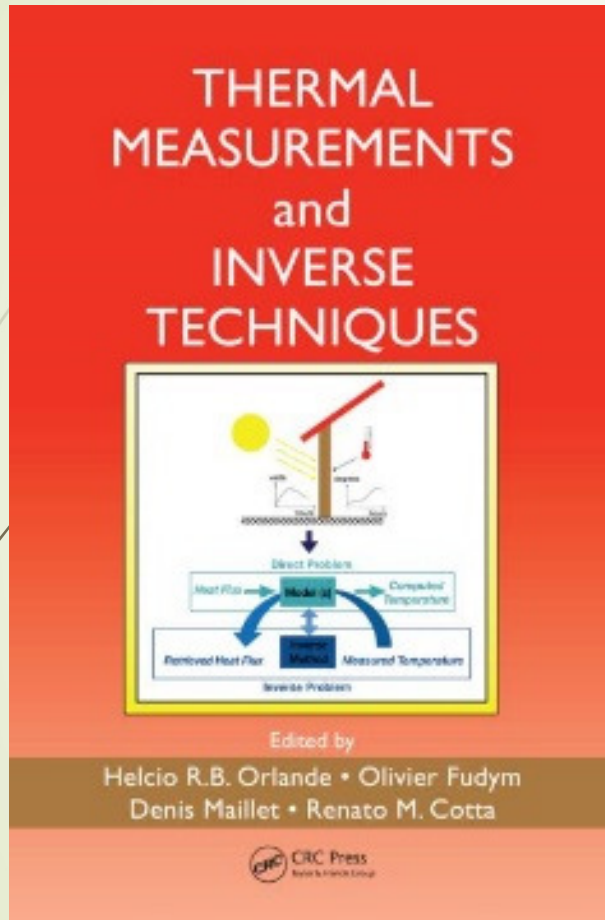
in Lorient : Welding, additive manufacturing, sintering...

in Brest: Welding, Bonding...

3 axis: Modelisation, characterisation and instrumentation.

- Multiphysic model (knowledge model for the heat input) and reduced model (for the calculation of mechanical effects: residual stresses and distortions)
- characterisation: definition of the parameters for the simulation
- instrumentation of the experimental characterisation and in situ experiments : thermocouples, infrared camera, speed camera, multispectral pyrometer...

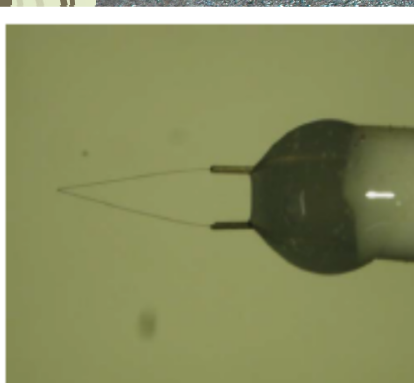
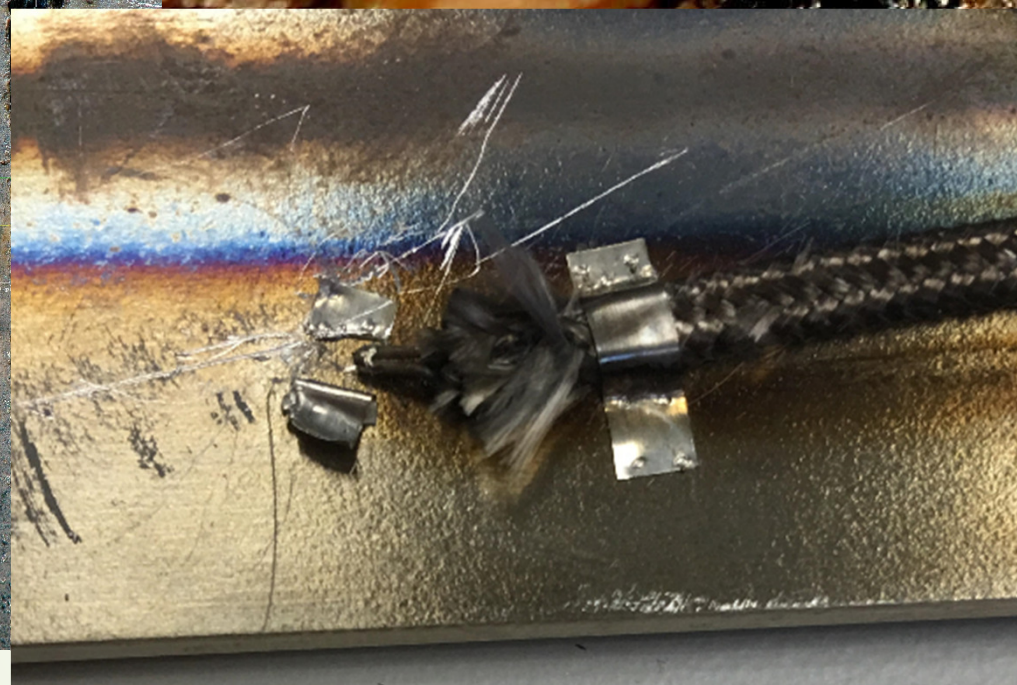




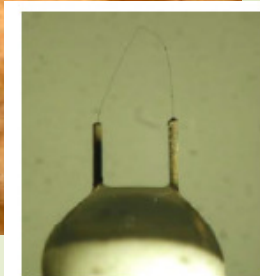
- H. R. B. Orlande, O. Fudym, D. Maillet, R. M. Cotta, *Thermal measurements and inverse techniques*, CRC Press, Taylor & Francis Group, Boca Raton, 2011.

... and the french engineering techniques.

Some examples of instrumentation



S type : 5 μm



S type : 0.5 μm

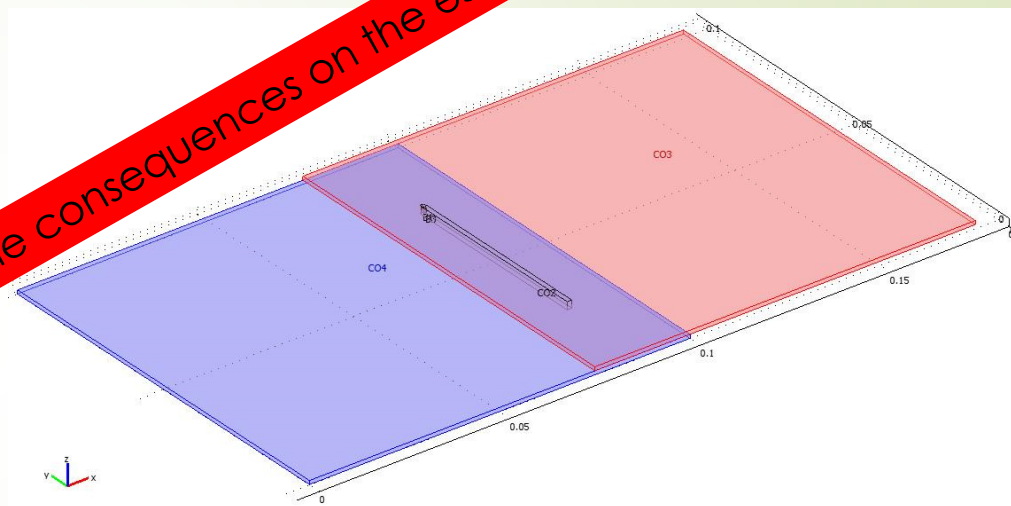
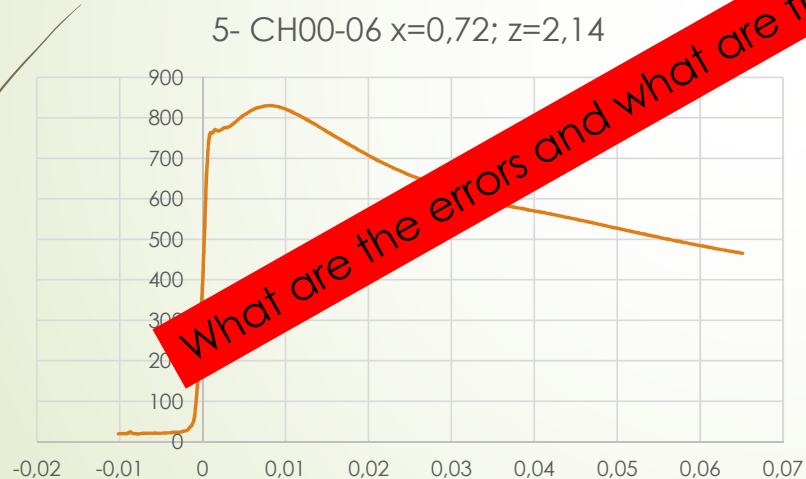
Questions

- What do we want to measure ?
 - What is the level of the temperature?
 - What is the speed of the phenomenon?
- Can I define all measurement errors? From:
 - The measurement chain
 - The acquisition system
 - The thermocouple calibration
 - The intrusive effect of the sensor.
- What does the thermocouple measure?
 - Can I define the thermal equilibrium of the thermocouple with the medium?
- Which measurement chain do I take?
- What is the strategy to define correctly the heat source term?
- Which estimation algorithm we can use?

What do we want to measure ?

- Example 1: For the estimation of a source term in a Laser welding
 - Welding speed : 8.3 m/min
 - Welding length: 7 cm
 - Welding time: 0.5 s
 - The transverse gradient during the welding : 800 °C for 0.7 mm
 - Thickness of the steel sheet: 1 mm

What are the errors and what are the consequences on the estimate ?

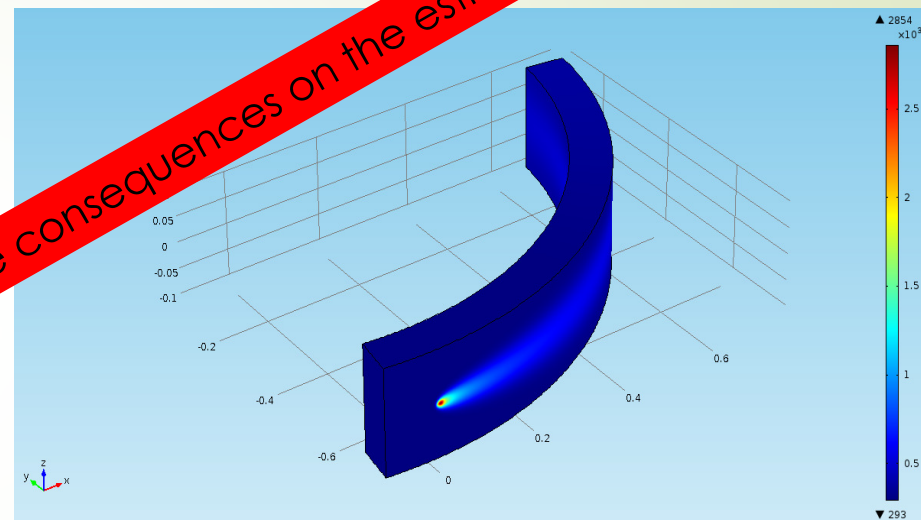
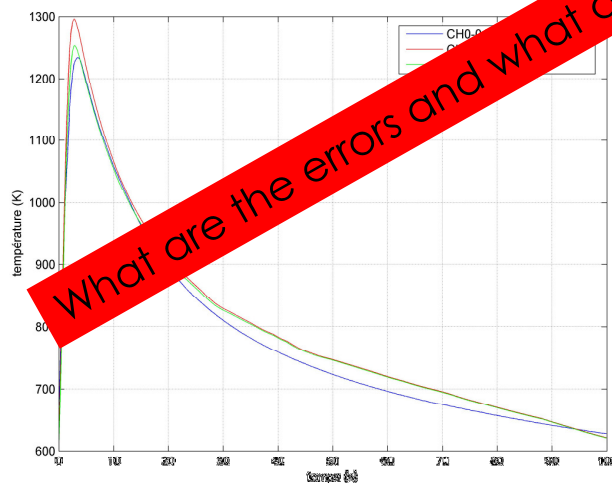


Thermocouple on the surface ; diameter: 25 µm



What do we want to measure ?

- Example 2: For the estimation of a source term in an electro arc welding
 - Welding speed : 0.15 m/min
 - Welding length: 4.72 m (1 turn of the cylinder)
 - Welding time: 600 s
 - Thickness of the steel sheet: 8 cm



What are the errors and what are the consequences on the estimate ?

15 Thermocouples inside the sheet.
diameter: 50 μm

Questions

- **Can I define all measurement errors? From:**
 - **The measurement chain**
 - **The acquisition system**
- the measurement errors can come from the filtering on the acquisition board. These filters can lead to damping of signal variation.
- the magnetic fields around the manipulation can lead to signal drift and noise up to +/- 50 ° C. the solution is to remove the wires from the thermocouples perpendicular to the magnetic field and sometimes to shield the wires.

Questions

- **Can I define all measurement errors? From:**
 - **The Thermocouple calibration**
- Temperature measurement:
 - Why? (History, Temperature: what is it?)
 - How? (principle, characterisation, time constant...)

Temperature measurement

- History (ref: Metti school – 2009 – Angra dos Reis)



Philon from Byzance (-250 ?)
Heron from Alexandria
(-200 to + 200 ?)
Time of the greek philosophy



The first steam machine
The hydraulic pump
**Heat and temperature
are connected ?**



Galien (131 - 210)
Greek doctor

Among more than 750
papers on science
and medicine,
**he introduced the
concept of "degrees
of heat and cold"**



Avicenne (980 - 1037)
Iranian doctor

Instrument for treating
fever, depending on
how hot, cold,
humidity, dry

Temperature measurement

Let's build instruments and temperature scales: the beginning of the adventure

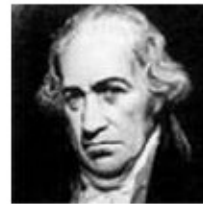


Galileo Galilei
1597



Santorrio Santorio
1612

Thermoscope :
Air/water
thermometer to
« measure » the body
temperature (fever)



Fahrenheit
1715

Mercury/alcool
thermometer
T° scale :
32-212
degrees
Reference =
salt/ice melting



Réaumur
1730

Mercury/alcool
thermometer
T° scale :
0-80 degrees
Reference = =
T° of a
larder...



Celsius
1742



Ice : 0 degree
Boiling water : 100
degrees

Problem: fixed points?

Temperature measurement

The first theoretical step:

1824 : reflexion on the motive power

is the potential work available from a heat source potentially unbounded?

Can heat engines be in principle improved by replacing the steam by some other working fluid or gaz ?

Towards the second law...

Efficiency is an intuition but

$$\eta = 1 - \frac{f(\theta_1)}{f(\theta_2)}$$

$f(\theta) = T$ Lord Kelvin

From Carnot to Kelvin



**Sadi Carnot
(1776-1832)**

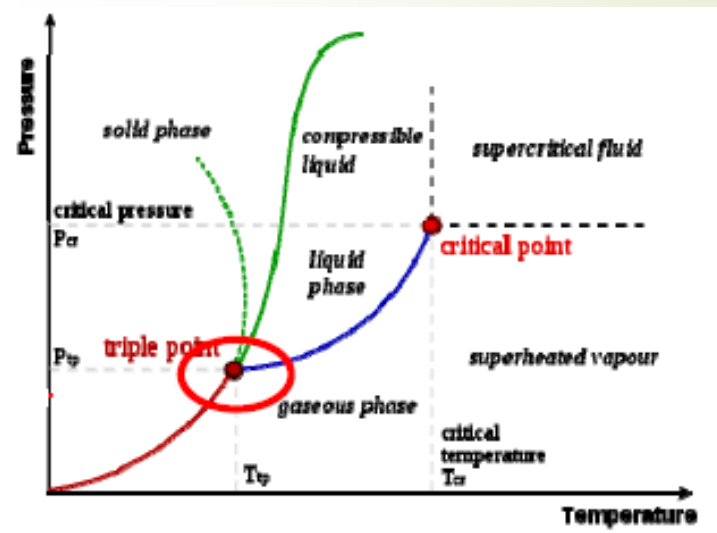
Temperature measurement

With Kelvin, the temperature becomes an absolute reality...



William Thomson
Lord Kelvin
(1824-1907)

The kelvin, unit of thermodynamic temperature, is equal to the fraction $1/273.16$ of the thermodynamic temperature of the triple point of water



Temperature measurement

Today,

Temperature scales are based on fixed points

From the first official international temperature scale (ITS) of 1927 to the future...

« Bureau International des Poids et Mesures (BIPM) »

1927 : ITS 27

1948 : ITS 48

1968 : ITS 68

1976 : ITS 76

1990 : ITS 90....

Temperature measurement

Fixed points of ITS 90

Temperature (K)	Element	Point
from 3 to 5	helium	vapor
13,803 3	hydrogen	triple
≈17	hydrogen (or helium)	vapor (or gas thermometer)
≈ 20.3	hydrogen (or helium)	vapor (or gas thermometer)
24.556 1	neon	triple
54.358 4	oxygen	triple
83.805 8	argon	triple
234.315 6	mercury	triple
273.16	water	triple
302.914 6	gallium	melting
429.748 5	indium	freezing
505.078	lead	freezing
692.677	zinc	freezing
933.473	aluminium	freezing
1 234.93	argent	freezing
1 337.33	gold	freezing
1 357.77	copper	freezing

Temperature measurement

Up to 1000°C :

- 1000 ° C - 1200 ° C : Mainly type K thermocouples (40 μ V / ° C), type N, T ...
- Difficulties with thermocouples: instability, inhomogeneities, temperature limits of 1100-1200 ° C for types K and N
- Up to 1500 ° C, Pt / Pd thermocouples are promising in terms of stability, but they are expensive and their fragility limits them to laboratory use only
- Beyond 1500 ° C, the W / Re family can reach up to 2300 ° C but stability is not clear

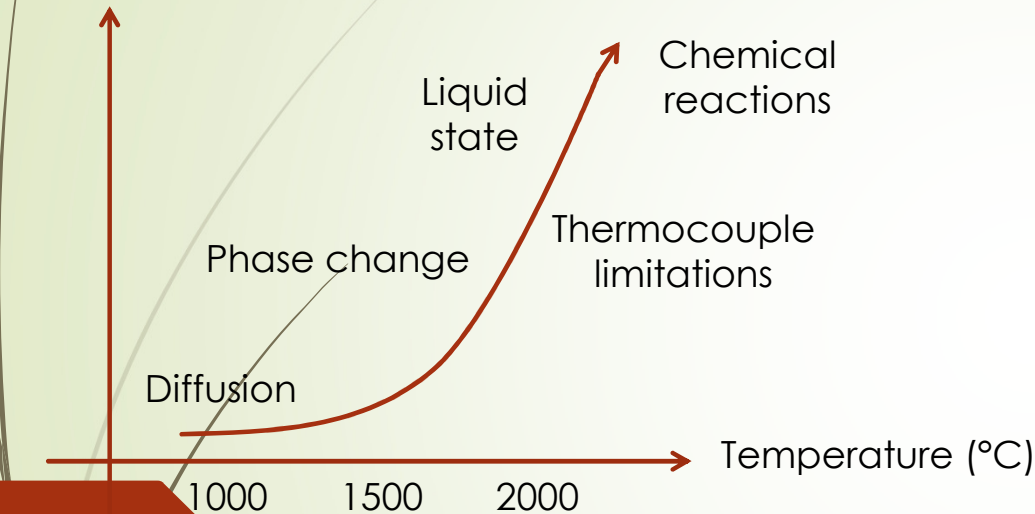
New thermocouples are being studied (Ir / Ir-Rh, Pt-20% Rh / Pt-40% Rh)

In use: non-guaranteed material compatibility, especially above 1500 ° C

Temperature measurement

Some problems encountered at high temperatures

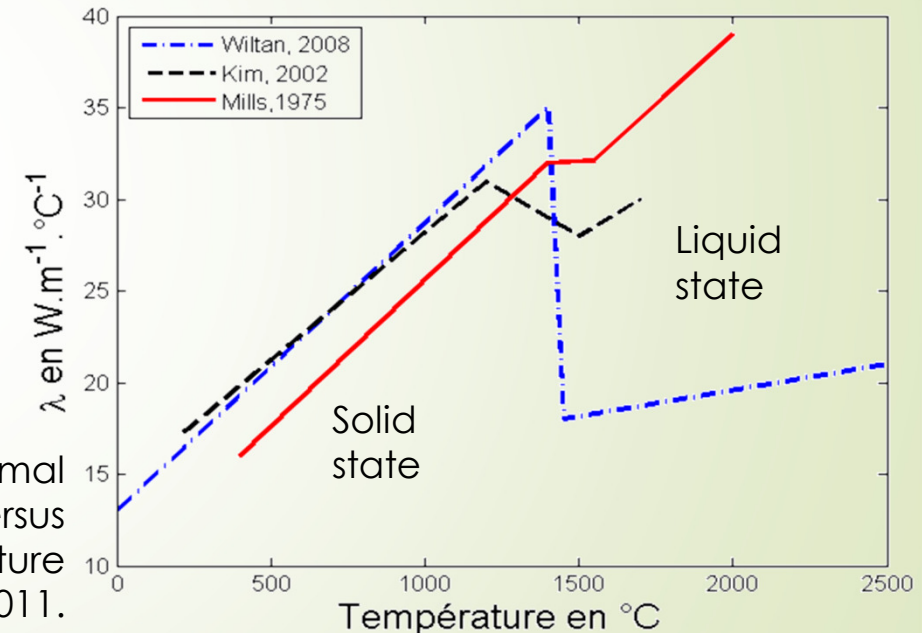
Experimental issues



316L steel thermal conductivity versus temperature
Dal, 2011.

The literature presents:

- **scarce high temperature thermal properties** compared to ambient temperature's ones
- **discrepancies** of the thermophysical properties between authors



Development of high temperature apparatuses dedicated to thermal characterization of solid and liquid materials and the thermocouple calibration.

Philippe Le Masson – IRDL – UBS.

Temperature measurement

Compatibility of materials at high temperature (~ 2000 ° C)

Example: Thermocouple W-Re

Thermocouples W-Re / sheath Mo
⇒+ Pearl ZrO₂ - 1750 °C



Thermocouples W-Re / sheath Ta
⇒+ overshath graphite - 1950 °C

Ta and C



Results after 50h – 1950°C

Association :	Molybdène	Tantale	Graphite pur
SiC	-	-	++
ZrO ₂ -8%Y ₂ O ₃	+	+	+
Graphite pur	-	+	/

Temperature measurement

Fixed points at high temperatures : objectives

The realization of the scale above 1000 ° C would be done by interpolation between these fixed points and not by extrapolation as currently: better uncertainties

Applications are as much in optical pyrometry as in contact thermometry. Traceability would be based on fixed points that could even be thermodynamic temperature vectors

Practical means for rapid checking of the stability of measuring instruments at working temperature

In-situ re-calibration of measuring and control instruments

- Completion and study since 2001
- Multiple comparisons
- Thermodynamic phase change temperatures determined
- New implementation of the kelvin HT definition (site [www BIPM](http://www.BIPM))

International projects: NIST, LNE (France)...

Philippe Le Masson – IRDL – UBS.

Temperature measurement

HOW?

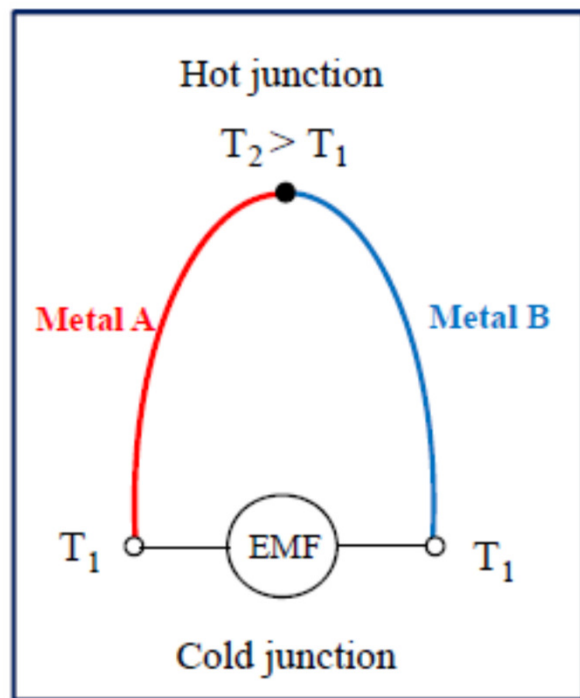
Optical methods

Spectroscopic methods

Temperature measurements

Resistance thermometers

Thermocouples



In 1821 T.J. Seebeck observed the existence of an electromotive force, EMF (μV) at the junction formed between two dissimilar metals (Seebeck effect) submitted to a temperature difference ($T_2 - T_1$).

Seebeck effect is actually the combined result of two other phenomenon, Thomson and Peltier effects

Peltier discovered that temperature gradients along conductors in a circuit generate an EMF.

Thomson observed the existence of an EMF due to the contact of two dissimilar metals and the junction temperature.

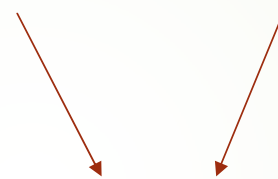
Thomson effect is normally much smaller in magnitude than the Peltier effect and can be minimized and disregarded with proper thermocouple design.

Temperature measurement

$$E_{AB}(T_2, T_1) = \Pi_{AB}^{T_1} - \Pi_{AB}^{T_2} + \int_{T_2}^{T_1} (\tau_A - \tau_B) dT$$

Peltier
Effect

Thomson
Effect



Seebeck effect

$$E_{AB}(T_2, T_1) = \sigma_{AB}(T_2 - T_1)$$

σ_{AB} is the Seebeck coefficient ($\mu\text{V}\cdot^\circ\text{C}^{-1}$), depends on the two materials A and B

Temperature measurement

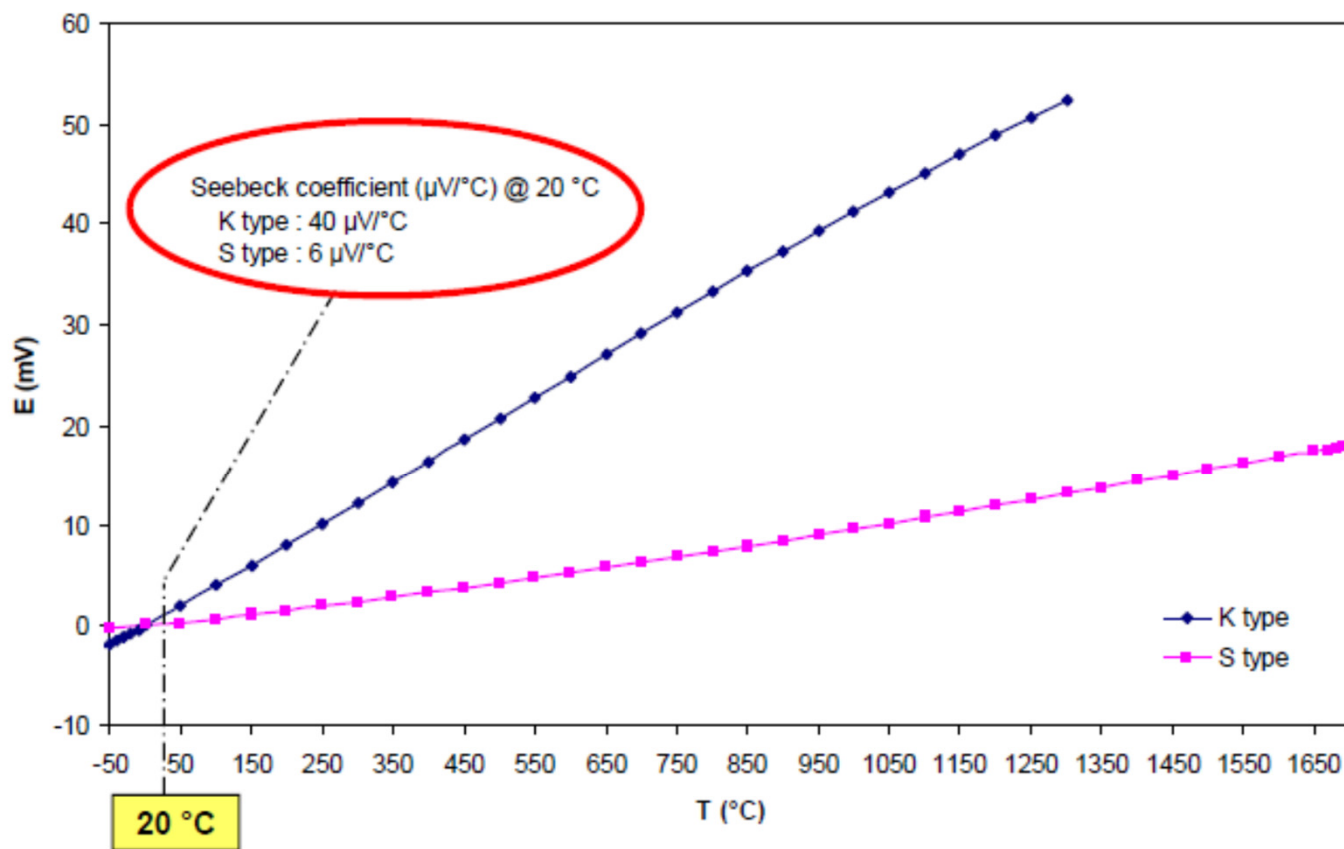
Material	Seebeck coefficient ($\mu\text{V}^\circ\text{C}^{-1}$)	Material	Seebeck coefficient ($\mu\text{V}^\circ\text{C}^{-1}$)
Bismuth	-72	Silver	6.5
Constantan	-35	Copper	6.5
Alumel	-17.3	Gold	6.5
Nickel	-15	Tungsten	7.5
Potassium	-9	Cadmium	7.5
Sodium	-2	Iron	18.5
Platinum	0	Chromel	21.7
Mercury	0.6	Nichrome	25
Carbon	3	Antimony	47
Aluminium	3.5	Germanium	300
Lead	4	Silicium	440
Tantalum	4.5	Tellurium	500
Rhodium	6	Sélenium	900

K type = Chromel/Alumel
 $\sigma = 21.7 - (-17.3) = 39 \mu\text{V}^\circ\text{C}^{-1} @ 0^\circ\text{C}$

T type = Copper/Constantan
 $\sigma = 1.7 - (-37.3) = 39 \mu\text{V}^\circ\text{C}^{-1} @ 0^\circ\text{C}$

$\sigma = 400 - (-15) = 415 \mu\text{V}^\circ\text{C}^{-1} \text{ at } 0^\circ\text{C}$

Temperature measurement



Electromotive force versus temperature
for S type and K type thermocouples (ITS-90)

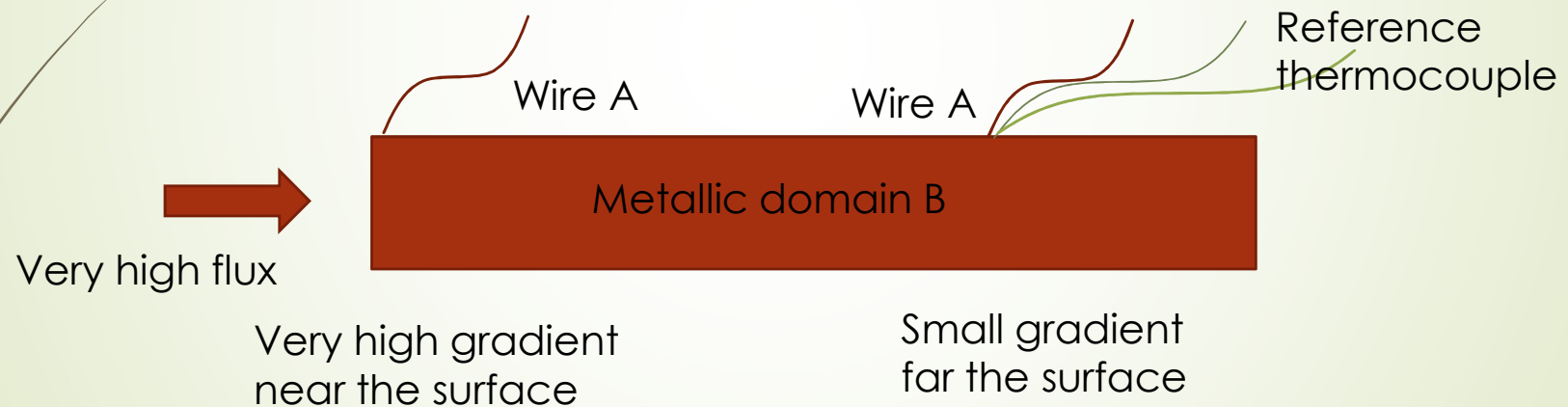
Temperature measurement

- semi-intrinsic thermocouple:

- suppose we wanted to use the support material as the element of the thermocouple: what should I do? What is the advantage and the disadvantage?

- Principle:

We have very transient phenomenon and we want use a very fin thermocouple.



What is the measure?

How I can make the calibration?

Temperature measurement

Advantages of thermocouples

- Cheap
- Wide temperature range : - 270°C to 2 100°C
- Small: from 0.5µm to.....
- easy to integrate into automated data systems

Disadvantages of thermocouples

- Small signals, limited temperature resolution
- Thermocouples wires have to extend from the measurement point to the readout. Signal generated wherever wires pass through a thermal gradient
- At high temperatures, thermocouples may undergo chemical and physical changes, leading to loss of calibration
- Recalibration of certain types of thermocouples or in certain applications is very difficult

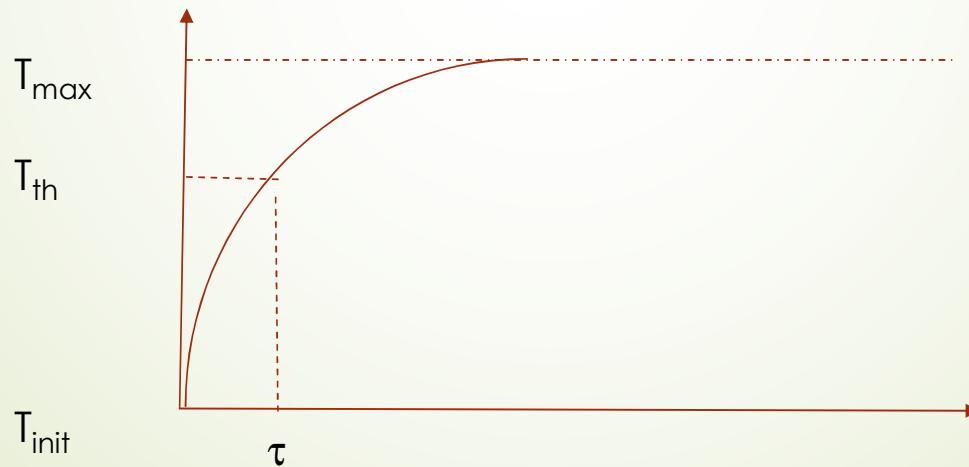
Temperature measurement

What is the constant time of a thermocouple τ ?

Is not a constant. τ depends on the heat transfer around the sensor : convection, conduction and radiation...

Theoretically, the time constant is defined for the 63% of the rise time

$$\frac{T_{max} - T_{th}}{T_{max} - T_{init}} = K \exp \left[-\frac{t}{\tau} \right]$$



The intrusive effect of the sensor

Analyse with an analytic model (J.P Bardon and B. Cassagne)

Measurement of surface temperatures

Sources of error in contact measurements: they can be classified into two categories:

- errors related to the measurement of the thermometric phenomenon (seen before);
- errors related to the disturbance of the thermal field caused by the application of the thermometer.

With a thermocouple, we measure the temperature of the thermocouple and not the temperature of the medium

The intrusive effect of the sensor

Analyse with an analytic model (J.P Bardon and B. Cassagne)

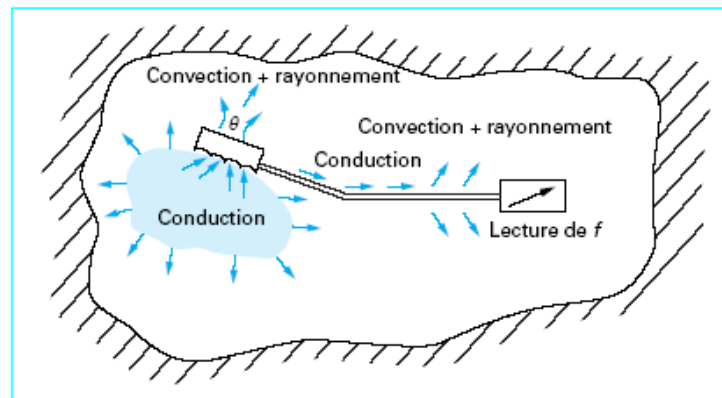


Figure 4 – Transferts de chaleur parasites du milieu vers le thermomètre, et du thermomètre vers l'extérieur

A sensor is attached to a sample. A heat flow is transmitted to the sensor which transmits heat flow through its wires to the external medium. The assembly, sensor and medium, exchanges with the environment by convection and radiation.

All these parasitic transfers induce a local perturbation of the temperature field, positive or negative, depending on whether there is a decrease or increase in transfers from the surface to the outside.

The **surface temperature** is no longer T but T_p . Moreover, the **temperature of the thermometer**, θ , is generally not equal to this perturbed temperature T_p , because the conditions of contact of the thermometer with the surface, always imperfect, cause its temperature θ to differ as much from T_p as the thermal contact resistance r_c is high, and the heat flux passing through the sensor-to-surface interface is large.

For measurements in variable regime are added the influences of the differences of thermal capacity between the thermometer and the medium, and of the initial temperatures.

The intrusive effect of the sensor

Analyse with an analytic model (J.P Bardon and B. Cassagne)

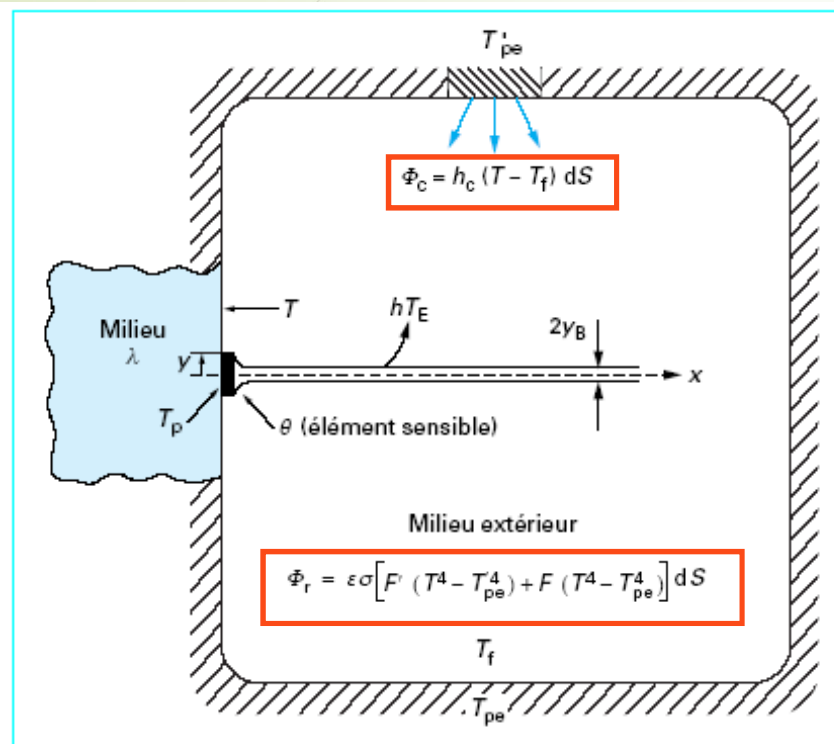


Figure 5 - Description du modèle

We consider a medium opaque to radiation, large dimension, limited on one side by a flat surface with uniform temperature T .

The sensitive element, which we assume to be infinitely thin, is in imperfect contact (contact resistance R_c per unit of apparent surface) with the plane face along a circle of radius y .

The connection with the outside is schematized by a bar of known characteristics, of radius y_B except at the section $x = 0$, assumed to be circular and of radius y .

The external environment is assimilated to a closed enclosure containing a fluid at temperature T_f which, for simplicity, we assume is transparent to thermal radiation.

It is also assumed that the wall of the enclosure can be assimilated to a black surface (emissivity $\epsilon = 1$) at a temperature T_{pe} close to T , except for a temperature element $T'_{pe} \gg T$

The intrusive effect of the sensor

Analyse with an analytic model (J.P Bardon and B. Cassagne)

Modeling the steady-state error

Without thermocouple, the surface temperature is T and the temperature of the environment T_E

With the sensor, a thermal disturbance causes a transfer of heat flow from the sensor to the outside. Let θ be the temperature of the sensor located at $x = 0$, ie the measured temperature. The measurement error $\delta \theta = T - \theta$ results from the conjunction of three effects.

Macroconstriction effect in the environment

It is caused by the convergence of the current lines to the measuring zone (πy^2). It follows that, at the level of this zone, the perturbed temperature T_p is connected to the temperature in the distance T , that is to say at the exact surface temperature before applying the thermometer to it, by the relation $T - T_p = r_M \Phi$ (1) r_M being the macroconstriction resistance; it is due to the convergence of the flux lines towards the contact circle. Its calculation, the hypothesis of a semi-infinite medium is classical; we obtain the two expressions:

$$r_M = \frac{1}{4y\lambda} \text{ ou } r_M = \frac{8}{3\pi^2 y\lambda}$$

depending on whether one assumes the isothermal contact circle or crossed by a flux of uniform density (λ is the thermal conductivity of the medium). The calculation also shows that most of the temperature perturbation is located in the immediate vicinity of the contact circle (94% of the $T - T_p$ drop occurs inside the sphere of center O and radius $10 y$).

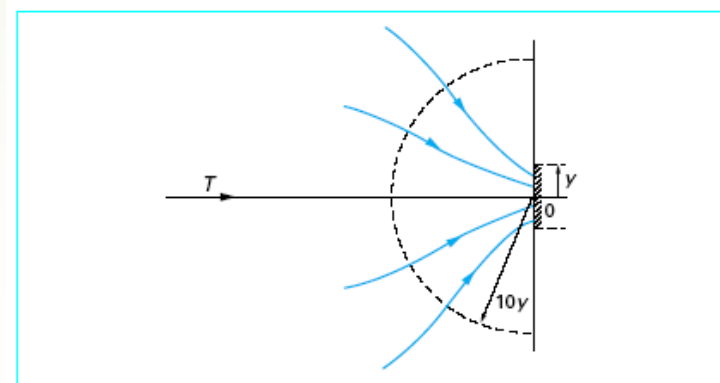
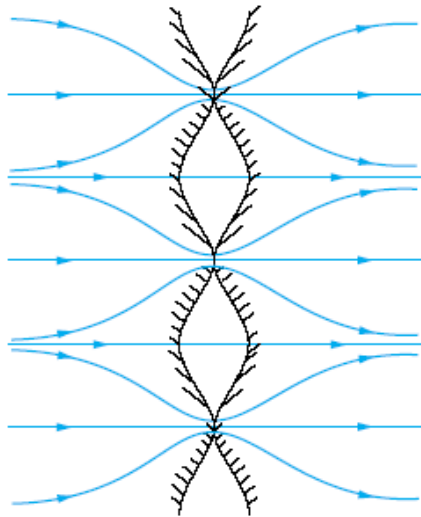


Figure 7 - Effet de macroconstriction au sein du milieu

The intrusive effect of the sensor

Analyse with an analytic model (J.P Bardon and B. Cassagne)



Second effect: Contact resistance effect at the medium-thermometer interface
 It is responsible for the temperature drop $T_p - \theta$ between disturbed temperature and measured temperature. We have $T_p - \theta = r_c \Phi$, where r_c represents the thermal contact resistance for the area πy^2 : $r_c = R_c / (\pi y^2)$.
 This effect is related to the imperfection of the contact, which results from the irregularities of the surfaces. Contact between two solid media occurs only in a number of small areas (1%) between which there remains an interstitial medium.

Figure 8 - Effet de résistance de contact à l'interface milieu-thermomètre

e (m)	25 E-6	2.5 E-6	0.25 E-6	0.025 E-6	0.025 E-6
$k \text{ air} = 0.025 \text{ W.m}^{-1}.\text{K}^{-1}$					
$R_c = e/k$	10^{-3}	10^{-4}	10^{-5}	10^{-6}	10^{-7}
Contact quality	bad				Very good

The intrusive effect of the sensor

Analyse with an analytic model (J.P Bardon and B. Cassagne)

Third Effect: Effect of fin

- the heat exchanges between the outer part of the thermometer and the ambient medium (between the face $x = 0$ at θ , and the external medium TE) :

$$\theta - TE = r_E \Phi$$

r_E representing the overall thermal resistance between the face $x = 0$ and the external medium. It defines global exchanges with the external environment. It depends in particular on the geometry, the overall surface transfer coefficient h and the thermal conductivity λ_E of this external connection.

The intrusive effect of the sensor

Analyse with an analytic model (J.P Bardon and B. Cassagne)

Conjunction of the three effects

From the three resistances, we deduce the measurement error: $\delta\theta = K(T - T_E)$ with $K = \frac{1}{1 + \frac{r_E}{r_C + r_M}}$ (5)

The error committed is therefore proportional to the difference between the temperature to be measured and the equivalent external temperature

the error coefficient K being all the smaller as the sum of the macroconstriction resistances r_M and the contact resistance r_C will be small in the resistance of the external connection r_E .

It should be noted that this model remains valid only as long as the hypotheses that allowed to linearize the radiative exchanges remain verified.

Important implications for steady-state contact measurement techniques

- even for perfect contact conditions $r_C = 0$, there is an error which depends on the ratio r_E / r_M .
- It will therefore be necessary to ensure that r_C is as low as possible and stable. The contact pressure must be strong and constant, the surface must be flat, without ripple, the most conductive interstitial medium possible (welding, grease)
- For measurements on an insulation (λ low), r_M is large and, in general, very much greater than r_C . The macroconvergence effect will play a major role in the error. It can be reduced by increasing the y-radius of the sensitive element without increasing the subsequent sections of the outer link. A contact disk of good thermal conductivity 1D will be used for this purpose.

The intrusive effect of the sensor

Analyse with an analytic model (J.P Bardon and B. Cassagne)

Example: applications.
Thermocouple measurement with and without contact disc.

Tableau 2 – Valeurs des résistances						
Nature de la paroi	Disque (1)	r_M (K.W ⁻¹)	R_c (K.m ² .W ⁻¹)	r_c (K.W ⁻¹)	r_E (K.W ⁻¹)	K
Conductrice ($\lambda = 100 \text{ W.m}^{-1}.\text{K}^{-1}$)	sans	5	10^{-4}	127	1 273	0,094
	avec	0,25	10^{-4}	0,32	1 293	0,0004
Isolante ($\lambda = 0,1 \text{ W.m}^{-1}.\text{K}^{-1}$)	sans	5 000	10^{-3}	1 270	1 273	0,831
	avec	250	10^{-3}	3,20	1 293	0,164

(1) $y = 10 \text{ mm}$, $\lambda_D = \lambda_B$.

The set of two wires of the thermocouple is assimilated to a bar of uniform circular cross-section with radius $y_B = 0.5 \text{ mm}$, infinite length, average conductivity $\lambda_B = 25 \text{ Wm}^{-1}\text{K}^{-1}$ and the heat transfer coefficient $h = 10 \text{ Wm}^{-2}\text{K}^{-1}$. The resistance of this bar is: $r_B = \frac{1}{\pi y_B \sqrt{2h y_B \lambda_B}}$ (solution of the bar)

$$r_E = r_B + \frac{1}{4y_B \lambda_D}$$

The resistance of the external connection is therefore: $r_E = r_B$ when there is no contact disk.

$r_E = r_B + \frac{1}{4y_B \lambda_B}$ with contact disc. $\frac{1}{4y_B \lambda_B}$ representing the resistance due to the convergence of the flux lines from y to y_B within the disk. It is clear from the table the preponderant influences of r_M for insulation measurements and r_c for measurements on the conductor.

The intrusive effect of the sensor

Analyse with an analytic model (J.P Bardon and B. Cassagne)

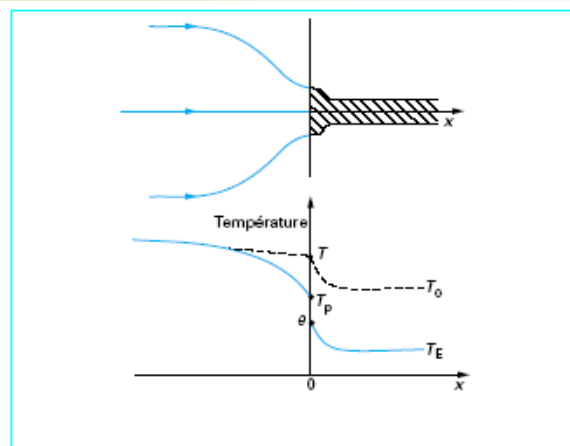


Figure 11 - Cas où un flux de chaleur important traverse l'aire de mesure

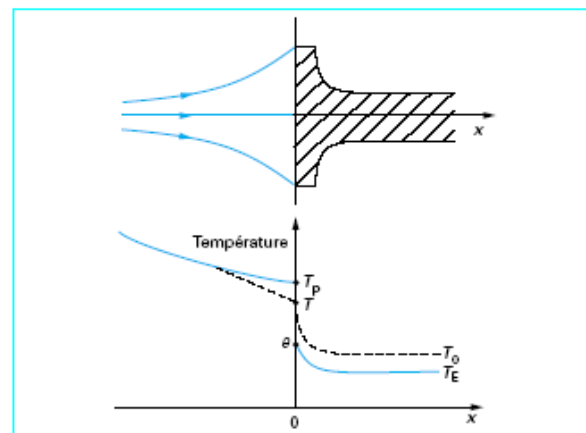


Figure 12 - Cas où l'application du thermomètre réduit les échanges superficiels

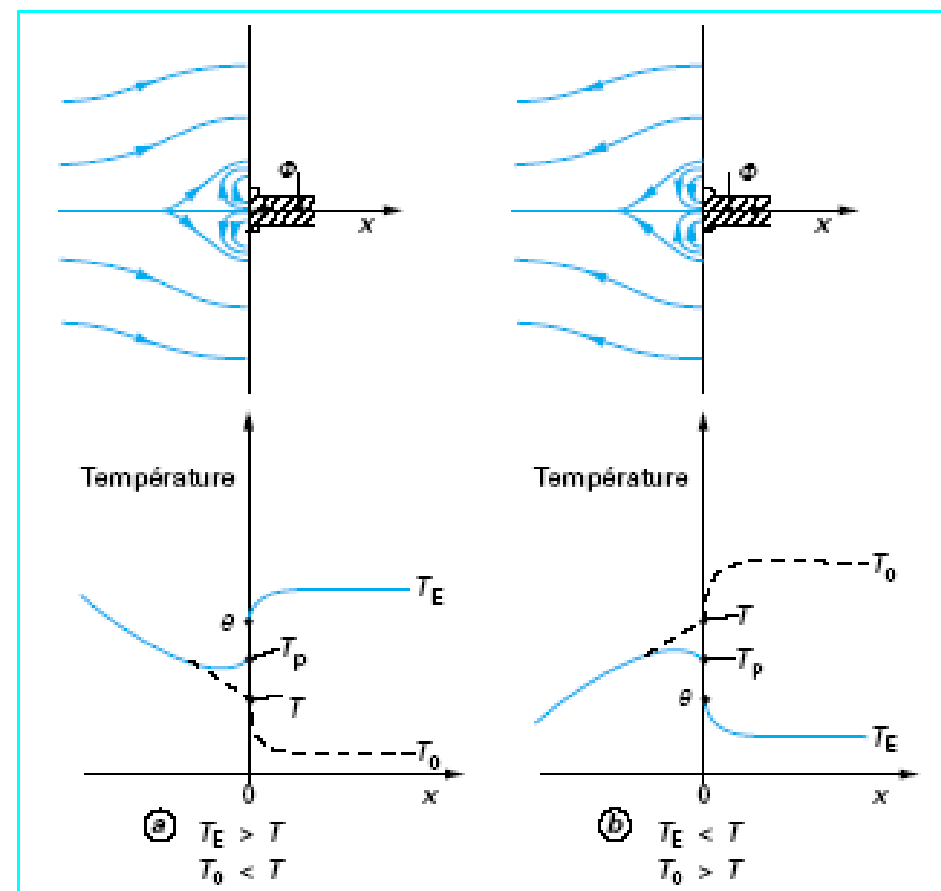


Figure 13 - Cas où l'application du thermomètre inverse les échanges superficiels

The intrusive effect of the sensor

Analyse with an analytic model (J.P Bardon and B. Cassagne)

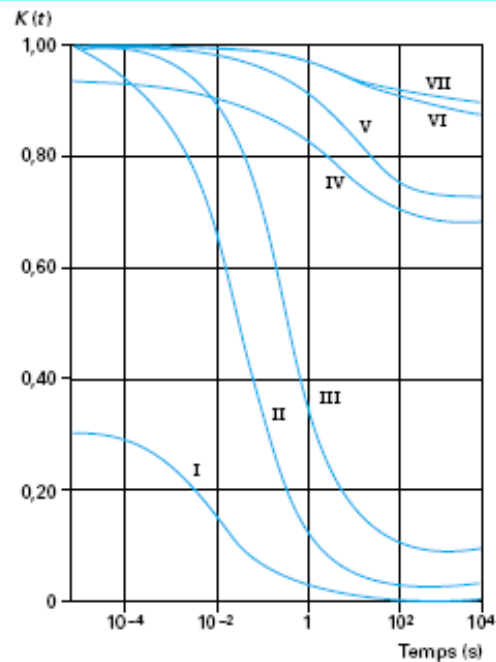
Modeling the transient error

For this study, the sensor is abruptly brought into contact with a surface. The sensor, initially at the equivalent uniform temperature T_E of the environment, is brought abruptly into contact with the medium assumed to have a uniform temperature T . On the contact circle, the temperature of the medium is $T_p(t)$ instead of T . Due to the imperfection of the contact, the measured temperature $\theta(t)$, at $x = 0$ of the bar, is different from T_p .

We suppose that it is still connected to T_p by the classical condition:

$$T_p(t) - \theta(t) = R_c \left(-\lambda_B \frac{\partial \theta}{\partial x} \right)_{x=0} \text{ with } R_c = r_c \pi y^2$$

The time evolution of the relative error $K(t)$ defined in the case of three media with different thermal characteristics and for several values of the contact resistance R_c between the thermometer and the medium.



Conducteur $\lambda = 100 \text{ W.m}^{-1}.\text{K}^{-1}$ $c\rho = 3,1 \times 10^6 \text{ J.m}^{-3}.\text{K}^{-1}$	} I $R_0 = 0$ } II $R_0 = 0,25 \times 10^{-4} \text{ K.m}^2.\text{W}^{-1}$ } III $R_0 = 10^{-4} \text{ K.m}^2.\text{W}^{-1}$
Isolant à forte capacité thermique volumique $\lambda = 0,19 \text{ W.m}^{-1}.\text{K}^{-1}$ $c\rho = 1,7 \times 10^6 \text{ J.m}^{-3}.\text{K}^{-1}$	} IV $R_0 = 0$ } V $R_0 = 5 \times 10^{-4} \text{ K.m}^2.\text{W}^{-1}$
Isolant à faible capacité thermique volumique $\lambda = 0,05 \text{ W.m}^{-1}.\text{K}^{-1}$ $c\rho = 8,4 \times 10^3 \text{ J.m}^{-3}.\text{K}^{-1}$	} VI $R_0 = 0$ } VII $R_0 = 5 \times 10^{-4} \text{ K.m}^2.\text{W}^{-1}$
Caractéristiques thermométriques de la barre :	
$\gamma = \gamma_B = 0,5 \text{ mm}$	$\lambda_B = 17 \text{ W.m}^{-1}.\text{K}^{-1}$
$c\rho_B = 3,4 \times 10^6 \text{ J.m}^{-3}.\text{K}^{-1}$	$h = 15 \text{ W.m}^{-2}.\text{K}^{-1}$

Figure 21 – Évolution de l'erreur relative $K(t)$ (brusque mise en contact)

Tableau 6 – Temps de réponse t_r (en secondes) (capteur mis brusquement en contact avec la surface)

Nature de la paroi	γ_B (m)	$R_c/\gamma_B =$			
		0	0,05 K.m.W ⁻¹	0,20 K.m.W ⁻¹	1 K.m.W ⁻¹
Conductrice (1)	5×10^{-5}	0,012	0,038	0,25	1
	5×10^{-4}	1,8	3,6	20	56
Isolante à forte capacité thermique (2)	5×10^{-5}	1,3	1,32	1,35	1,4
	5×10^{-4}	91	94	101	110
Isolante à faible capacité thermique (3)	5×10^{-5}	2,5	2,54	2,63	2,8
	5×10^{-4}	298	302	307	316

(1) $\lambda = 100 \text{ W.m}^{-1}.\text{K}^{-1}$; $c\rho = 3,1 \times 10^6 \text{ J.m}^{-3}.\text{K}^{-1}$
 (2) $\lambda = 0,19 \text{ W.m}^{-1}.\text{K}^{-1}$; $c\rho = 1,7 \times 10^6 \text{ J.m}^{-3}.\text{K}^{-1}$
 (3) $\lambda = 0,05 \text{ W.m}^{-1}.\text{K}^{-1}$; $c\rho = 8,4 \times 10^3 \text{ J.m}^{-3}.\text{K}^{-1}$

Inertia of measurement

It is characterized by the evaluation of the response time t_r

defined by: $\frac{K(t_r) - K(\infty)}{K(0) - K(\infty)} = 0.05$

$K(\infty)$ identifying with the steady-state error coefficient.

this response time depends very much on the characteristics of the medium. For a measurement on a conductor, it depends very much on the contact conditions. It grows very rapidly with R_c , which appears to be the main cause of the inertia of the thermometer.

For a measurement on an insulator, the response times are much greater but practically independent of the contact conditions considered. All this shows that the response time is not a specific characteristic of the sensor but of the medium - sensor - environment.

Break.... Before the applications

Analyse the measurement errors

Objectives:

- Estimation of a source term for a TIG welding experiment – PVR experiment: **Programmierter-Verformungs-Riß Versuch (PVR)**.

Context:

Hot cracking test

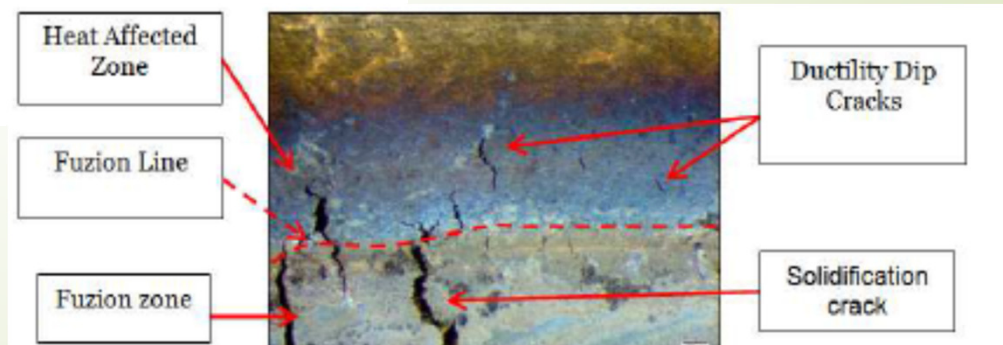
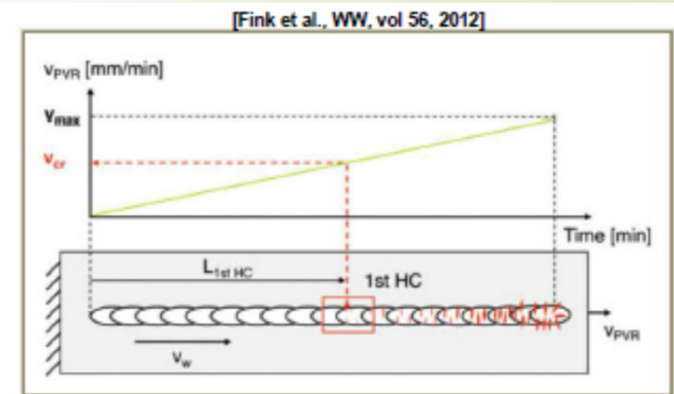
Simultaneous realization of a melting line and a tensile stress:

- Constant energy melting line
- Travel speed of traverse at constant acceleration (scanning of a range of high deformation velocity with a single test piece)

Discriminant observations for the segregation cracks

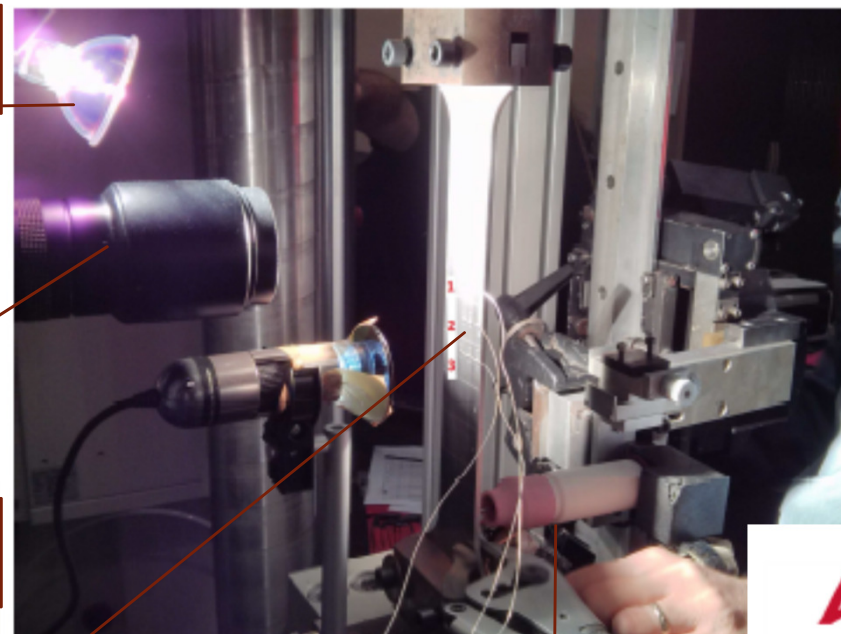
(liquation + solidification) for quantification of the criteria:

- Critical crossing distance and / or speed of occurrence of the first crack
- Crack density on a defined area



- TIG process is stable
- Easily instrumentable
 - Test parameters: U, I, Vs, F
 - Temperature measurements (Thermocouples)
 - Arc and Bath Vision
 - Measurement of distortions
 - Macrography
- Fusion line without addition of material
- Low Intensity

Halogen lamps



Speed camera

Thermocouples

TIG process

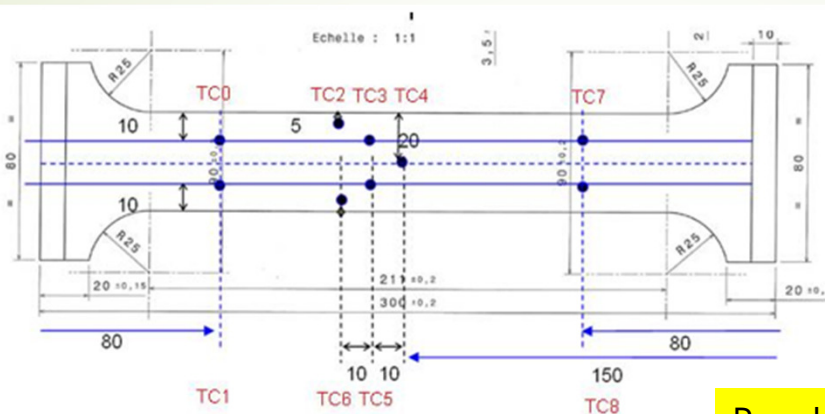
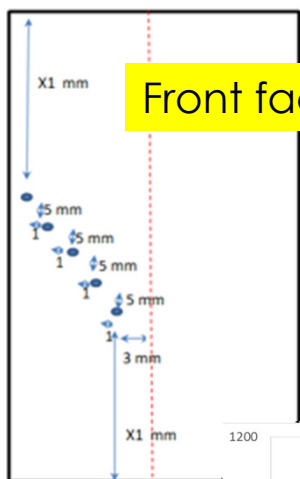
A
AREVA
l'avenir pour énergie

A
AREVA
Technical Center

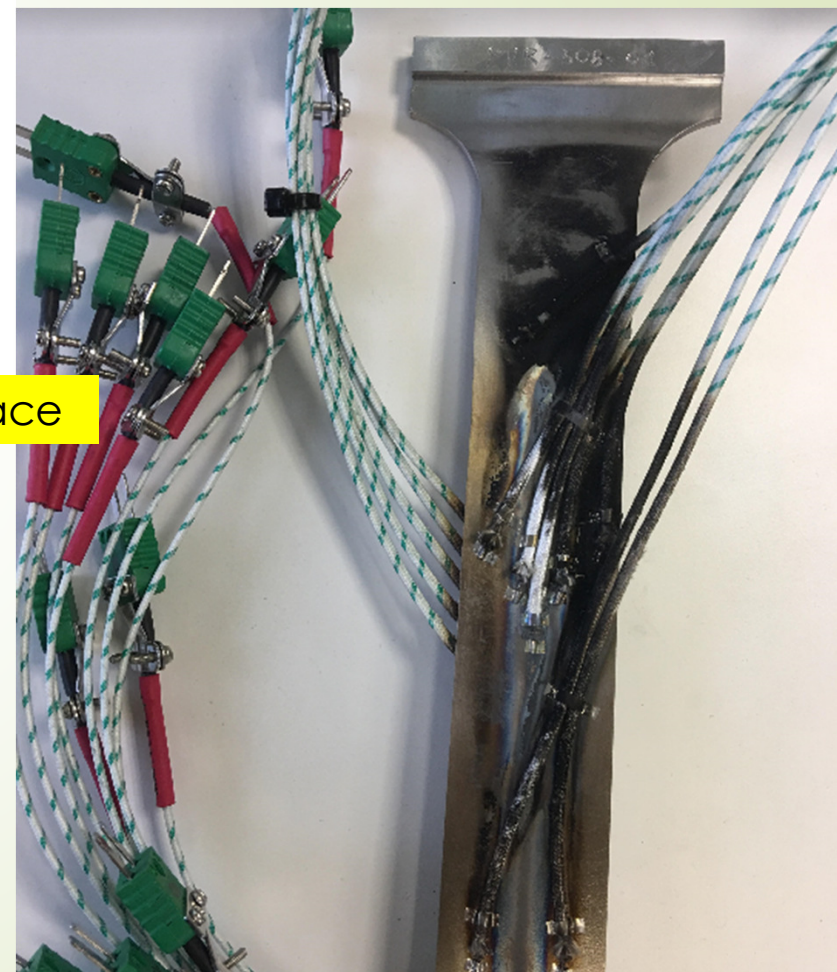
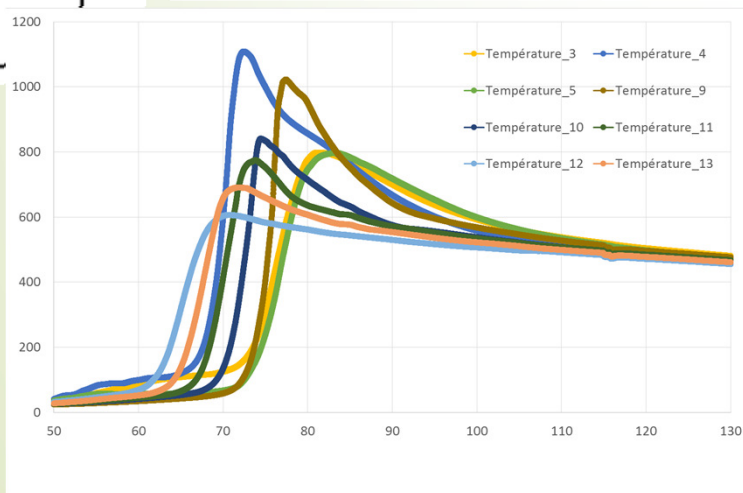
- The thermocouple instrumentation: 14 thermocouples

Front face

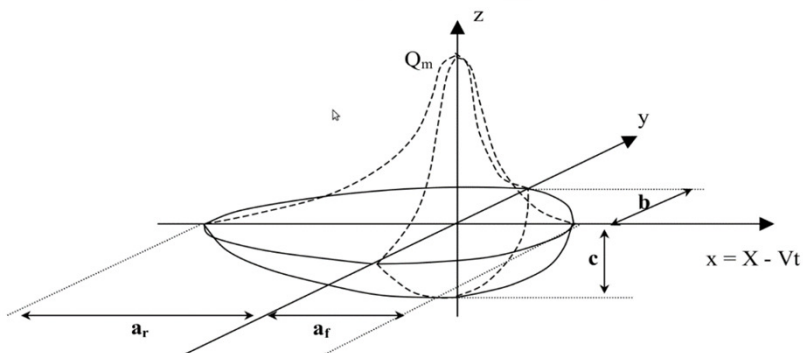
TC13
TC12
TC11
TC10
TC9



Back face



- The heat source term : Goldak type – 7 parameters

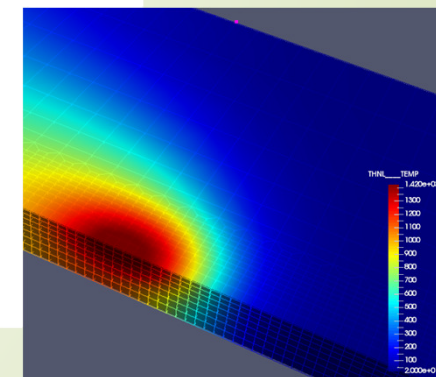
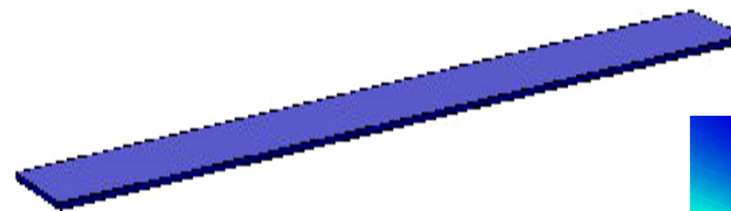


$$q(X, Y, Z) = \frac{Q_0 \cdot 6\sqrt{3}}{abc\sqrt{\pi}^3} \cdot \exp \left[-\frac{3(X - X_0)^2}{a^2} - \frac{3(Y - Y_0)^2}{b^2} - \frac{3(Z - Z_0)^2}{c^2} \right]$$

For the estimation, we use 8 thermocouples...
With a levenberg Marquardt algorithm.

Conclusion: we find parameters but it is impossible to have a fused zone.
Question: Why???????

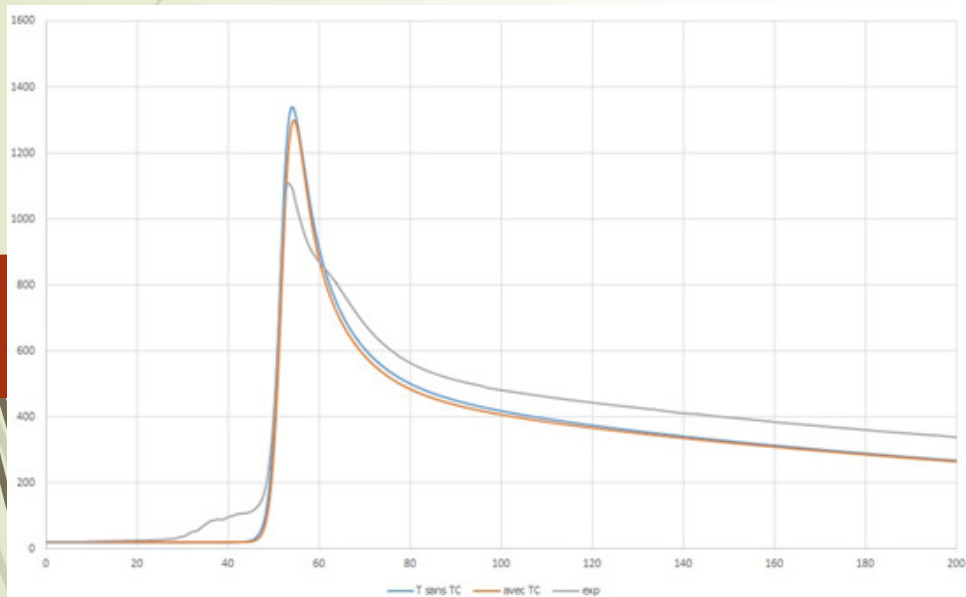
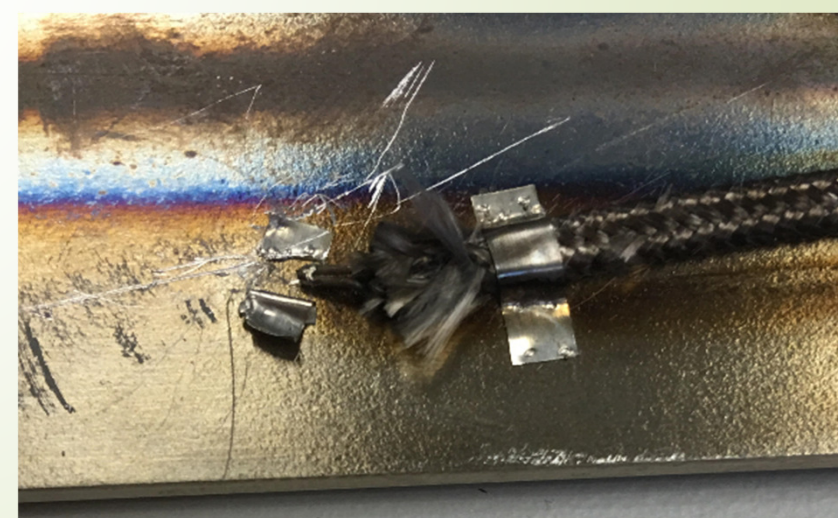
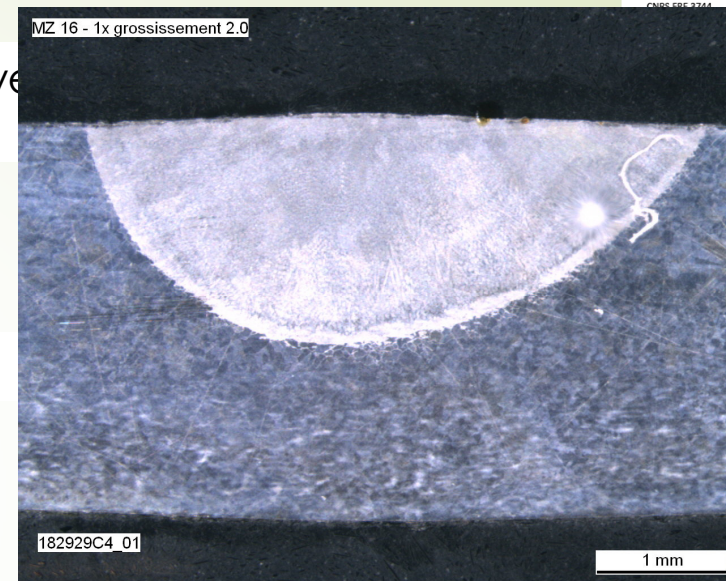
Philippe Le Masson – IRDL – UBS.



Analyse the measurement errors – PVR experiment

- With the macrograph, we have defined the parameters and we can define a fused zone.

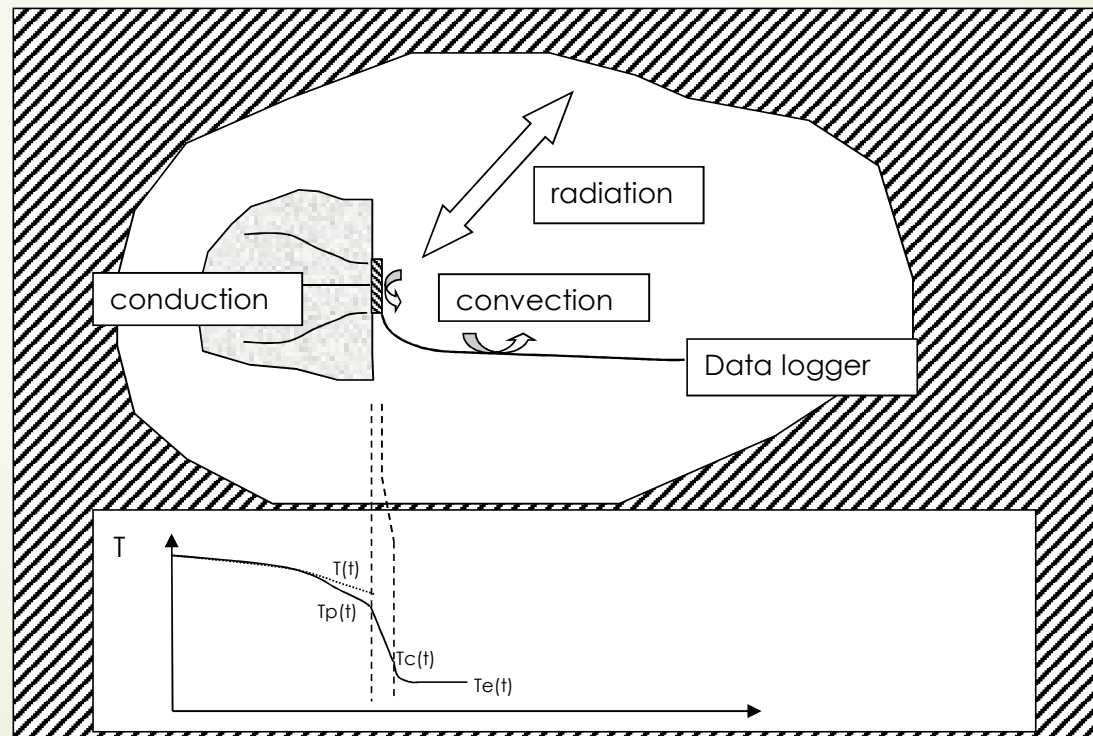
- Comparison: theoretical and experimental measurements



The modelisation of the error (METTI School)

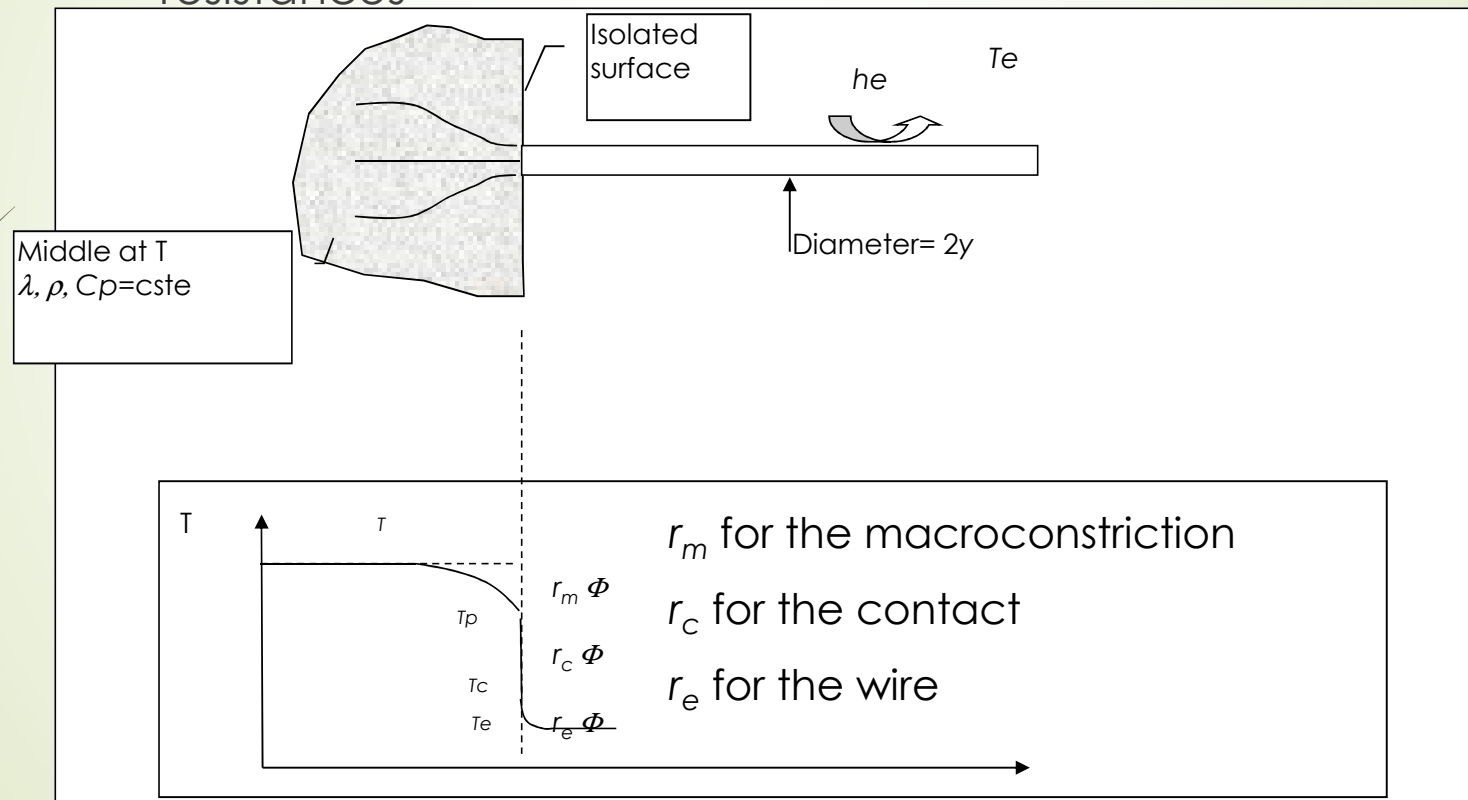
- In a steady state case and for a thermocouple on a surface, we have this scheme:

$$\varepsilon(t) = T(t) - T_c(t)$$



The modelisation of the error

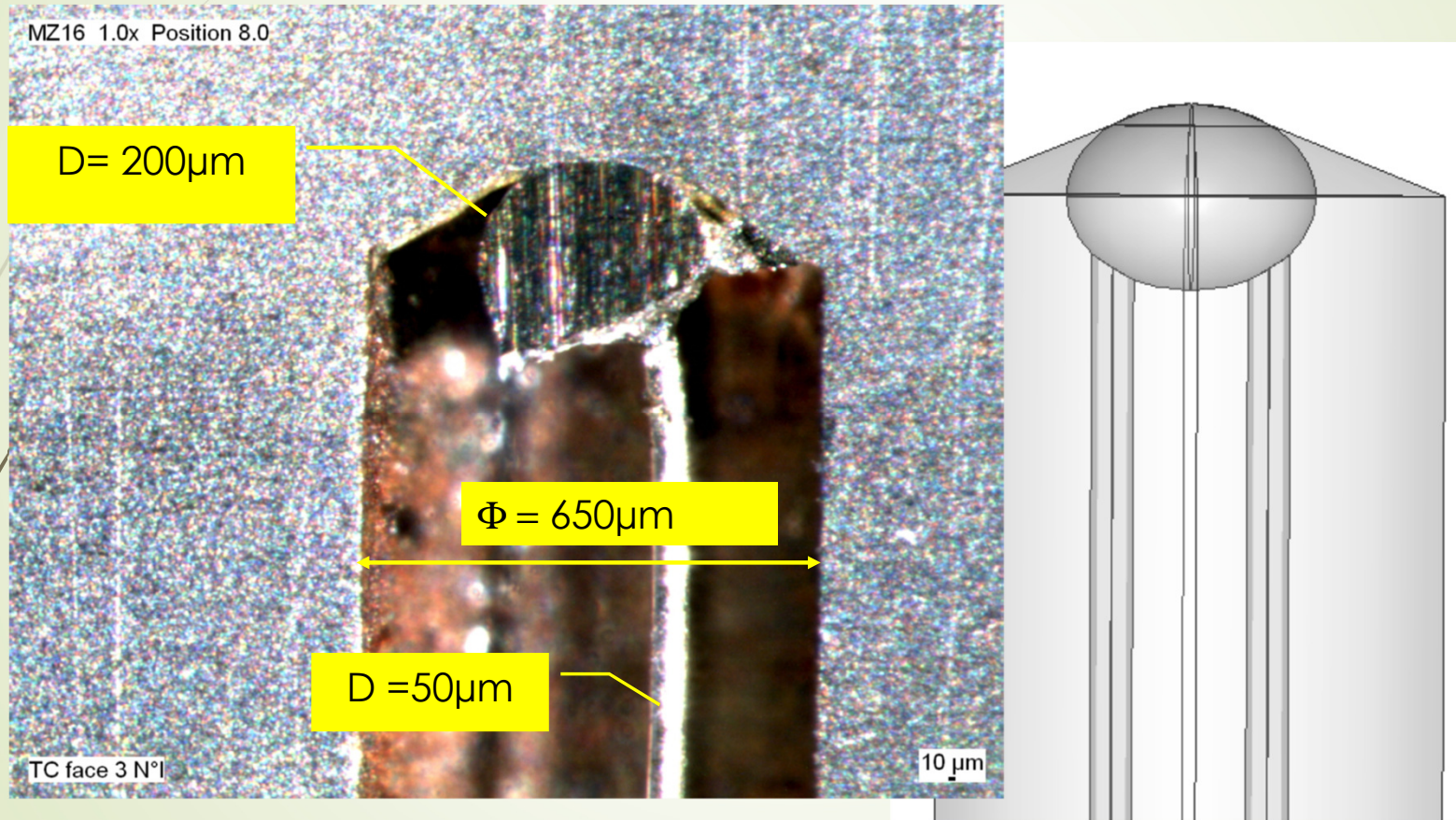
- For this case, in the model in steady state, we define three resistances



Modelisation of the welding problem with thermocouples

- ▶ With the software « Comsol Multiphysics », we realize a simulation of the welding problem. But, in the second time, we modelise the thermocouples.
- ▶ Two configurations are studied:
 - ▶ For the first one, the holes for the thermocouples are perpendiculars of the heat flux and the fused zone.
 - ▶ For the second, the holes are parallels of the fused zone.
- ▶ Moreover, we compute different contact resistances between the thermocouples and the material ($R_c = e/\lambda$, $\lambda = 0.025 \text{ W/m/K}$):
 - ▶ $R_c = 10^{-3}$ or $10^{-4} \text{ m}^2\text{K/W}$ for a bad contact ($e = 25\mu\text{m}$ or $2.5\mu\text{m}$)
 - ▶ $R_c = 10^{-5}$ or $10^{-6} \text{ m}^2\text{K/W}$ for a mean contact ($e = 0.25\mu\text{m}$ or $0.025\mu\text{m}$)
 - ▶ $R_c = 10^{-7} \text{ m}^2\text{K/W}$ for a good contact ($e = 0.0025\mu\text{m}$)

The modelisation of the thermocouples



Results of the first estimation

- ▶ Analyze the results for a “crime inverse”:
 - ▶ The criterion decreases
 - ▶ After the first iteration, we have:

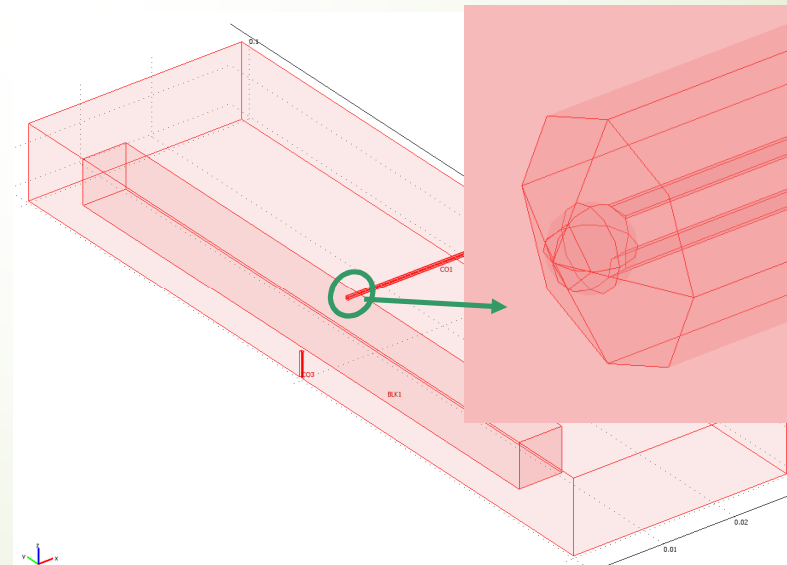
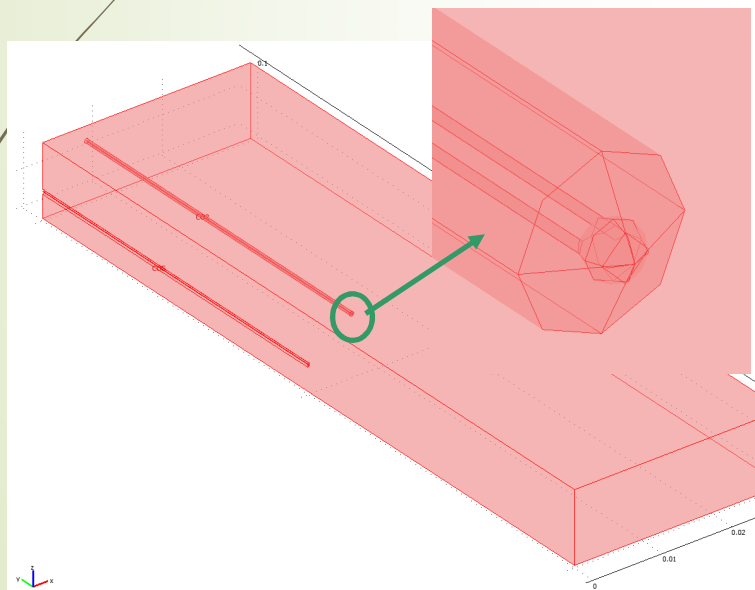
iteration	Q	Criterion
Initial values	100	$187 \cdot 10^6$
First	3988	1800
second	4000	0.001

- ▶ After 2 iterations, we obtain the good value $Q = 4000$

Modelisation of the welding problem with thermocouples

with “Comsol Multiphysics” the two configurations.

Parallele configuration Perpendicular configuration





Modelisation of the welding problem with thermocouples

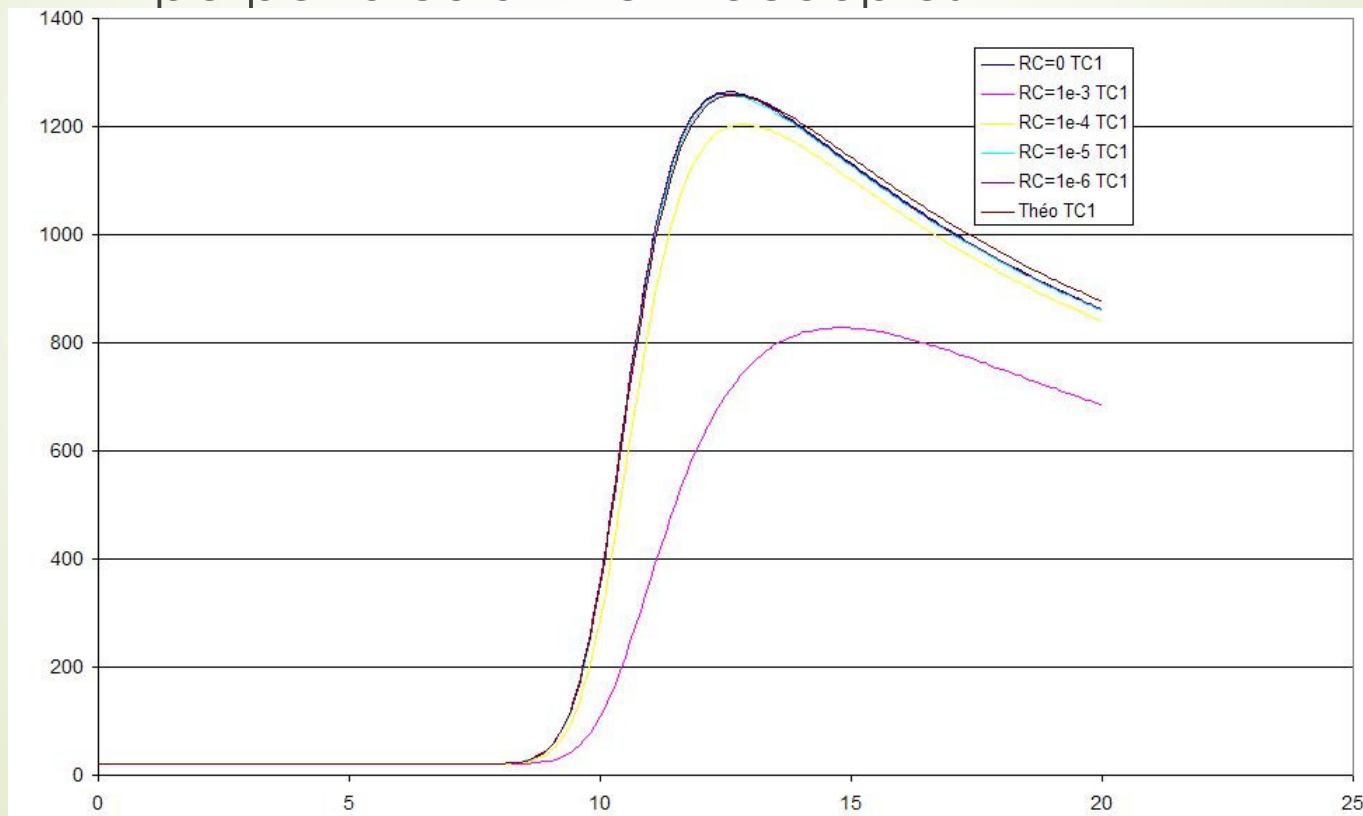
We execute these configurations with different contact resistances and we use the thermogrammes in the first optimisation loop with a direct problem without the thermocouples.

With this work, we can underline:

- The measurement errors
- The estimation errors of Q

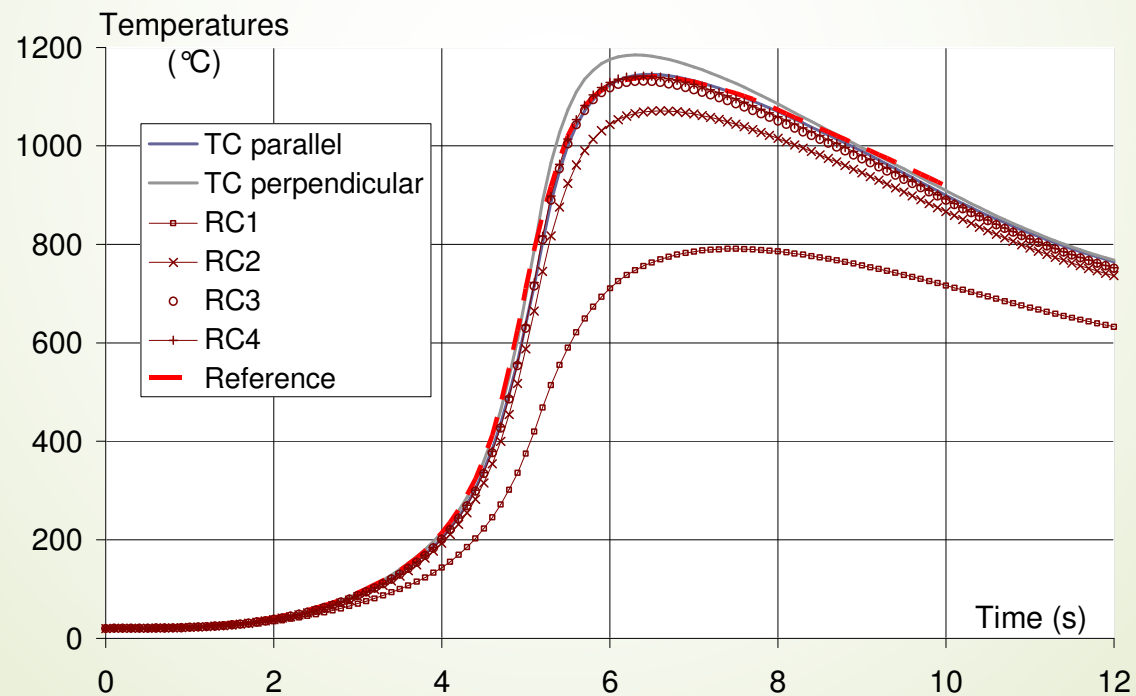
Modelisation of the welding problem with thermocouples

Visualisation of the measurements errors for perpendicular thermocouples

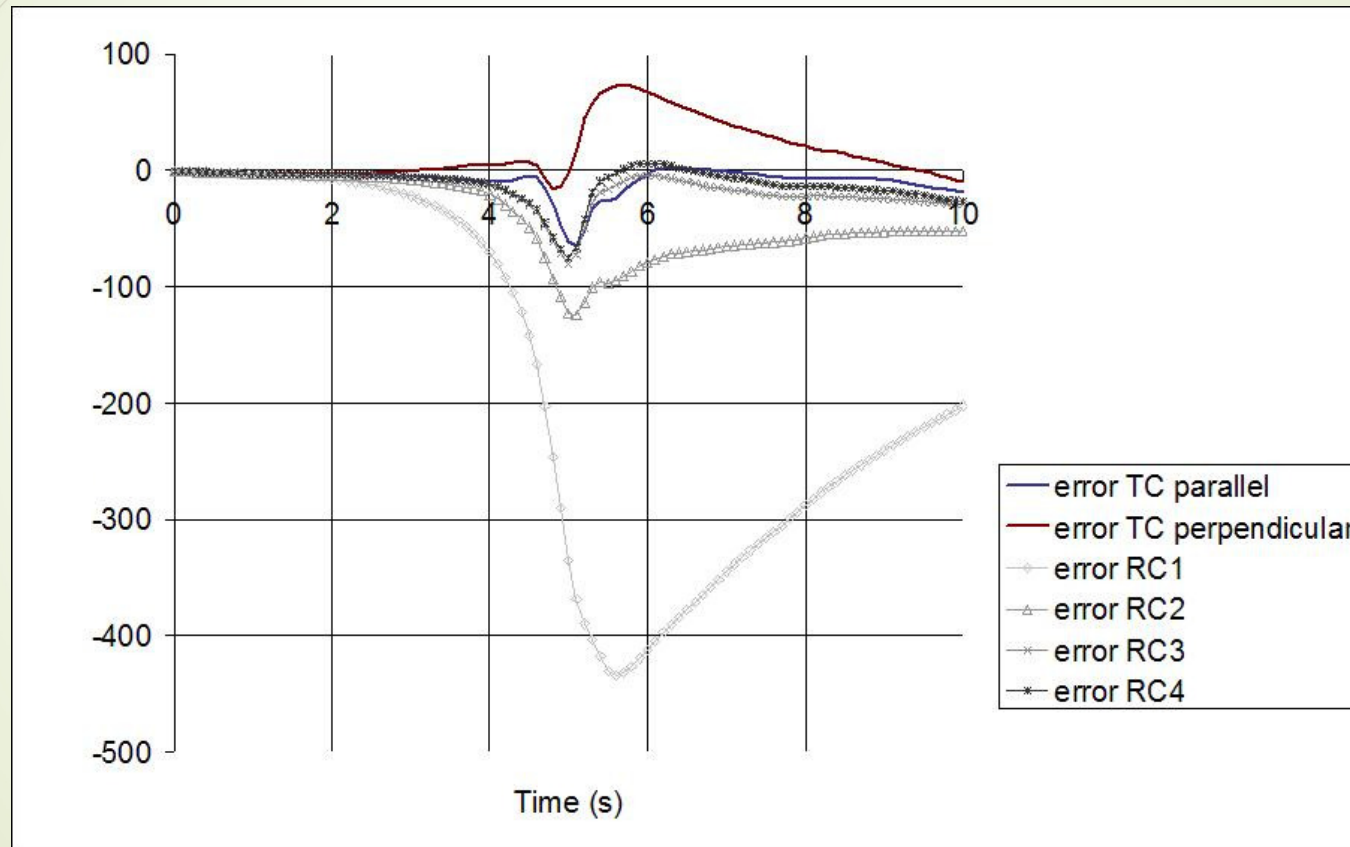


Modelisation of the welding problem with thermocouples

Visualisation of the measurements errors and comparisons between the two configurations



Modelisation of the welding problem with thermocouples



Modelisation of the welding problem with thermocouples

Conclusions for the two configurations

- 1- With the thermocouples in an isotherm, we have less errors.
- 2- It's very important to have a good contact between the thermocouple and the material
- 3- We must define correctly the space domain to have the less errors.

Modelisation of the welding problem with thermocouples

for 7 iterations	RC= 1e-3		RC= 1e-4		RC= 1e-5		RC= 1e-6		RC= 0	
TC perpendicular	2907	37,60%	3788	5,60%	3923	1,96%	4064	1,57%	4061	1,50%
TC parallel	2600	53,85%	3854	3,79%	3987	0,33%	4010	0,25%	3985	0,38%

Modelisation of the welding problem with thermocouples

Conclusions for the two configurations

- 1- An estimation which don't take into account the real instrumentation leads to an error.
- 2- This error can be higher if we have bigger thermocouples (here the diameter of the wire is $50\mu\text{m}$). It's impossible to define the characteristic time for the thermocouple. In fact, we study the interaction between the thermocouple with the domain
- 3- At last, if we use thermocouples, we must analyze the transfer between the thermocouple and the material (R_c and heat transfer coefficient between the wires and the environment). And, we have to try to use a real experimental direct problem in the optimization loop. Or eventually, we must quantify the measurement corrections

NET TG4 : general hypothesis

Specimen geometry considered in the simulation

Plate 194 × 150 × 18

Slot 80 mm long ; 6 mm deep

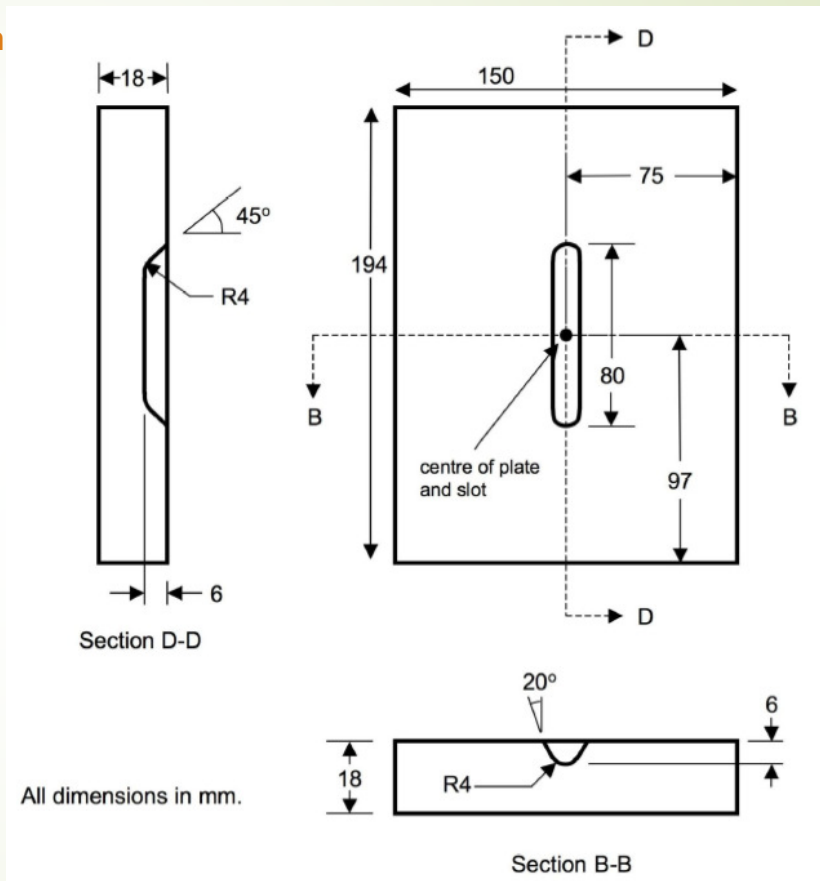
Material :

316L austenitic steel

Welding parameters :

GTAW – 3 weld passes	Pass 2	Pass 3
U = 10 V	U=10 V	U= 10V
I = 150 – 180 A	I= 204 A	I = 196 A
V = 1.667 mm/s	V=76.2mm/mn (1.27mm/s)	V=76.2mm/mn (1.27mm/s)
E = 0.7 to 1.0 KJ/mm	1.675 KJ/mm	1.768 KJ/mm
Interpass T° < 80 °C	T < 60 °C	T < 60 °C

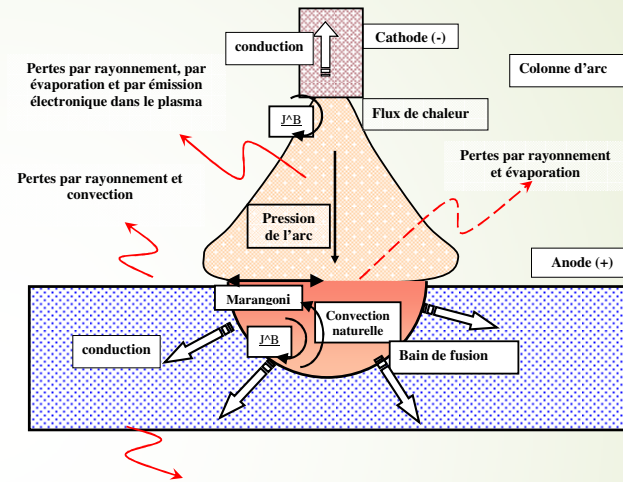
philippe.le-masson@univ-ubs.fr / Garching June 2010



Simulation

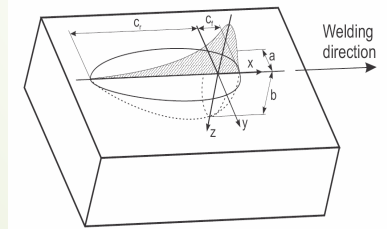
➔ 2 approaches:

➔ Multiphysics:



➔ Equivalent heat sources:

Goldak model



CIN model

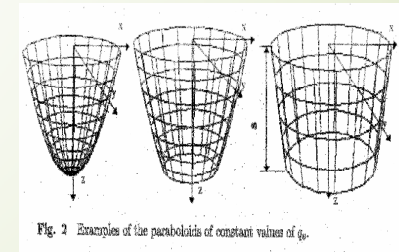
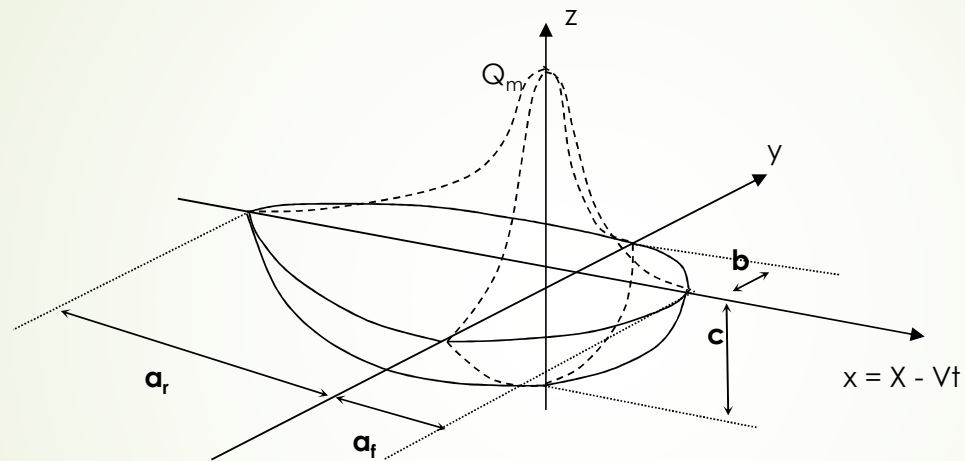


Fig. 2 Examples of the paraboloids of constant values of θ_w .

Heat input : hypothesis

→ Double ellipsoid $Q = f(X, Y, Z, t)$ over the weld deposit and the test piece



$$q(x, y, z) = Q_0 \cdot \frac{6\sqrt{3} \cdot f_\xi}{a_\xi \cdot b \cdot c \cdot \pi^{3/2}} \exp\left(\frac{-3x^2}{a_\xi^2}\right) \cdot \exp\left(\frac{-3y^2}{b^2}\right) \cdot \exp\left(\frac{-3z^2}{c^2}\right) \quad \int_V q(x, y, z) \cdot dV = P_0$$

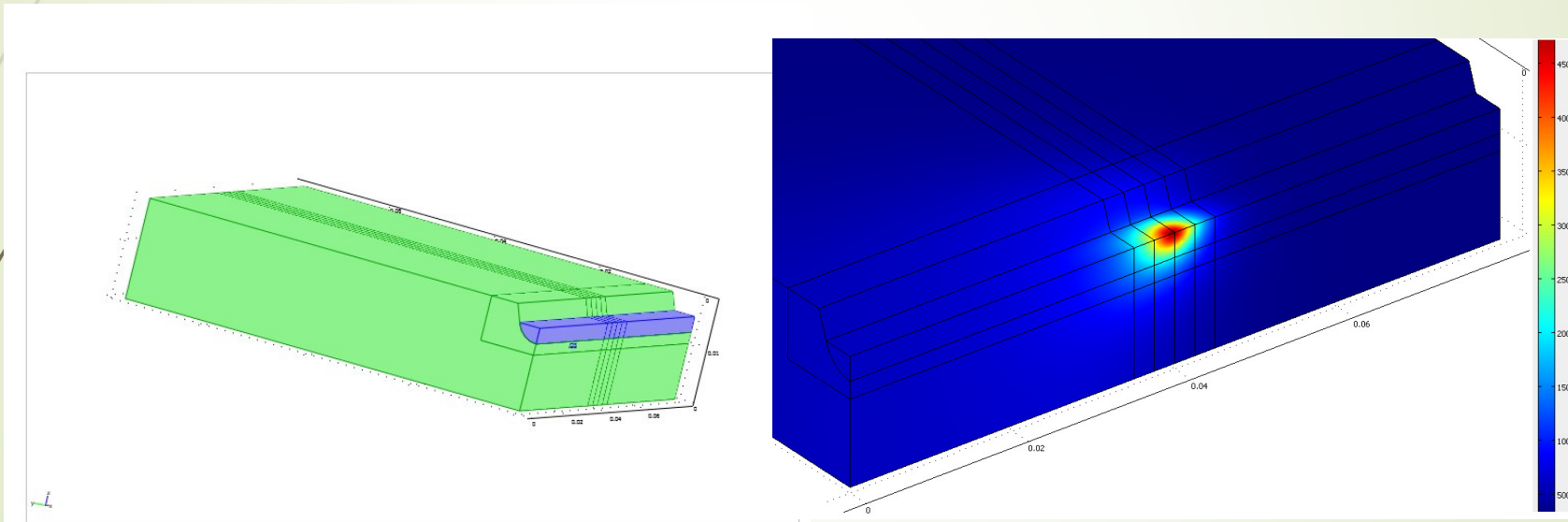
With this function: 7 parameters: a_r , a_f , b , c , Q_0 , f_f and f_r . Moreover, $f_f + f_r = 2$ and $a_f(2 - f_r) = a_r f_f$

Direct and inverse problems

-For the numerical resolution, we use:

-The software “Comsol Multiphysics” for the direct problem

-Matlab for the inverse problem (Levenberg Marquardt Algorithm)



Solution for the pass1 in a quasi steady state simulation

philippe.le-masson@univ-ubs.fr / Garching June 2010

Gauss-Newton or Levenberg-Marquardt Method

$$\mathbf{P}^{k+1} = \mathbf{P}^k + \left[\mathbf{J}^T \mathbf{W} \mathbf{J} + \lambda^k \mathbf{\Omega}^k \right]^{-1} \left\{ \mathbf{J}^T \mathbf{W} \left[\mathbf{Y} - \mathbf{T}(\mathbf{P}^k) \right] \right\}$$

where λ^k is a parameter and $\mathbf{\Omega}^k$ a diagonale matrix (= I for example)

For uncorrelated measurements

$$\mathbf{W} = \begin{bmatrix} 1/\sigma_1^2 & & & 0 \\ & 1/\sigma_2^2 & & \\ & & \ddots & \\ 0 & & & 1/\sigma_1^2 \end{bmatrix}$$

The sensitivity matrix

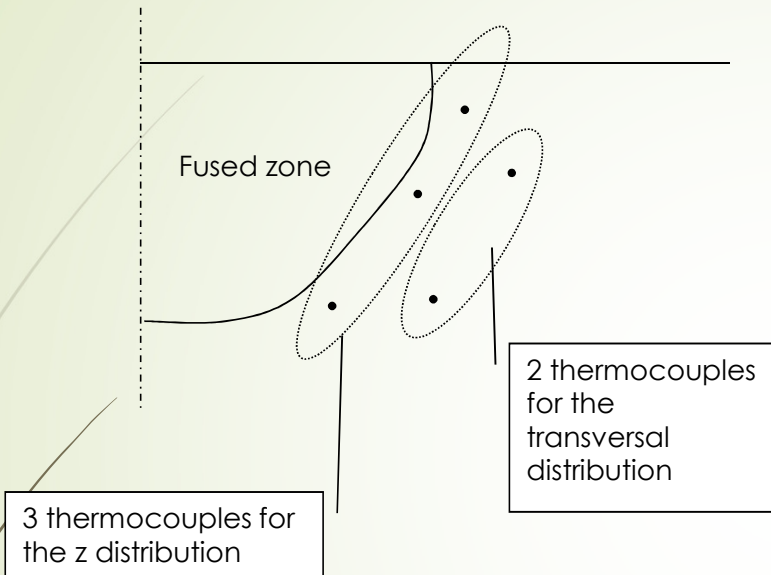
$$\mathbf{J} = \left[\frac{\partial \mathbf{T}^T}{\partial \mathbf{P}} \right]^T = \begin{bmatrix} \frac{\partial T_1}{\partial P_1} & \frac{\partial T_1}{\partial P_2} & \frac{\partial T_1}{\partial P_3} & \dots & \frac{\partial T_1}{\partial P_N} \\ \frac{\partial T_2}{\partial P_1} & \frac{\partial T_2}{\partial P_2} & \frac{\partial T_2}{\partial P_3} & \dots & \frac{\partial T_2}{\partial P_N} \\ \vdots & \vdots & \vdots & \ddots & \vdots \\ \frac{\partial T_I}{\partial P_1} & \frac{\partial T_I}{\partial P_2} & \frac{\partial T_I}{\partial P_3} & \dots & \frac{\partial T_I}{\partial P_N} \end{bmatrix}$$

$$J_{ij} \cong \frac{T_i(P_1, P_2, \dots, P_j + \epsilon P_j, \dots, P_N) - T_i(P_1, P_2, \dots, P_j - \epsilon P_j, \dots, P_N)}{2\epsilon P_j}$$

For the definition of the measurement points:

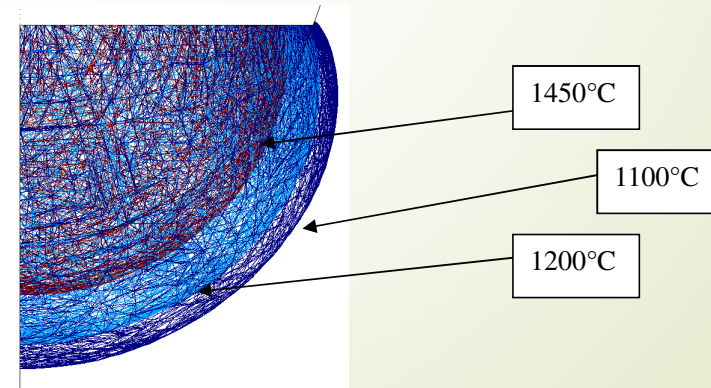
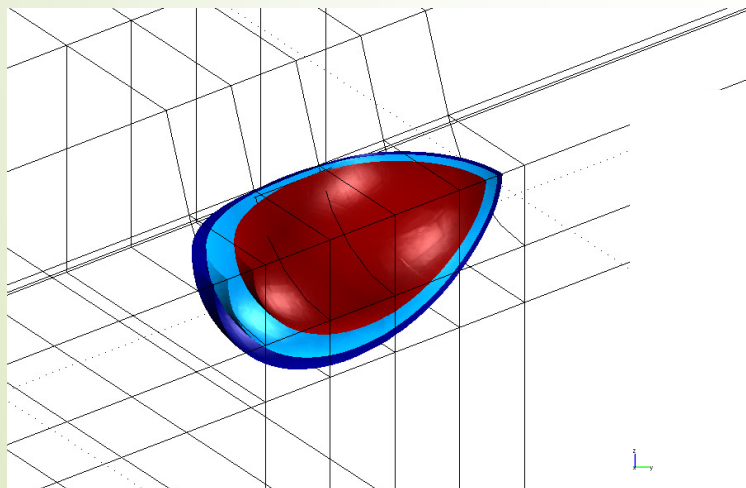
- We can analyse the evolution of the reduced sensitivity coefficients to define the best positions for the measurement points and analyze if the parameters are correlated over the whole time range of study
- analyze the determinant of the matrix $[\mathbf{J}^T \mathbf{J}]$ to define the final measurement time

Instrumentation



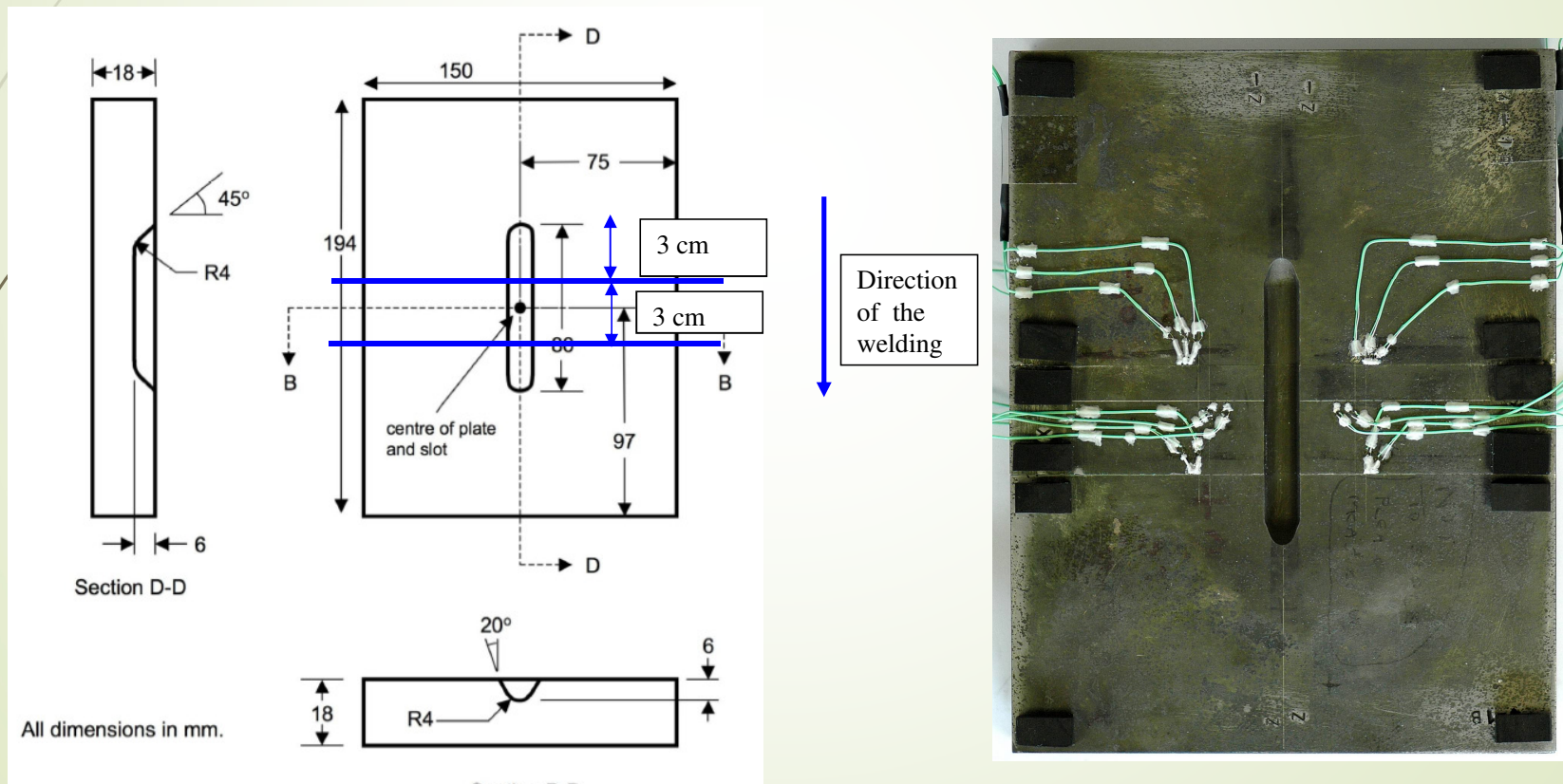
For each estimation, we put thermocouples on two isotherms. In this case, we can obtain the heat distribution in the depth, in the transversal direction and in the longitudinal direction (time)

With the simulation and a comparison with micrographs, we define the instrumentation



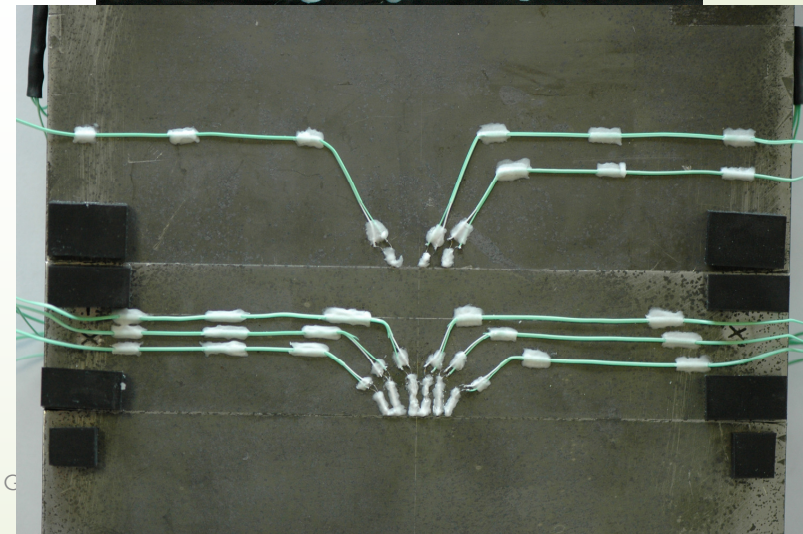
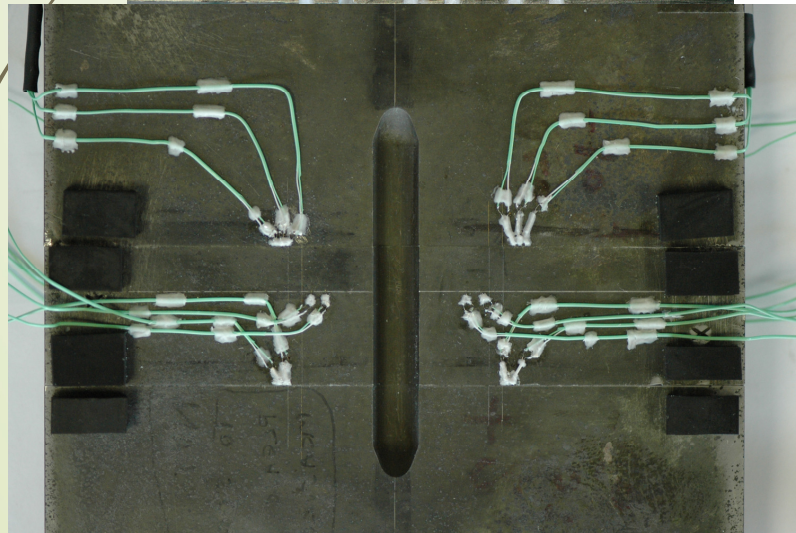
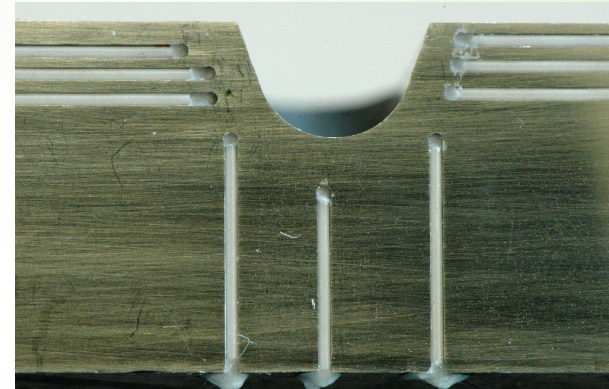
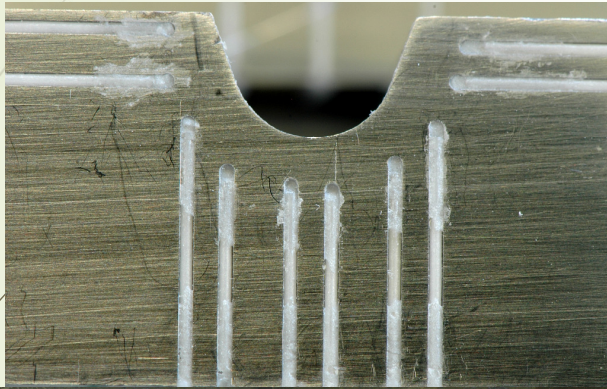
Instrumentation

For the measurements with thermocouples, we make holes in the specimen. We have a perturbation in the heat diffusion. So we must put the thermocouple wires in an isotherm for a length that around ten diameter. For this experience, we had cut the specimen in three parts



Instrumentation

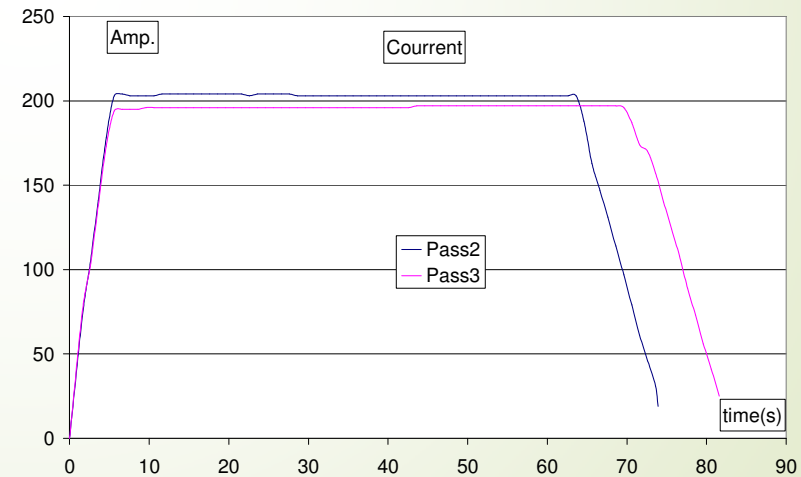
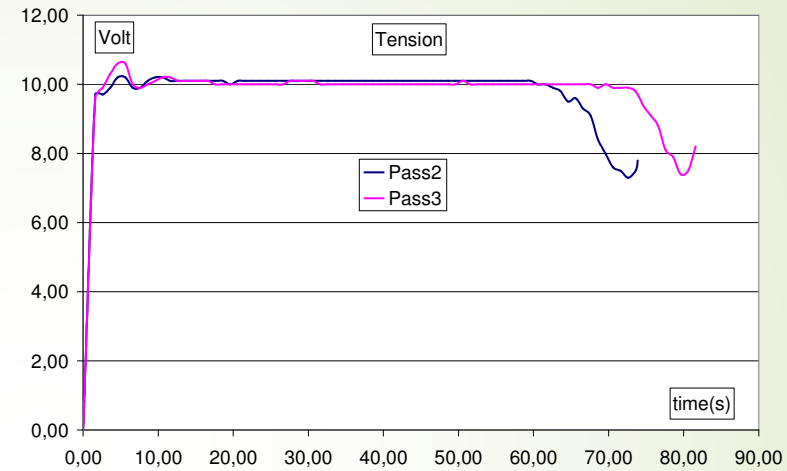
We had 23 thermocouples. These thermocouples were welded in holes: depth 7mm, diameter: 0,65mm. The wires were protected by alumina tubes.



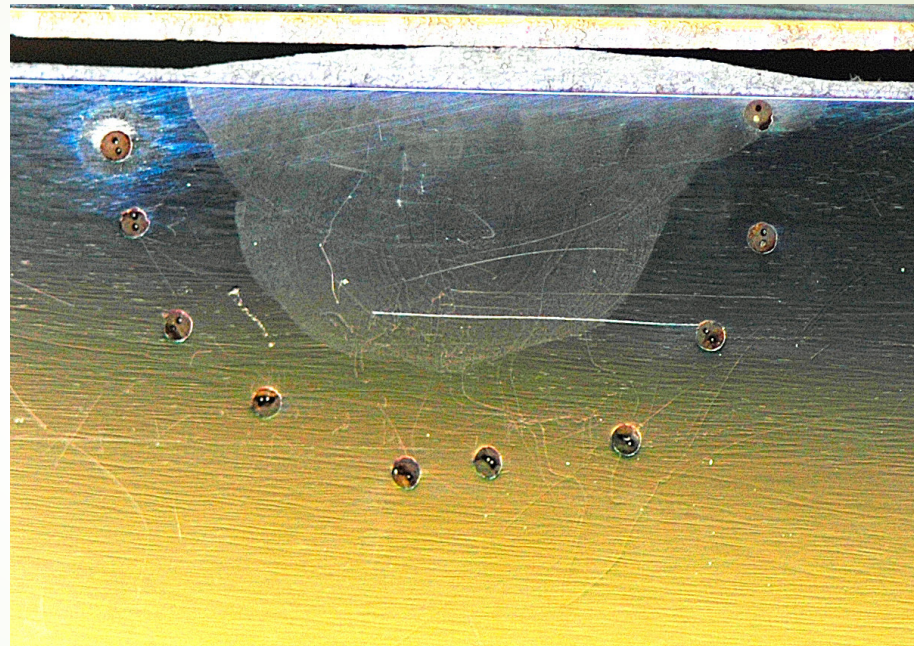
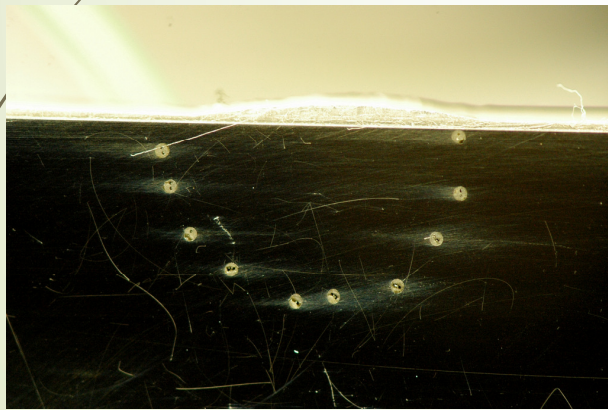
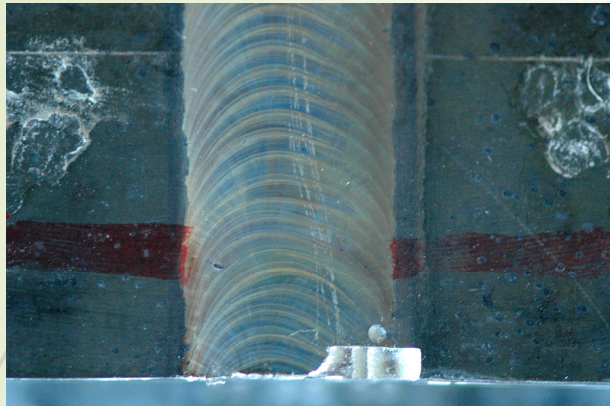
NET TG4 : general hypothesis

Welding parameters :

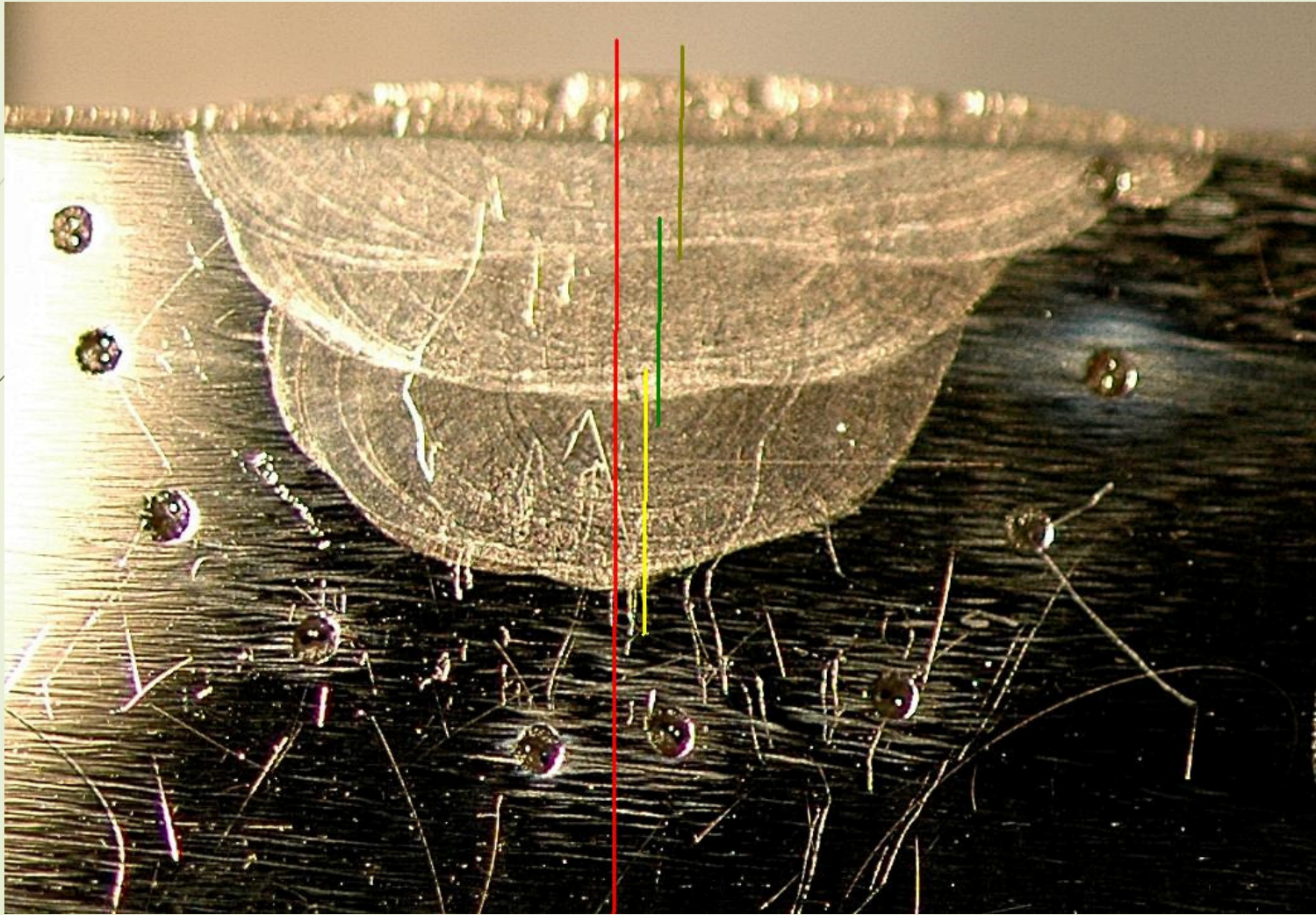
	PASS 2	PASS 3
JOB NO	0	0
WELD NO	0	0
RUN NO	0	0
WELDER	"G LITTLE"	"G LITTLE"
DATE	22-Oct-09	22-Oct-09
TIME	10:27 AM	11:24 AM
CURRENT	185	180
VOLTS	9,8	9,9
WIRE SPEED	0,1	0,0
TRAVEL SPEED	0,0	0,0
ARC TIME	73,9	81,6
WELD LENGTH (mm)	80	82
ENERGY (kJ)	134	145
HEAT INPUT (J/mm)	1675	1768
GAS FLOW (Lt/Min)	0,0	0,0
INTERPASS TEMP	0,0	0,0
WIRE CONSUMED (mt)	0,0	0,0
GAS TYPE	0,0	0,0



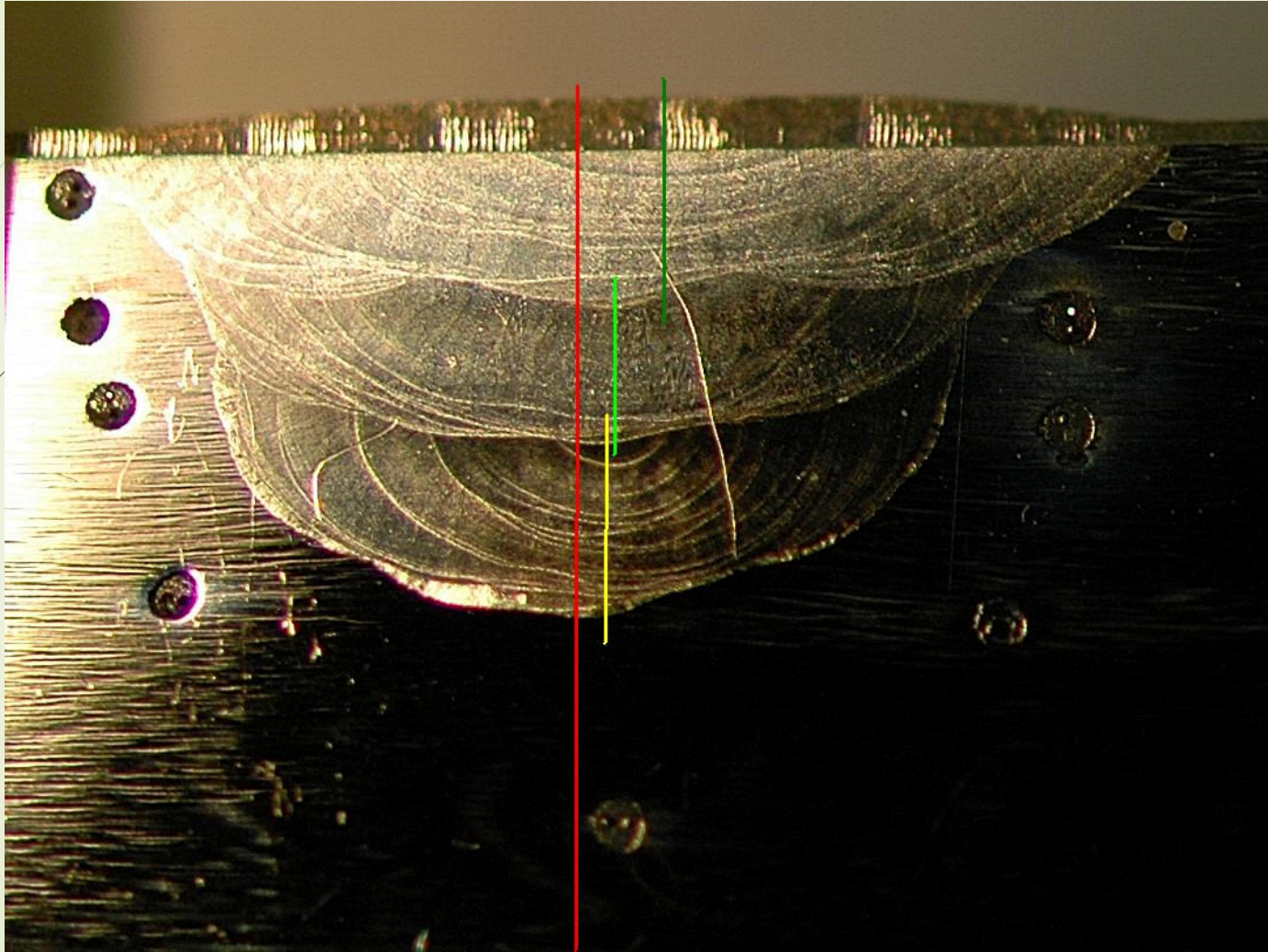
Exploitation



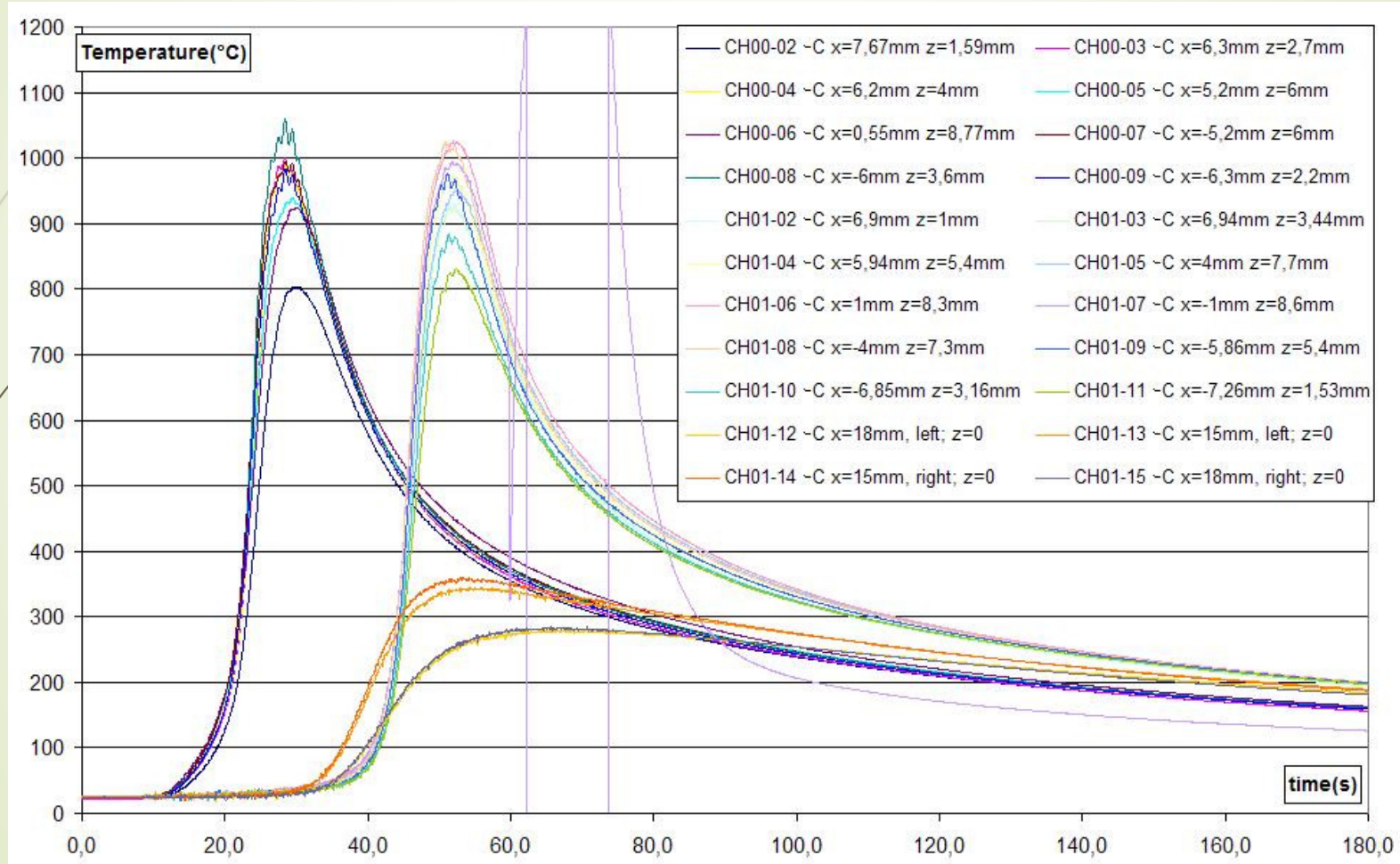
Welding axis



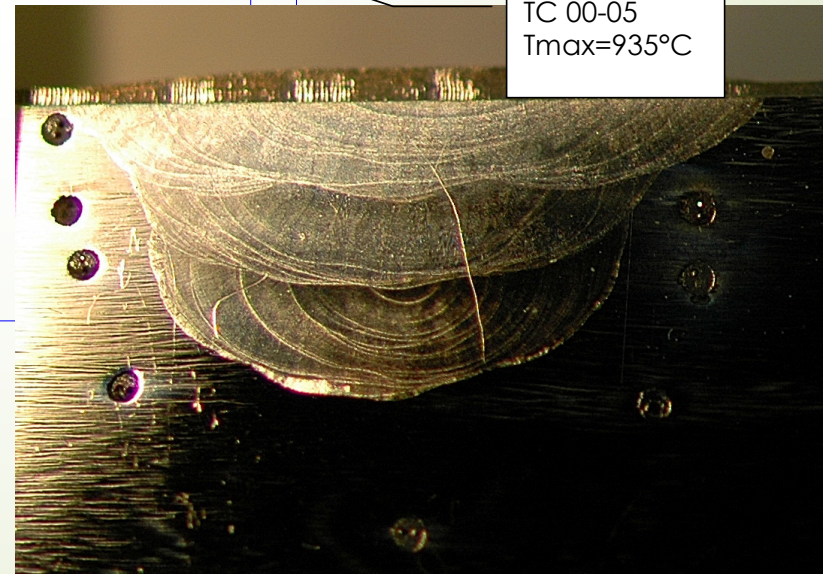
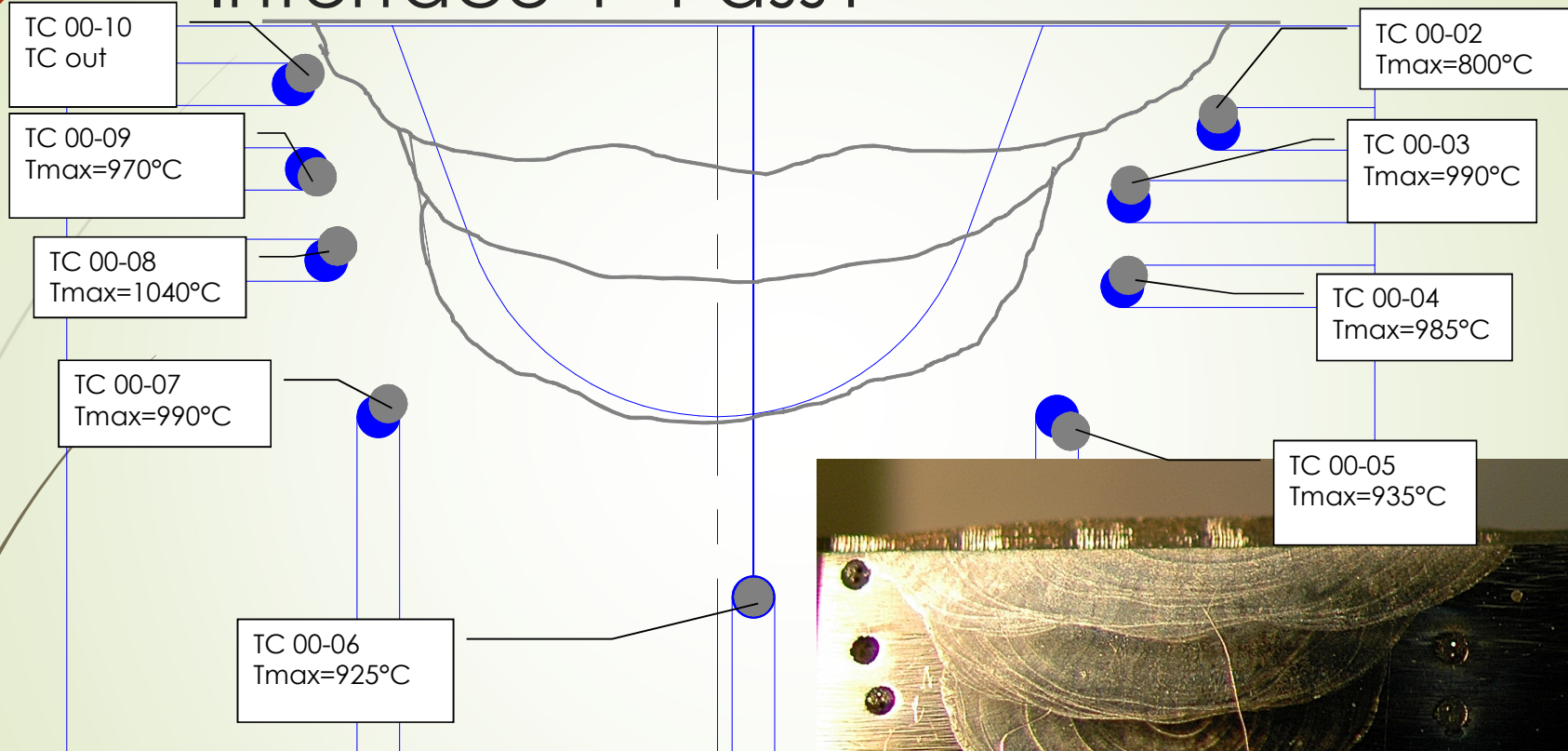
Welding axis



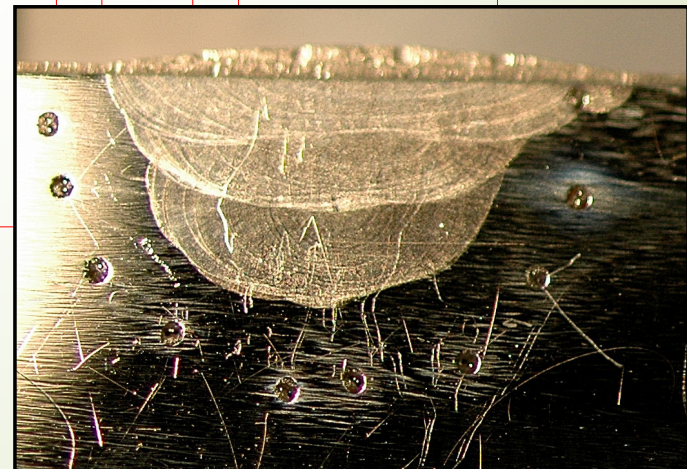
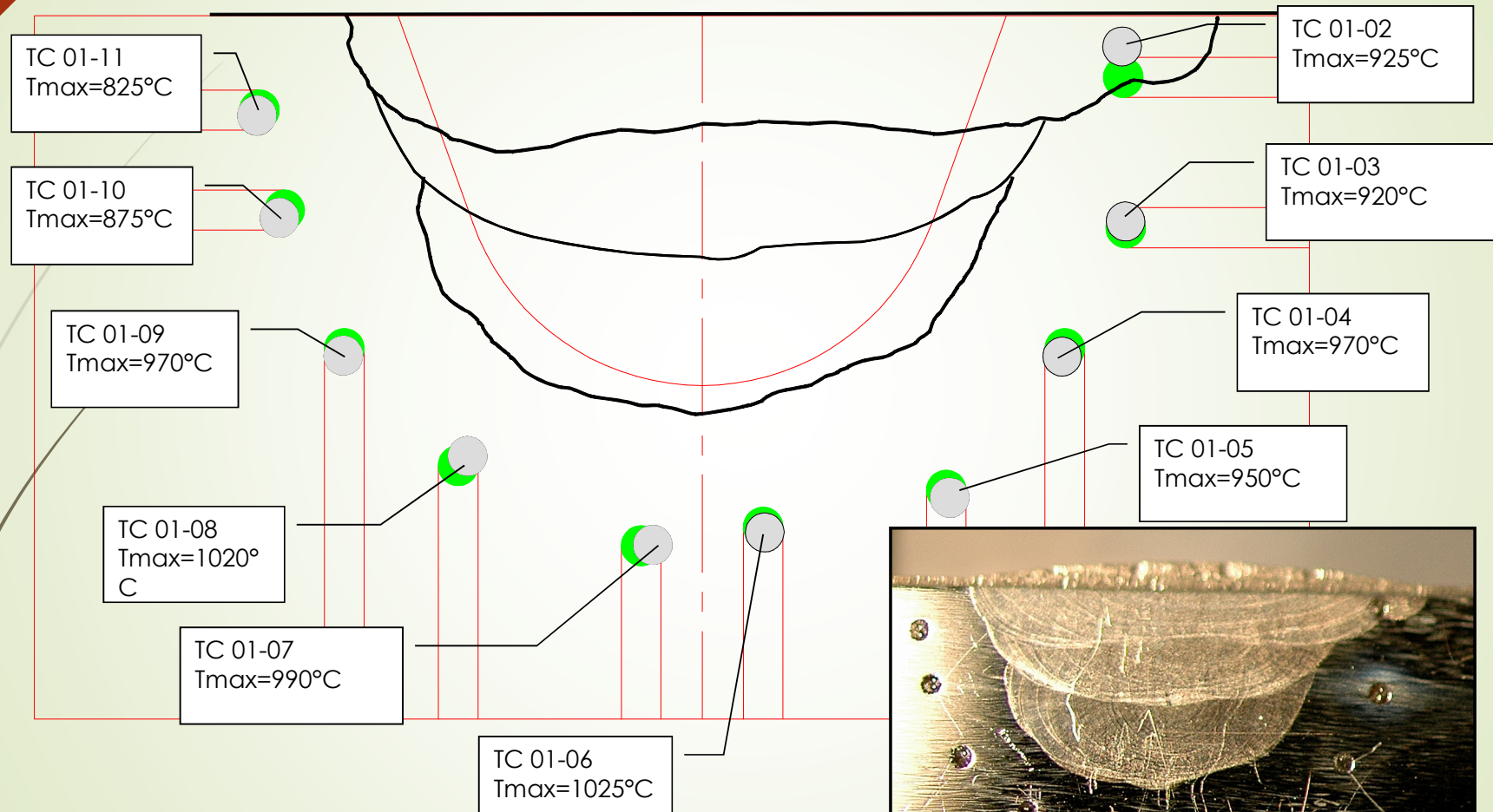
Pass 1



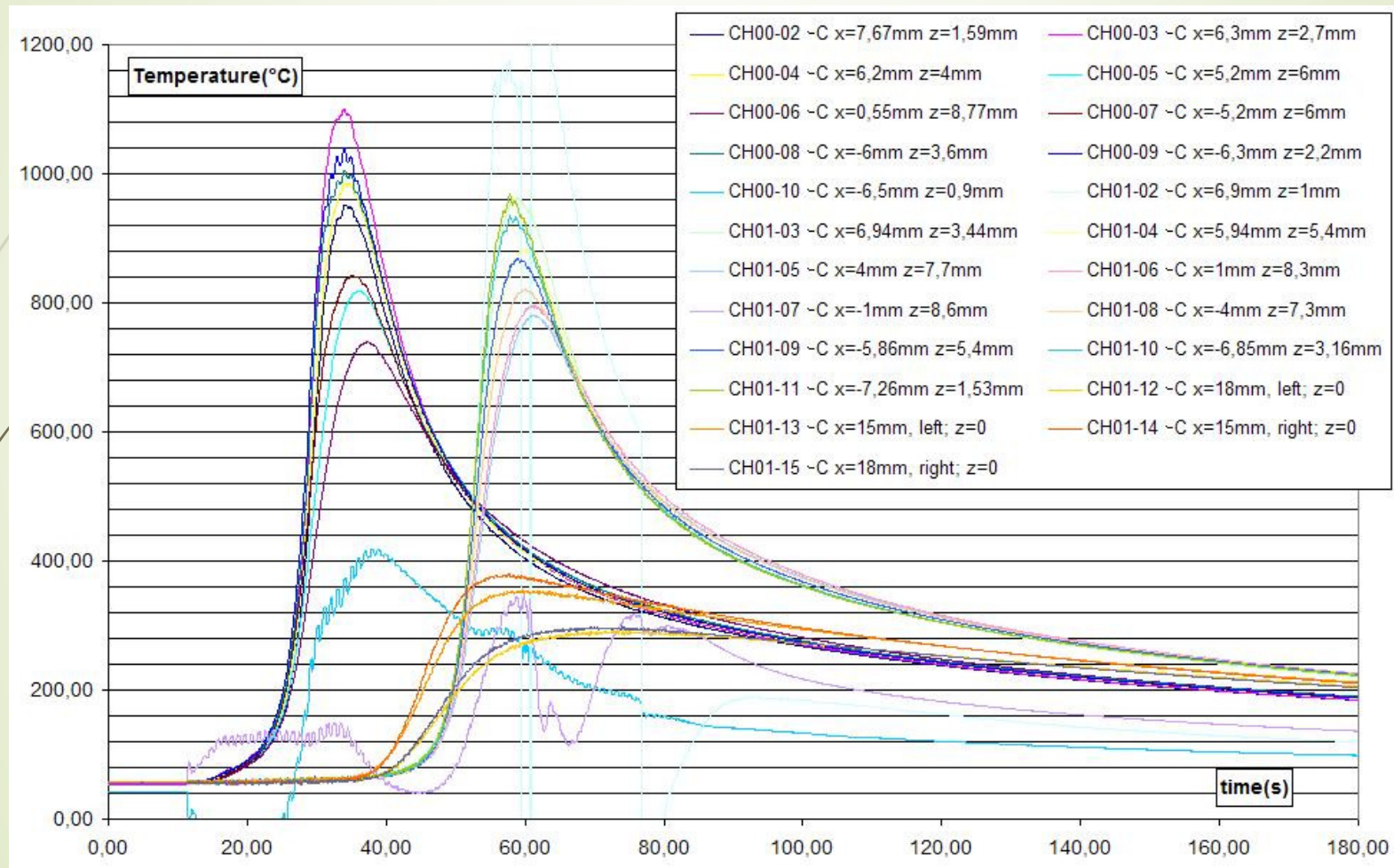
Interface 1- Pass1



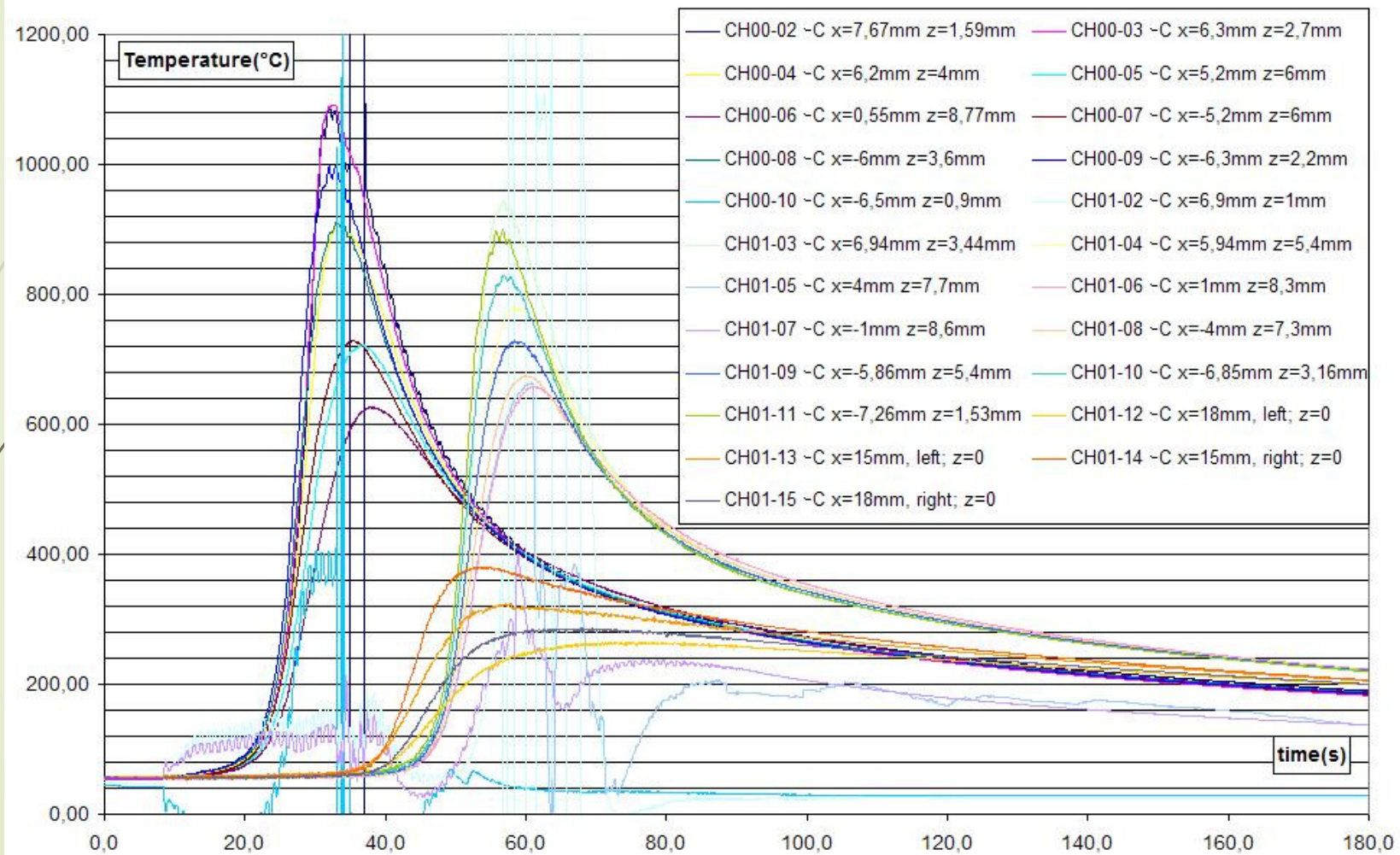
Interface 2- Pass1



Pass2



Pass3

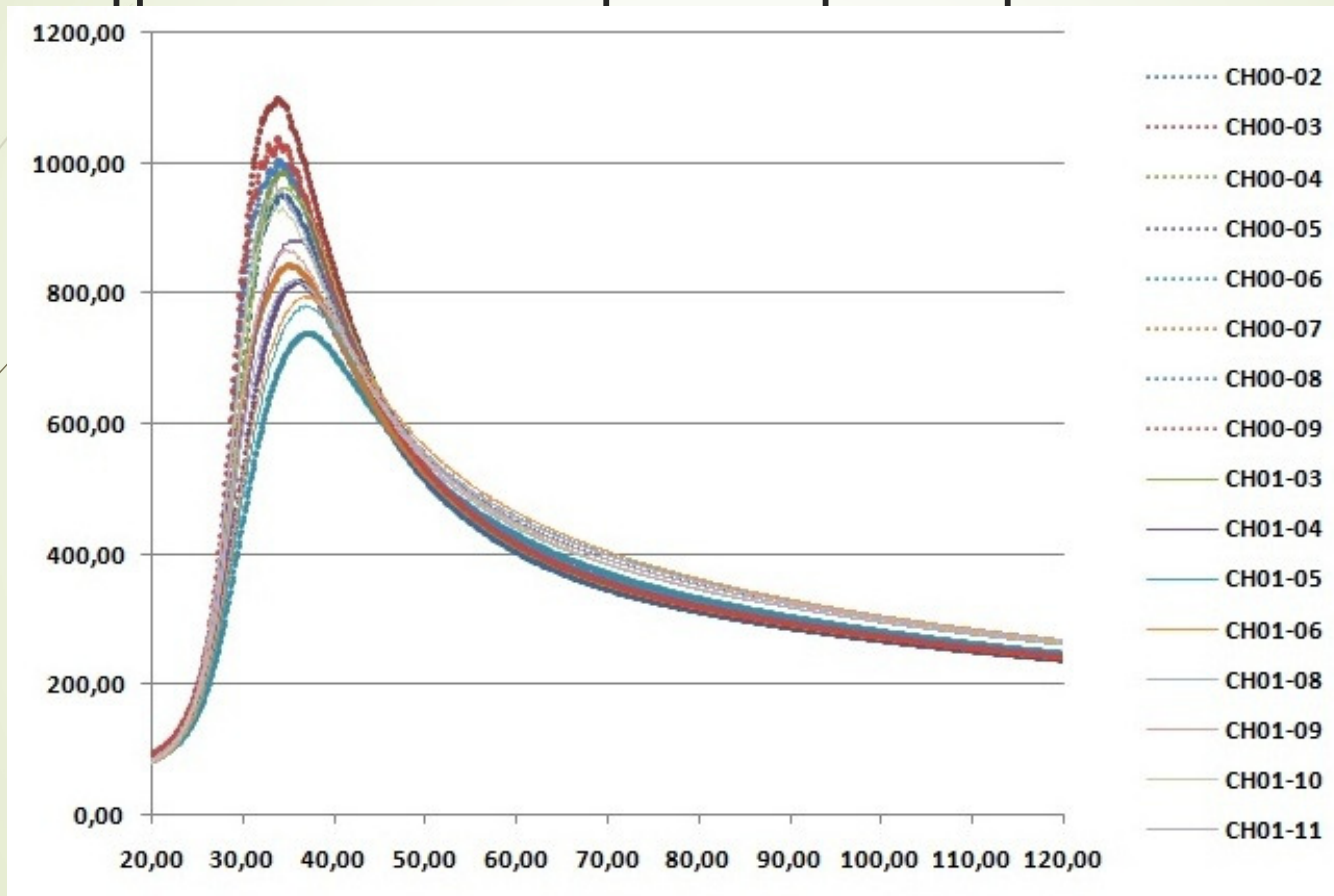


Hypothesis for the simulation

- ▶ equivalent heat sources
- ▶ The thermo physical characteristics are taken in function of the temperature (ρ ; c_p ; k).
- ▶ In the fused zone, we impose an equivalent conductivity to take into account the displacement of the metal: $k = 200 \text{ W/m.K}$
- ▶ The fused zone is defined around 1450°C for the comparison with the macrograph
- ▶ On the surface, we define a heat transfer coefficient:

$h_{eq} = hcv + \varepsilon \cdot \sigma \cdot (T^2 + Tamb^2) * (T + Tamb)$ where $\varepsilon = 0.8$ (the emissivity), and the parameter hcv (heat convective coefficient) is estimated.

We use only the second interface for



philippe.le-masson@univ-ubs.fr / Garching June 2010

1 pass

- Goldak heat source:

$$Q_{av}(x, y, z) = \frac{\eta 6\sqrt{3}}{ab_{fo}c\pi^{3/2}} f_{fo} Q e^{-3\left(\frac{y}{a}\right)^2} e^{-3\left(\frac{x}{b_{fo}}\right)^2} e^{-3\left(\frac{z}{c}\right)^2}$$

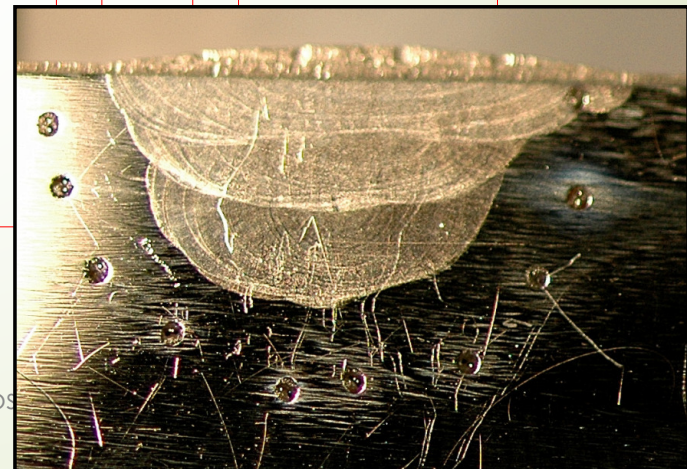
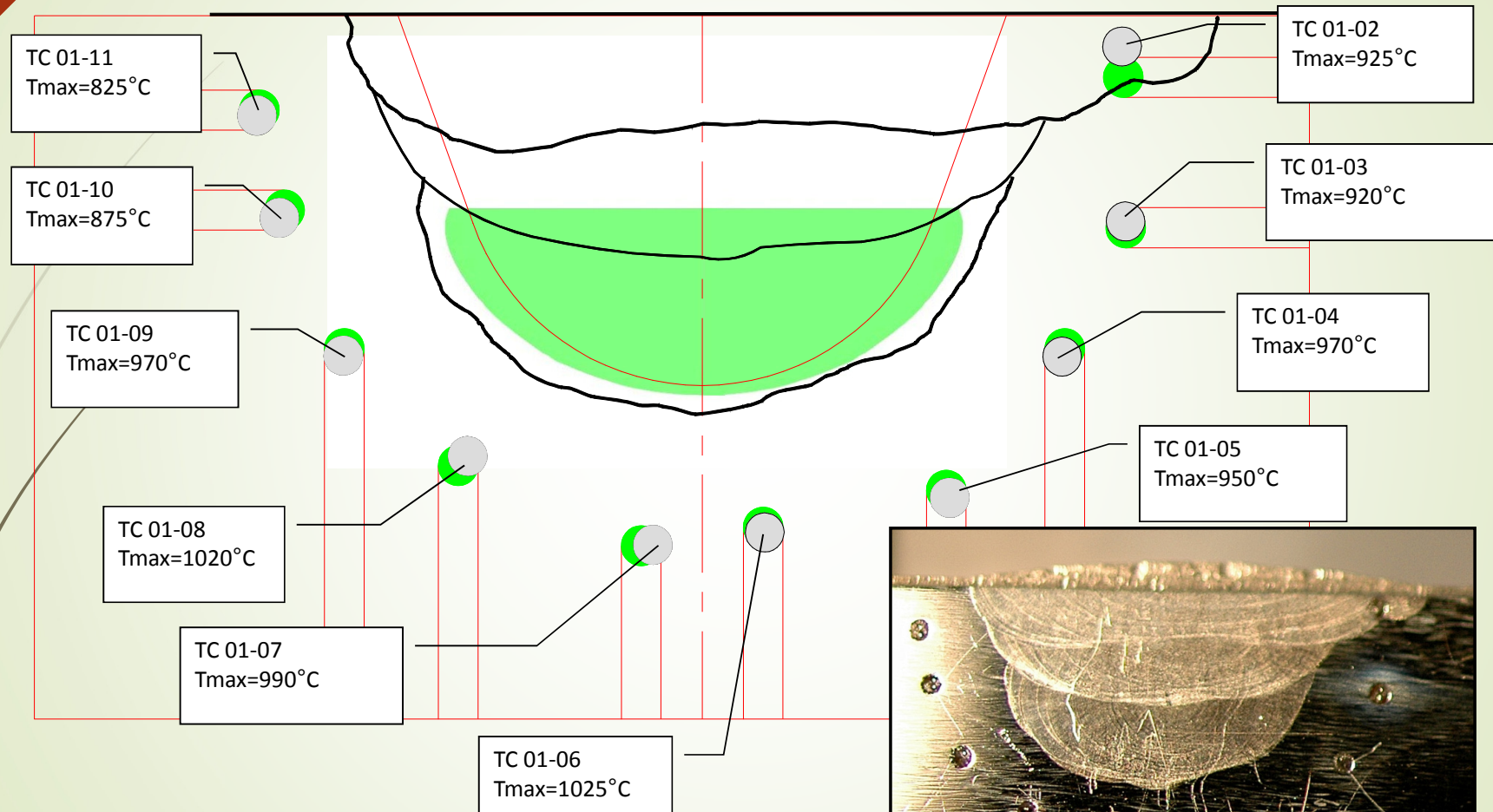
$$Q_r(x, y, z) = \frac{\eta 6\sqrt{3}}{ab_r c\pi^{3/2}} f_r Q e^{-3\left(\frac{y}{a}\right)^2} e^{-3\left(\frac{x}{b_r}\right)^2} e^{-3\left(\frac{z}{c}\right)^2}$$

The standard deviation = 13°C

	1 Pass
Parameter	Values
a (mm)	5.894
c (mm)	1.5
b_r (mm)	11.8977
b_f (mm)	3.719
f_{fo}	1.143726
f_r	$2 \cdot f_{fo}$
η	0.8849
hcv (W/m ² .k)	115.1775

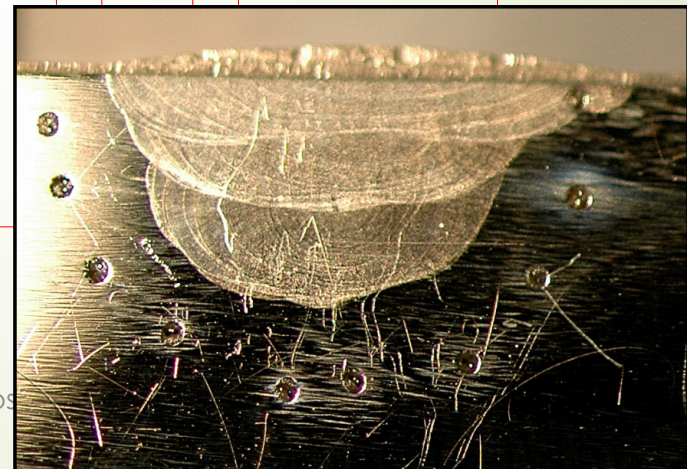
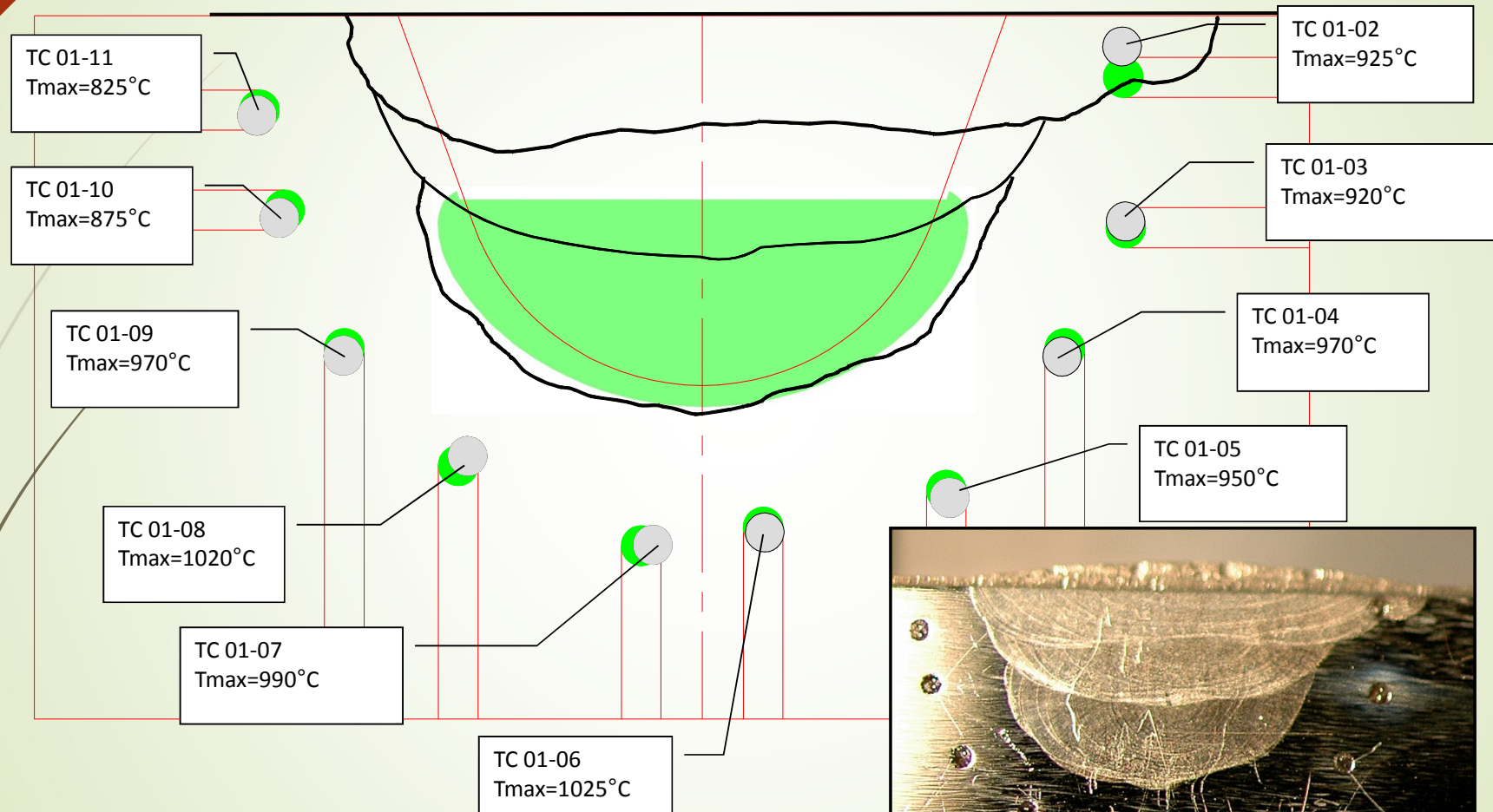
Interface 2- Pass1

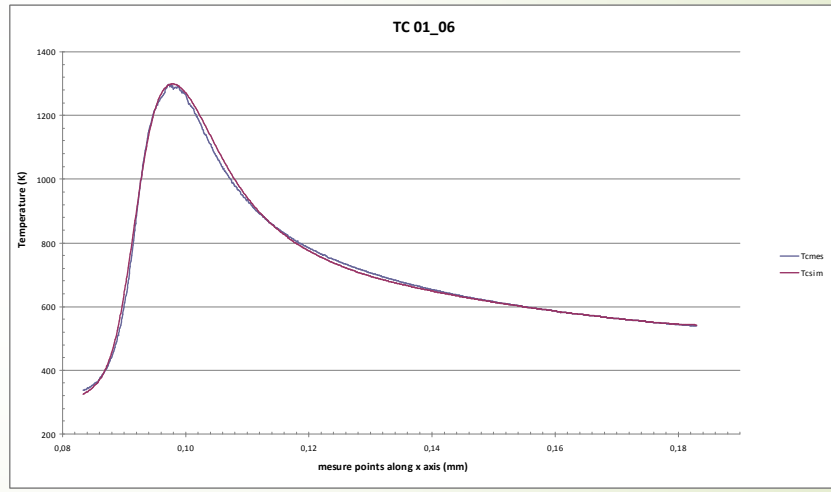
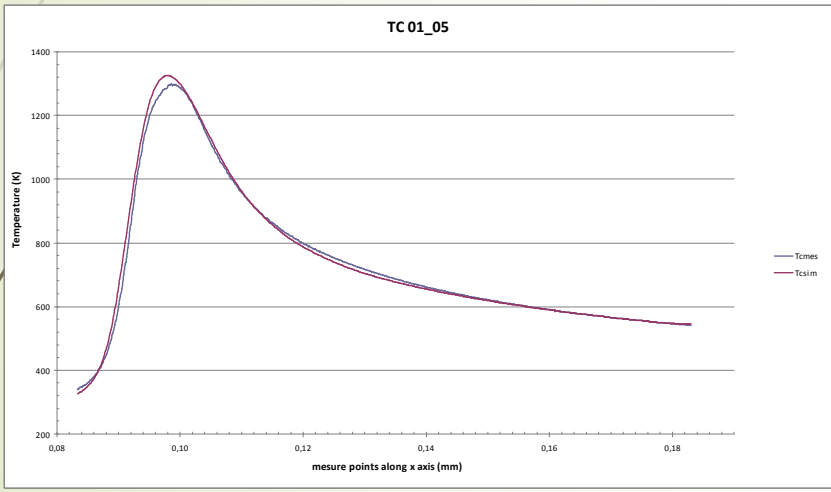
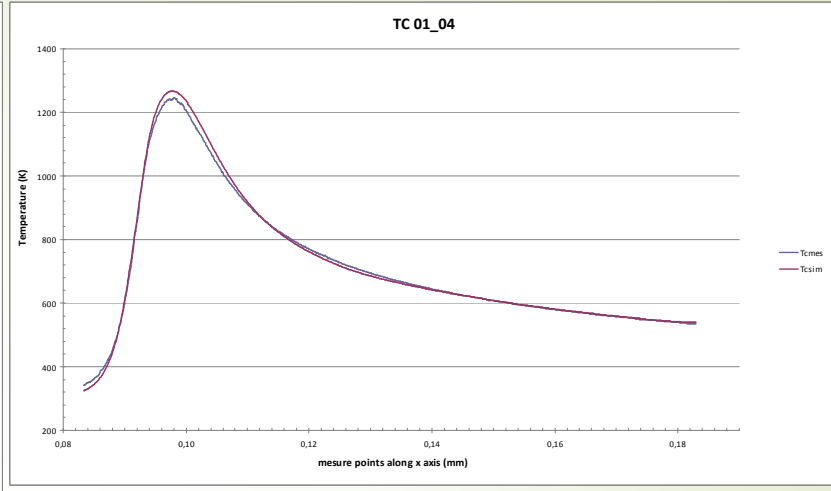
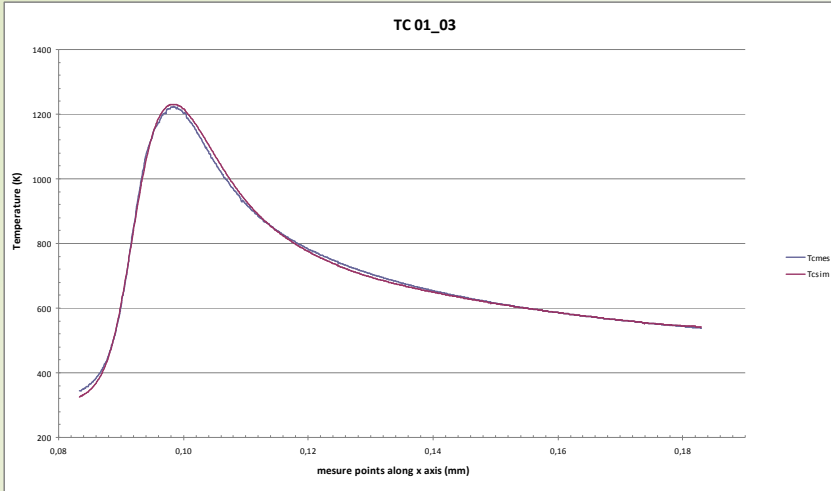
warning
 $T_f=1450^{\circ}\text{C}$



Interface 2- Pass1

warning
 $T_f=1400^{\circ}\text{C}$





2nd pass

► Truncated Goldak heat source:

for $z > H$

$$Q_{av}(x, y, z) = \frac{\eta 6 \sqrt{3}}{ab_{fo}c\pi^{3/2}} f_{fo} Q \cdot e^{-3\left(\frac{y}{a}\right)^2} e^{-3\left(\frac{x}{b_{fo}}\right)^2} e^{-3\left(\frac{z}{c}\right)^2}$$

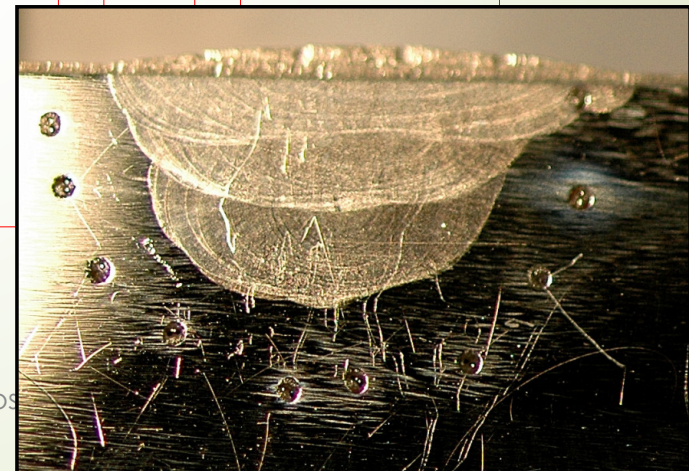
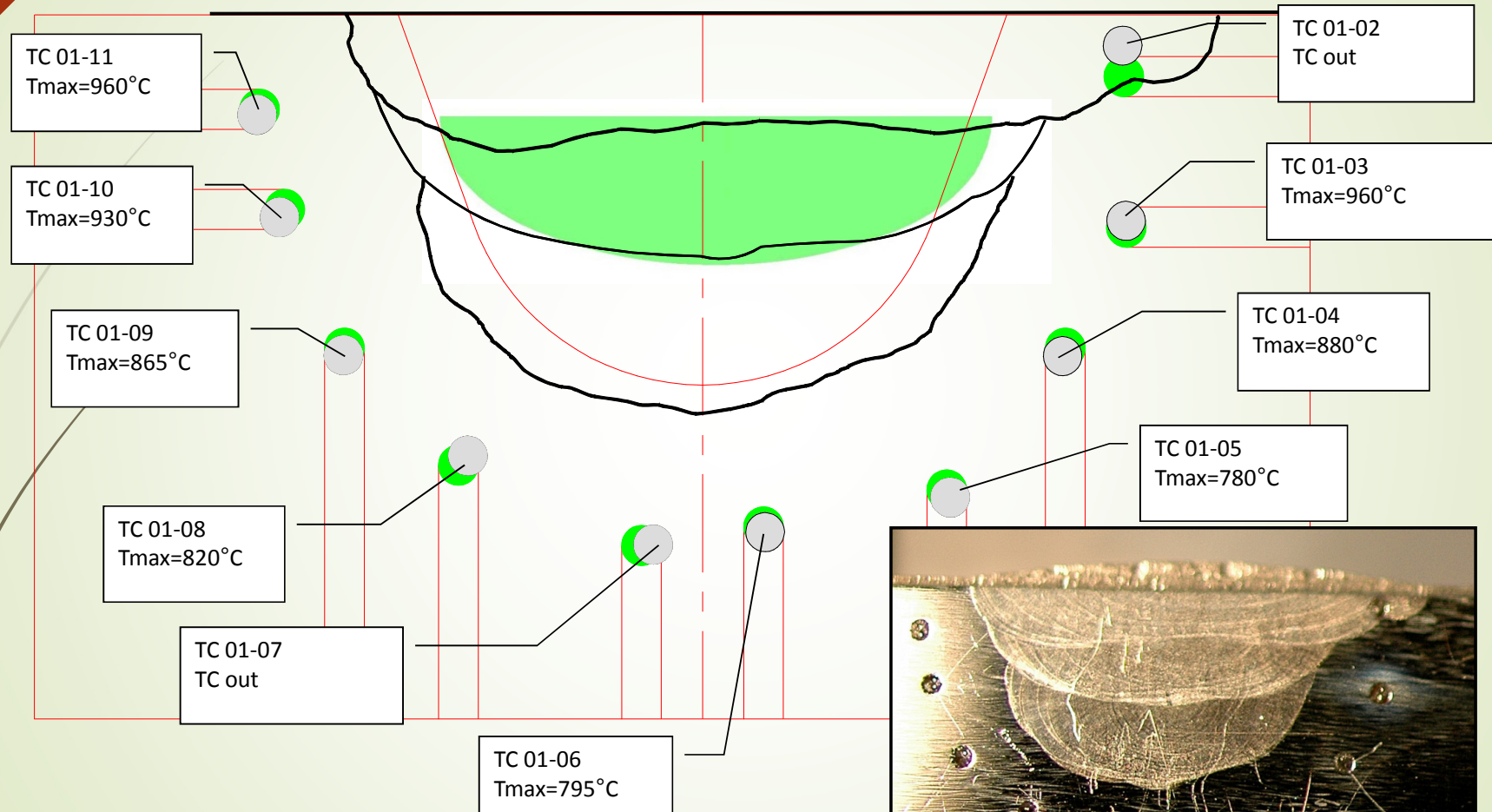
$$Q_r(x, y, z) = \frac{\eta 6 \sqrt{3}}{ab_r c \pi^{3/2}} f_r Q \cdot e^{-3\left(\frac{y}{a}\right)^2} e^{-3\left(\frac{x}{b_r}\right)^2} e^{-3\left(\frac{z}{c}\right)^2}$$

The standard deviation = 15°C

2nd Pass	
Parameter	Values
a (mm)	8.92
c (mm)	4.992
b_r (mm)	9.71
b_f (mm)	5.12
f_{fo}	1.0866
f_r	$2 \cdot f_{fo}$
η	1.42062
hcv (W/m ² .k)	103.58
H (mm)	14.681

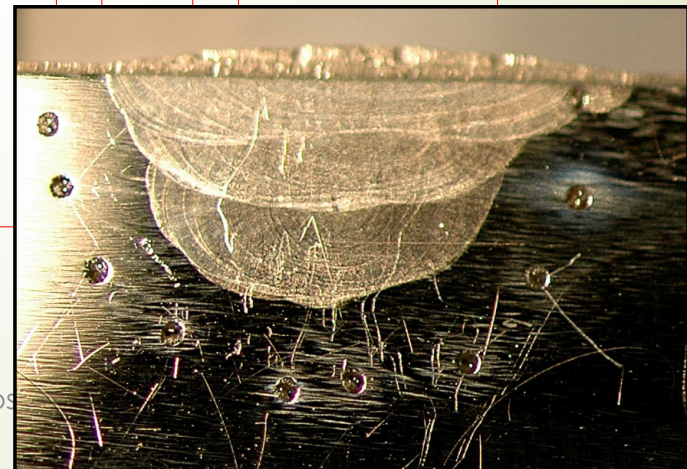
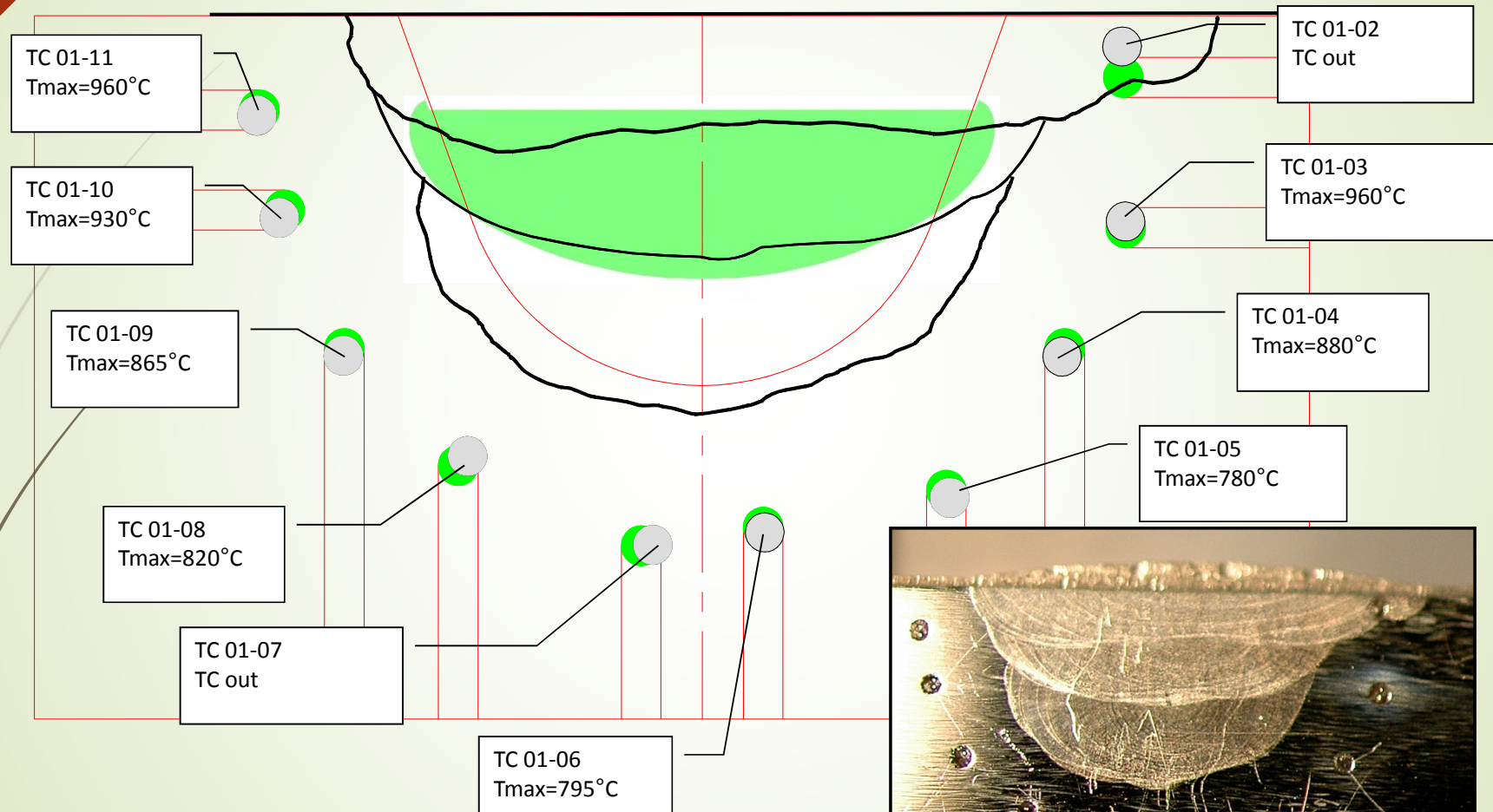
Interface 2- Pass2

warning
 $T_f=1450^{\circ}\text{C}$



Interface 2- Pass2

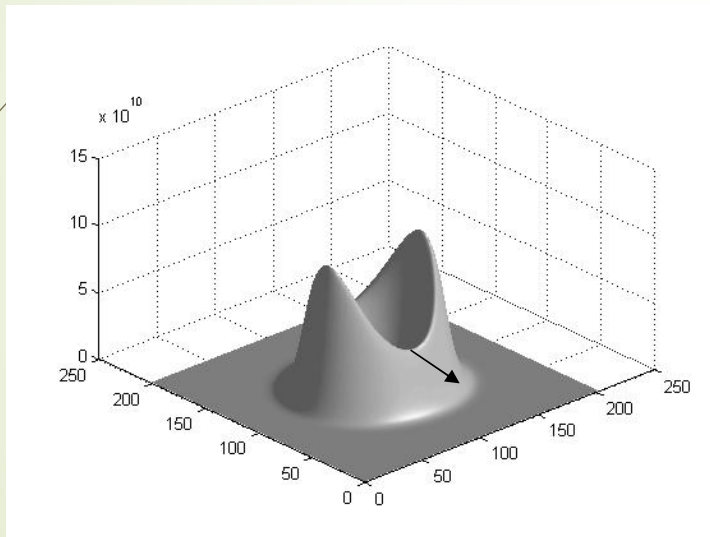
warning
 $T_f=1400^{\circ}\text{C}$



3th pass

- Annular heat source with gaussian source in the center:

$$Q = \left[\frac{\text{eta_A} * P}{\pi * R^2 * e} * e^{\left[\frac{rt^2}{ra^2}\right]} + \frac{\text{eta_B} * P}{\pi * R^2 * e} * e^{\left[\frac{(rt-b)^2}{rb^2}\right]} \right] * e^{\left[\frac{x^2}{rc^2}\right]} * (z > H)$$

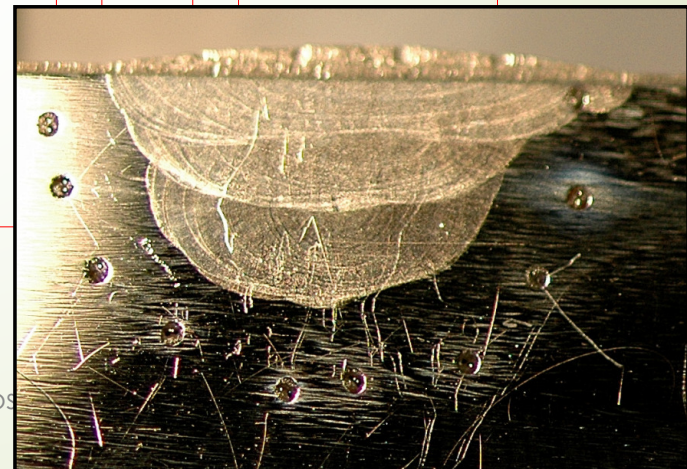
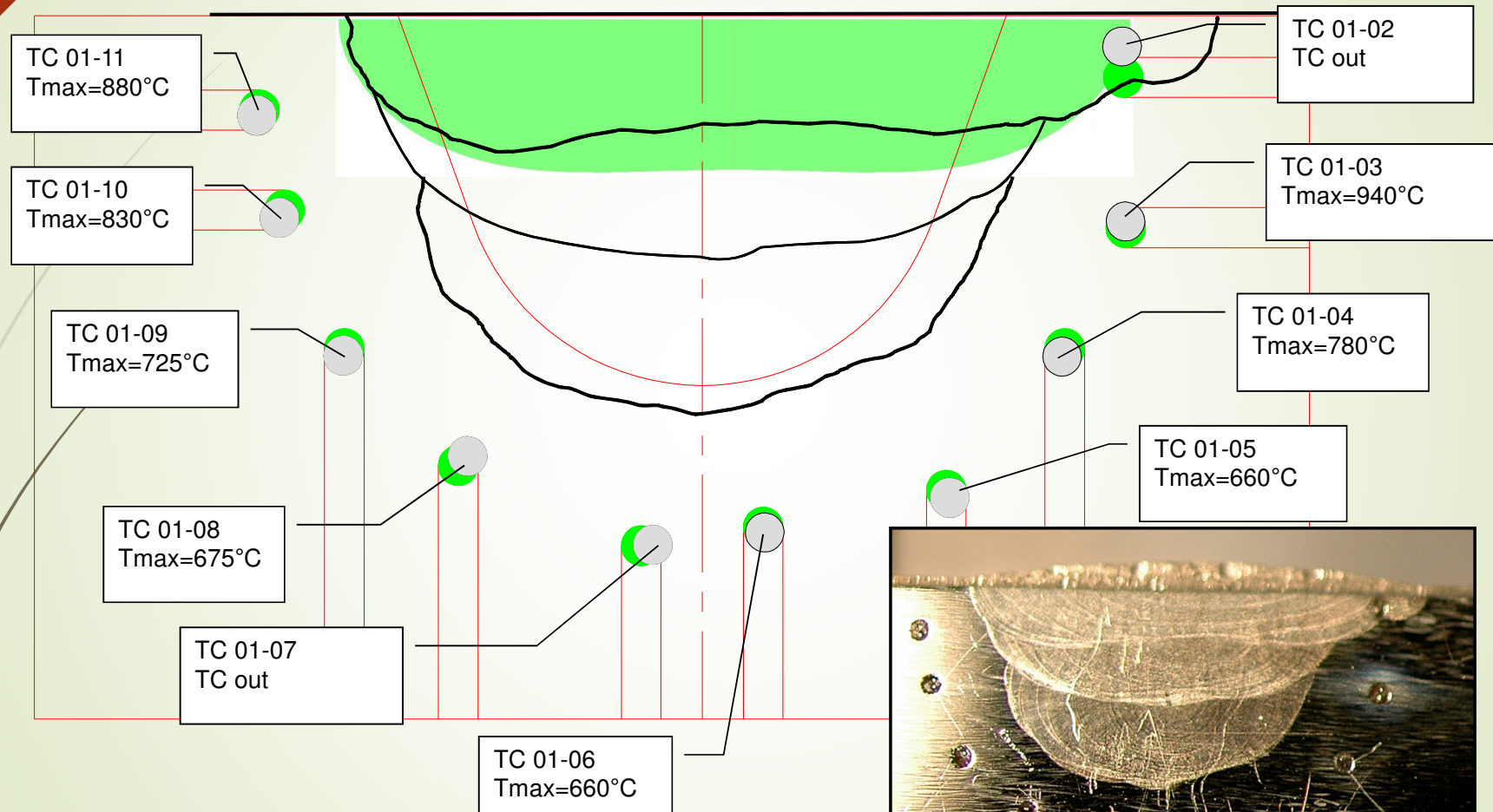


The standard deviation = 9.5°C

3th pass	
Parameter	Values
e (mm)	0.5
ra (mm)	1.2
rb (mm)	1.16
rc (mm)	4
b (mm)	3.95
eta_A	0
eta_B	0.75
R (mm)	2.149

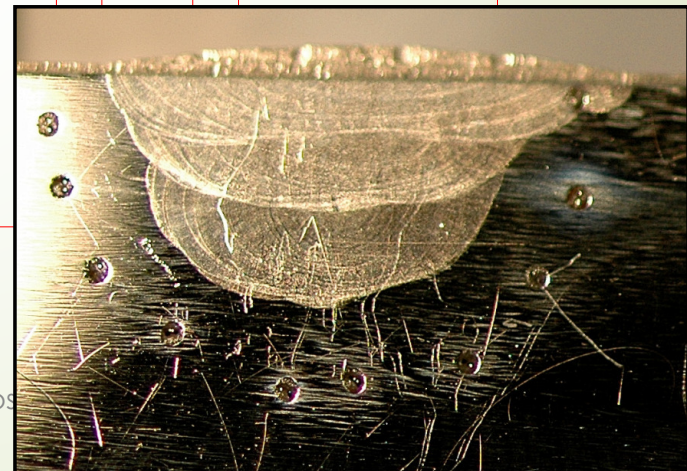
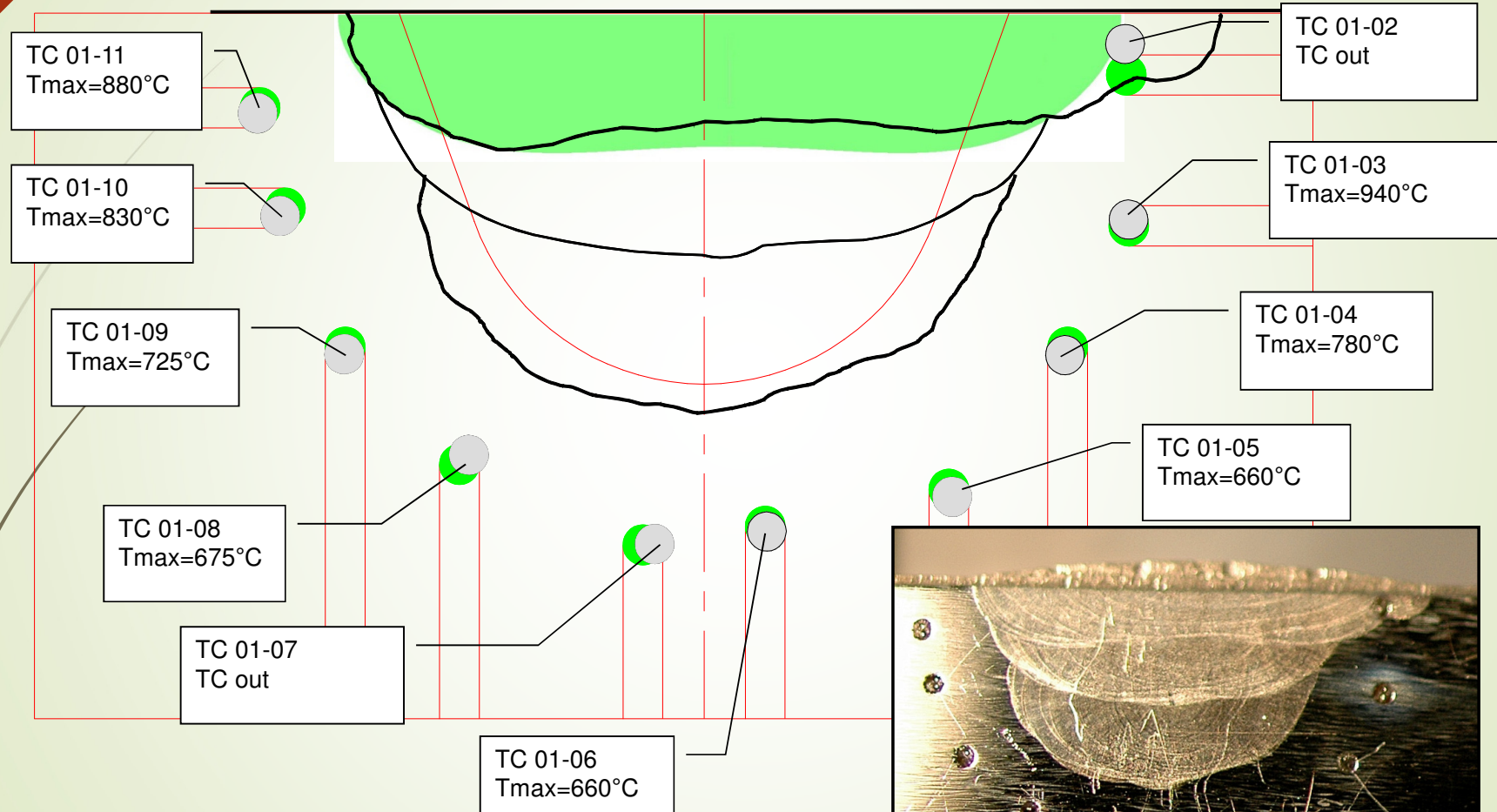
Interface 2- Pass3

warning
 $T_f=1450^{\circ}\text{C}$



Interface 2- Pass3

warning
 $T_f=1488^\circ\text{C}$





Conclusions

With the real positions of the thermocouples, the measured temperatures and the macrographs (fused zones), we can obtain the equivalent heat sources.

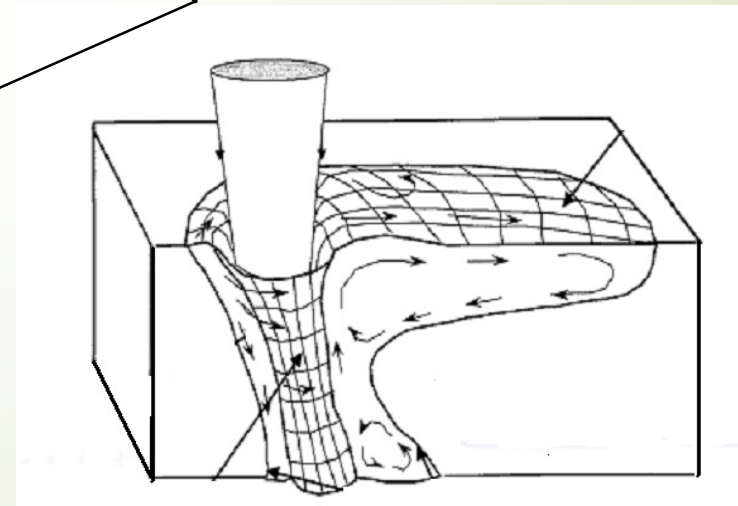
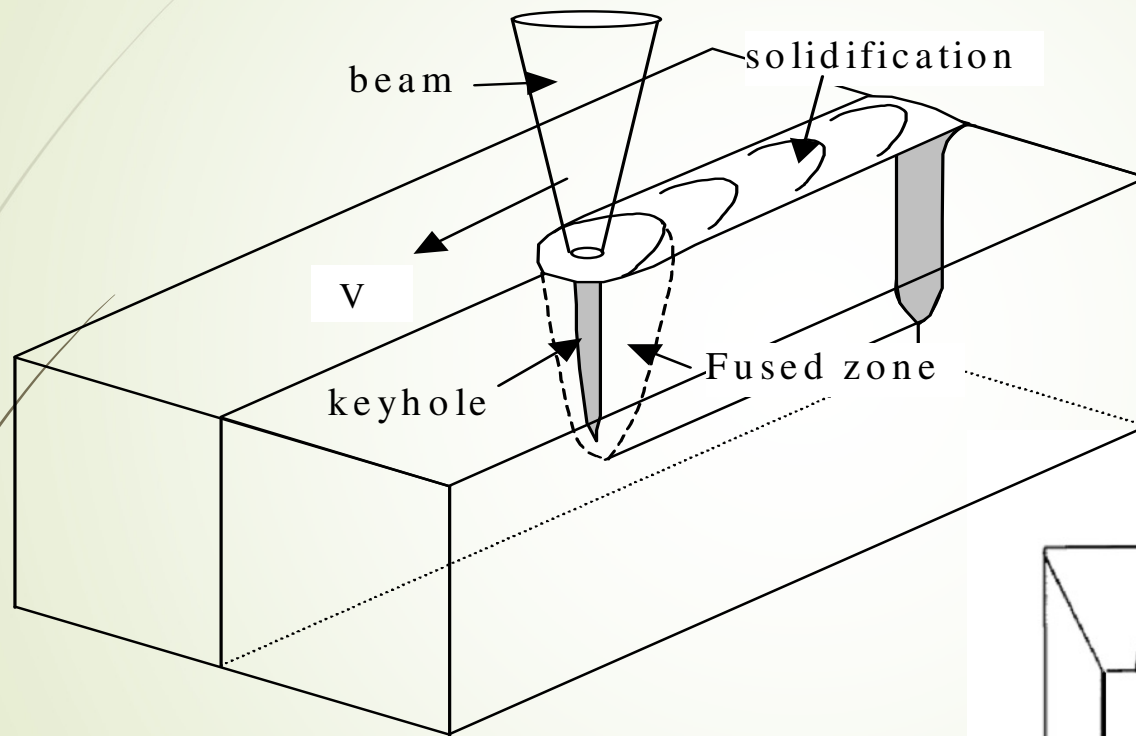
For the first and second pass, we obtain the shapes of the fused zones with the Goldak model (or a truncated model) and we have a good agreement between the measured and simulated temperatures. But for the third pass, where the fused zone is extended, it is more difficult to use this model. We use an annular model.

Now, with these equivalent heat sources, we can simulate the mechanical effects... One point stays on the definition of the heat source at the beginning and at the end of the weld.....

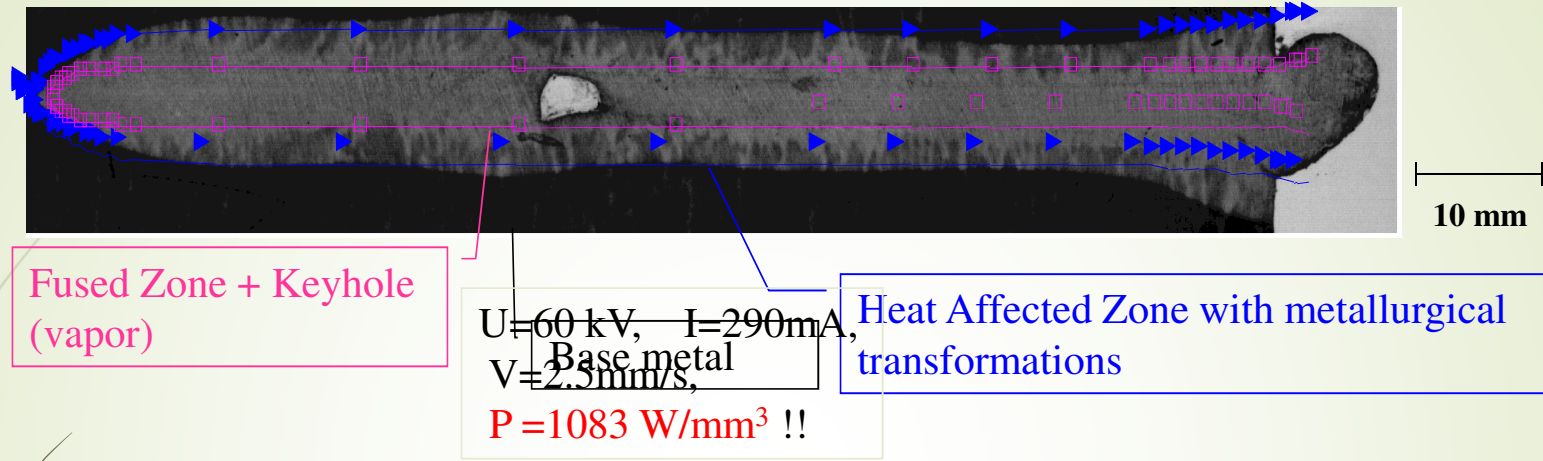
[flyer.pdf](#)

The electron beam welding : the principle

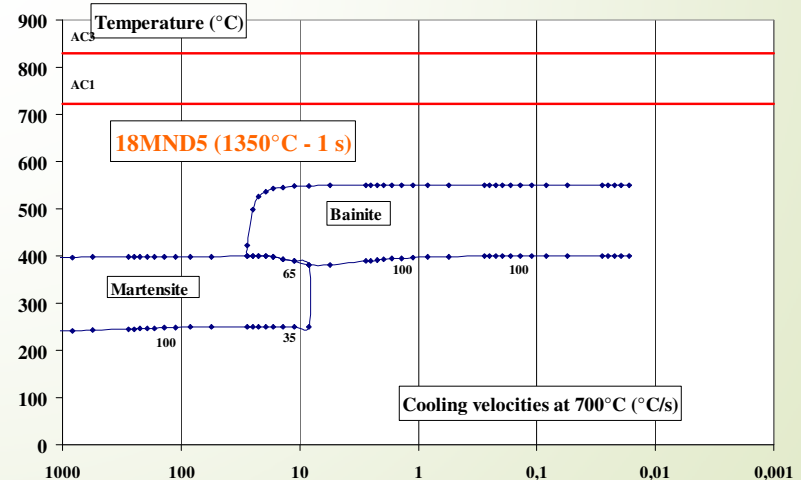
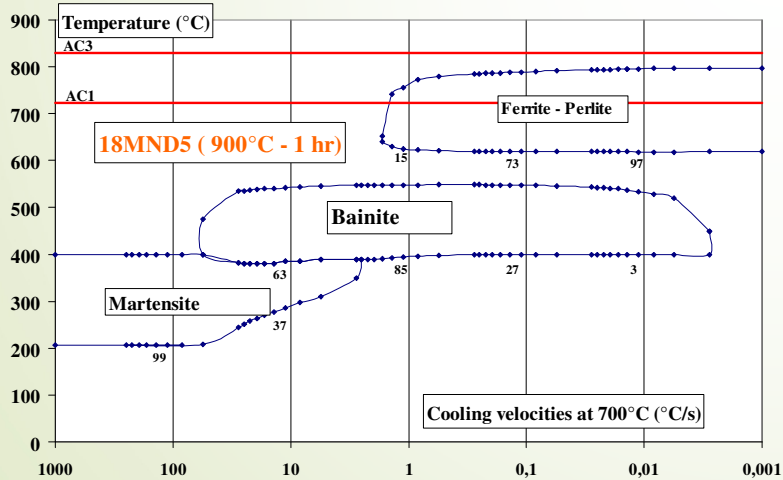
89



Numerical simulation of EB welding of 18MND5 steel



Microstructural simulation in HAZ

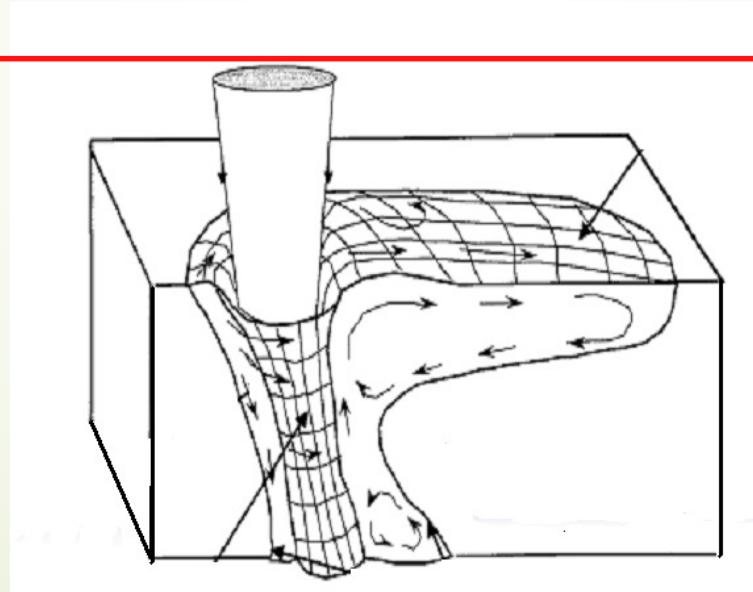


The electron beam welding : the simulation

91

In our problem :

1. *The keyhole is defined as a volumic source*
2. *A conductive model for the fused and vapor zones*
3. *metallurgical transformations in the heat affected zone*



The direct problems

92

$$\rho(T) C_p(T) \frac{\partial T}{\partial t} = \frac{\partial}{\partial x} \left(\lambda(T) \frac{\partial T}{\partial x} \right) + \frac{\partial}{\partial y} \left(\lambda(T) \frac{\partial T}{\partial y} \right) + \frac{\partial}{\partial z} \left(\lambda(T) \frac{\partial T}{\partial z} \right) + \frac{\partial P_\alpha}{\partial t} (x, y, z, t) L(T) - \rho \frac{\partial H}{\partial t} + S(x, y, z, t)$$

avec

$$C_p(T) = \sum_{\text{phases}} R_i C_{p_i}(T)$$

$$\lambda(T) = \sum_{\text{phases}} R_i \lambda_i(T)$$

$$\rho(T) = \sum_{\text{phases}} R_i \rho_i(T)$$

$$L(T) = (\rho_\gamma H_\gamma - \rho_\alpha H_\alpha)$$

Leblond-Devaux

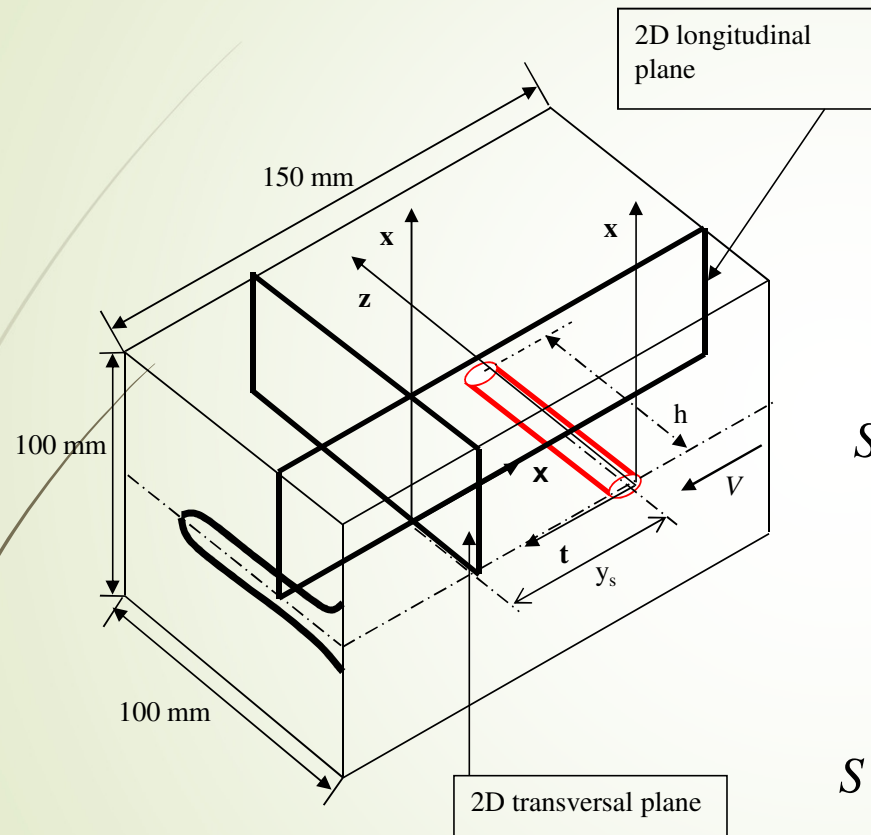
$$\frac{dP}{dt} = \frac{P_{eq}(T) - P}{\tau(T)} f\left(\frac{dT}{dt}\right)$$

Koistinen-Marburger

$$P = P_{max} \left\{ 1 - \exp[-b(T - M_s)] \right\} \quad \text{pour } T < M_s$$

$$\begin{aligned} DH &= 2.59 \cdot 10^5 \text{ J/Kg} & 1450 \text{ }^\circ\text{C} < T < 1550 \text{ }^\circ\text{C} \\ DH &= 6.59 \cdot 10^6 \text{ J/Kg} & 2600 \text{ }^\circ\text{C} < T < 2700 \text{ }^\circ\text{C} \end{aligned}$$

The direct problems



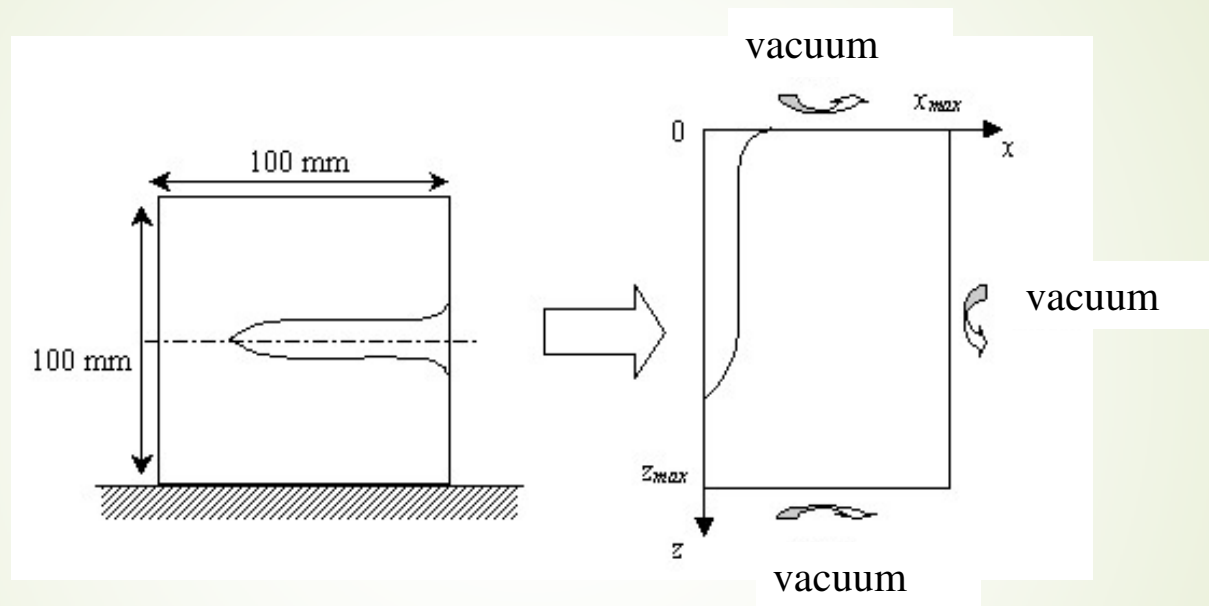
$$\eta = 0,9, U = 60 \text{ kV}, I_b = 0,29 \text{ A}, \\ V = 2,5 \text{ mm/s}, h = 0,071 \text{ m}, \\ w_0 = 0,15 \text{ mm} (\Phi_0 = 0,6 \text{ mm}), \\ z_e = 0,041 \text{ m}.$$

$$S(x, z, t) = \frac{\eta U I_b}{2\pi\omega_0^2 h} \exp\left(-\frac{x^2 + (Vt - y_s)^2}{2\omega_0^2}\right)$$

$$\xi = Vt$$

$$S(x, \xi) = \frac{\eta U I_b}{2\pi\omega_0^2} \exp\left(-\frac{x^2 + (\xi - y_s)^2}{2\omega_0^2}\right)$$

The direct problem: the transversal plane



$$\rho(T) C_p(T) \frac{\partial T}{\partial t} = \frac{\partial}{\partial x} \left(\lambda(T) \frac{\partial T}{\partial x} \right) + \frac{\partial}{\partial z} \left(\lambda(T) \frac{\partial T}{\partial z} \right) + \frac{\partial P_\alpha}{\partial t} (x, z, t) L(T) - \rho \frac{\partial H}{\partial t} + S(x, z, t)$$

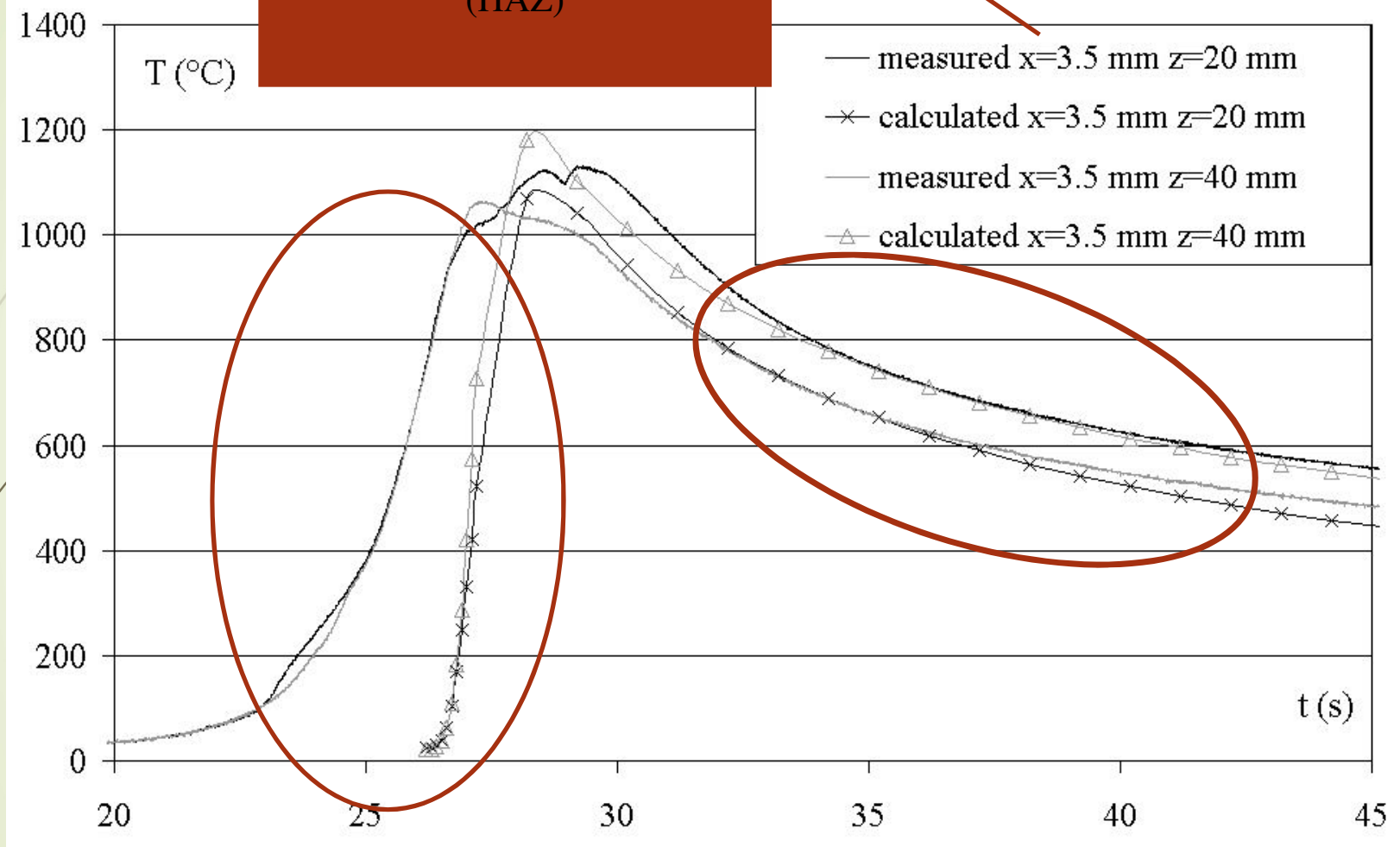
$$T(x, z) = T_0 = T_{inf} \quad P_\alpha(x, z, 0) = 1$$

The data

- ❑ The phase change enthalpy $L_{\alpha\gamma}(T) = \rho_\gamma H_\gamma - \rho_\alpha H_\alpha$ for the metallurgical transformations
- ❑ The phase change enthalpies « solid-liquid and liquid-vapor »
- ❑ The emissivity $\varepsilon=0.8$
- ❑ The initial and external temperatures $T_0=20^\circ\text{C}$
- ❑ The initial and finishing transformation temperatures of all phases (C.C.T. diagram of 18MND5 steel)
- ❑ The thermophysical characteristics $\lambda(T)$, $\rho(T)$ et $C(T)$ of the metallurgical phases.
- ❑ The source term:

$$S(x, z, t) = \frac{\eta U I b}{2\pi\omega_0^2} \exp\left(-\frac{x^2 + (Vt - y_s)^2}{2\omega_0^2}\right) \frac{2}{h} \left(1 - \frac{z}{h}\right)$$

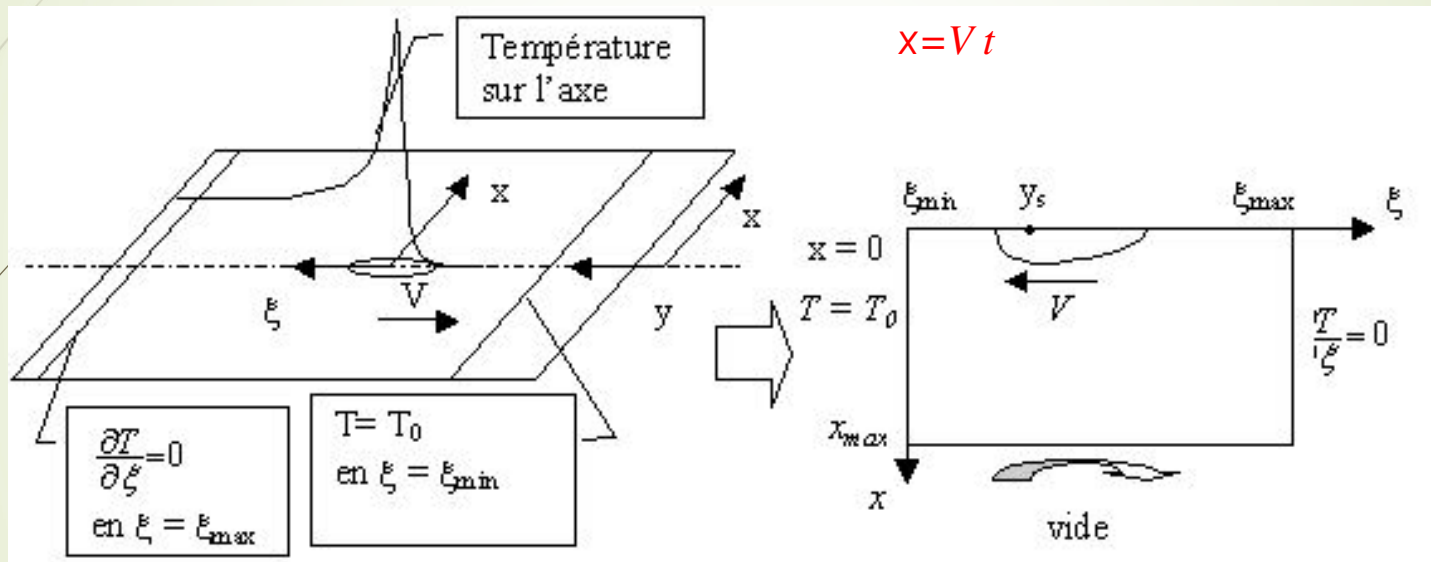
Measurements in the solid zone
(HAZ)



The direct problem: the longitudinal plane

97

The 2D quasi steady longitudinal problem

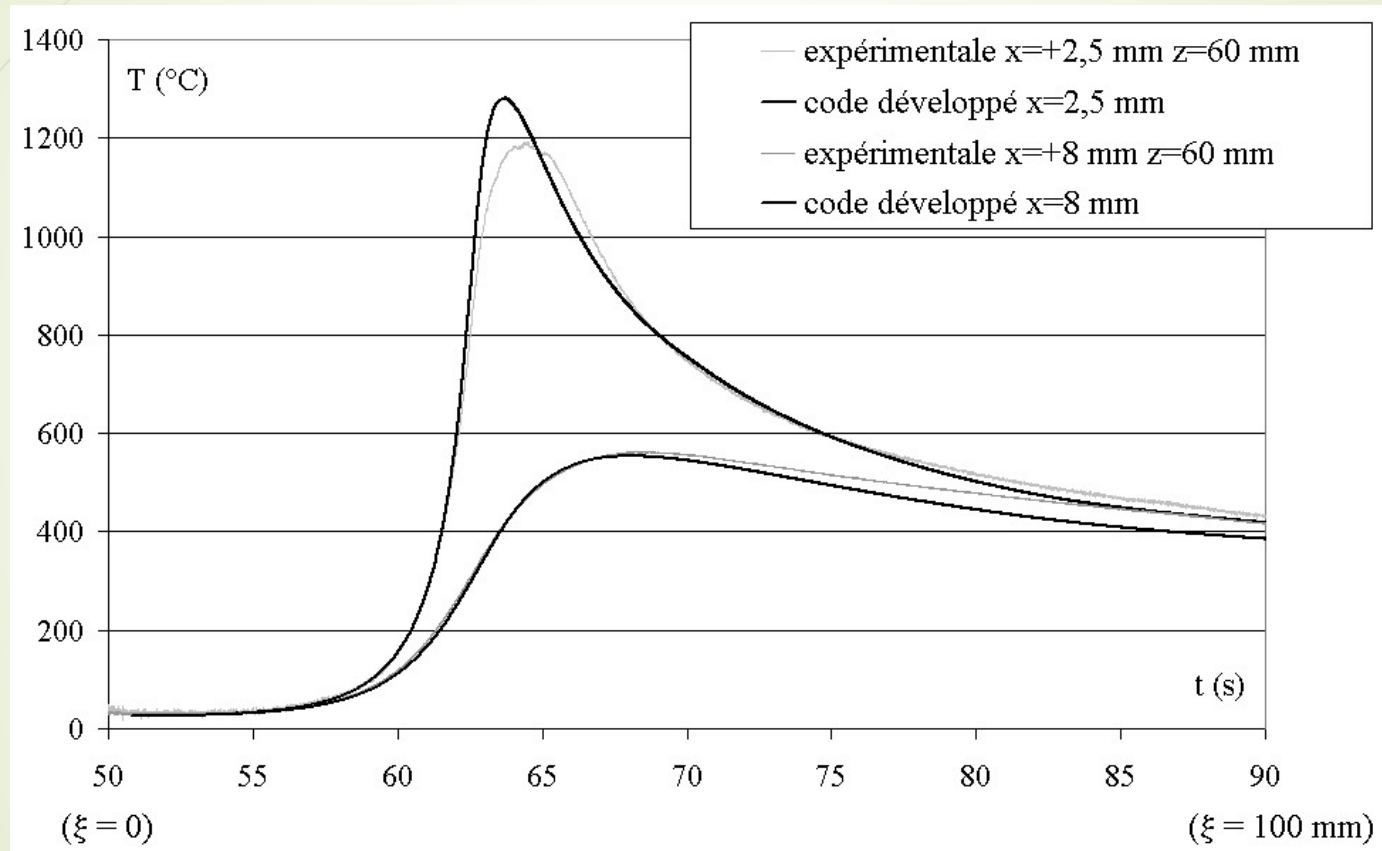


$$V\rho(T)C_p(T)\frac{\partial T}{\partial \xi} = \frac{\partial}{\partial x}\left(\lambda(T)\frac{\partial T}{\partial x}\right) + \frac{\partial}{\partial \xi}\left(\lambda(T)\frac{\partial T}{\partial \xi}\right) + V\frac{\partial P_\alpha}{\partial \xi}(x,\xi)L(T) - V\rho\frac{\partial H}{\partial \xi} + S(x,\xi)$$

$$T(x,\xi_{\min}) = T_0 = T_{inf} \quad P_\alpha(x,\xi_{\min}) = 1 \quad \text{en } x = 0$$

The direct problem: the longitudinal plane

98



The direct problems: conclusions

- ✓ The developed codes are validated with regard to commercial codes.
- ✓ Differences exist however between the experimental and calculated kinetics
- ✓ The estimation of a source term is thus interesting.

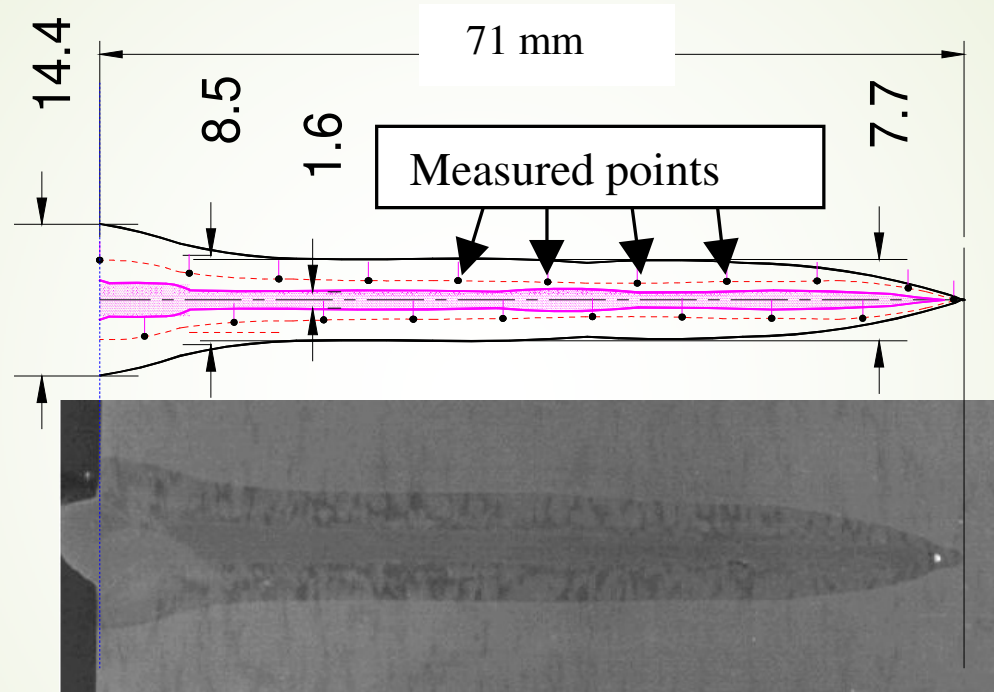
The inverse techniques

- ✓ Parameter estimation
- ✓ Function estimation

$$J(S) = \frac{1}{2} \sum_i [T(\bar{x}_i; S) - f_i]^2$$

1. The Levenberg Marquardt method
2. The iterative regularisation method

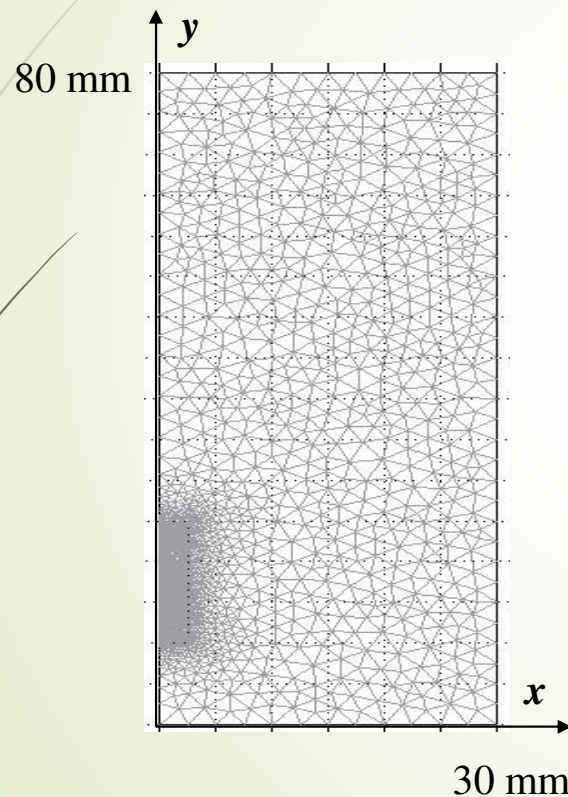
The sample



The Levenberg Marquardt method

102

The linear model in the 2D quasi steady longitudinal plane



$$S(x, y) = \frac{P_W}{W_{FE}^2} \exp \left[-\frac{x^2 + (y - y_s)^2}{W_{FE}^2} \right]$$

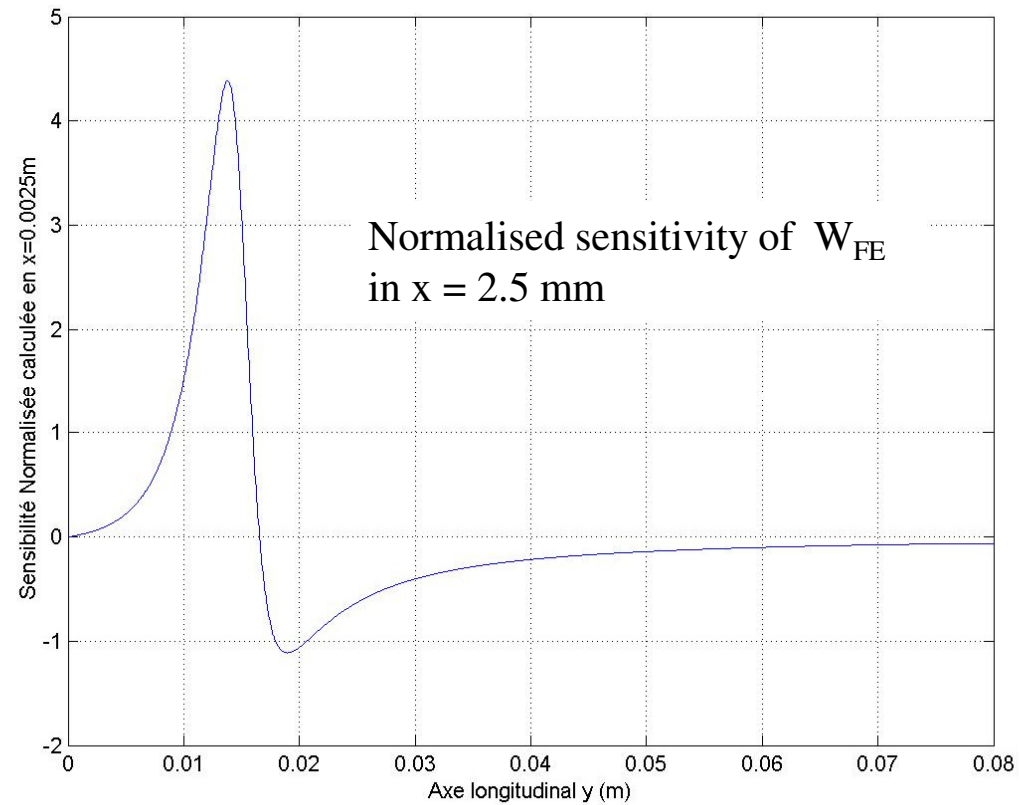
$$\bar{P} = \{P_W, W_{FE}, y_s\}$$

$$P_W = \frac{2}{h} \left(1 - \frac{z_e}{h} \right) \frac{\eta U I_b}{\pi} \quad W_{FE} = \sqrt{\frac{\Phi_0^2}{8}}$$

avec $P_W = 60000$ W/m, $y_s = 15$ mm, et $W_{FE} = 0,353$ mm ($F_0 = 1$ mm)

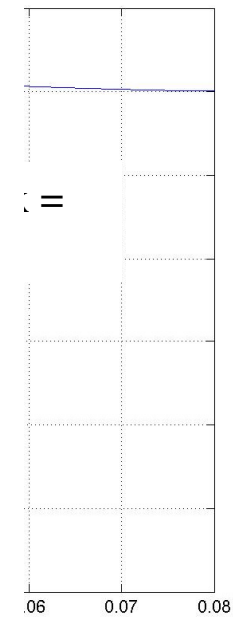
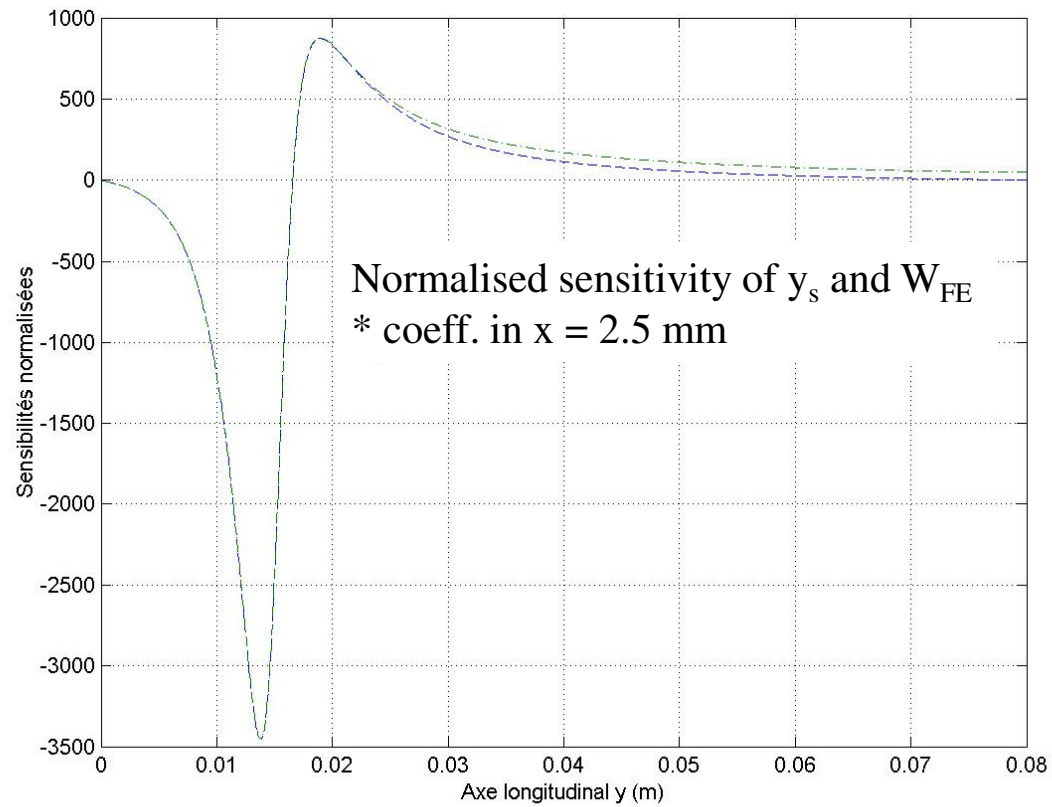
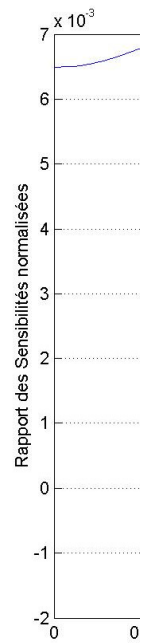
The Levenberg Marquardt method:

Sensitivity analysis



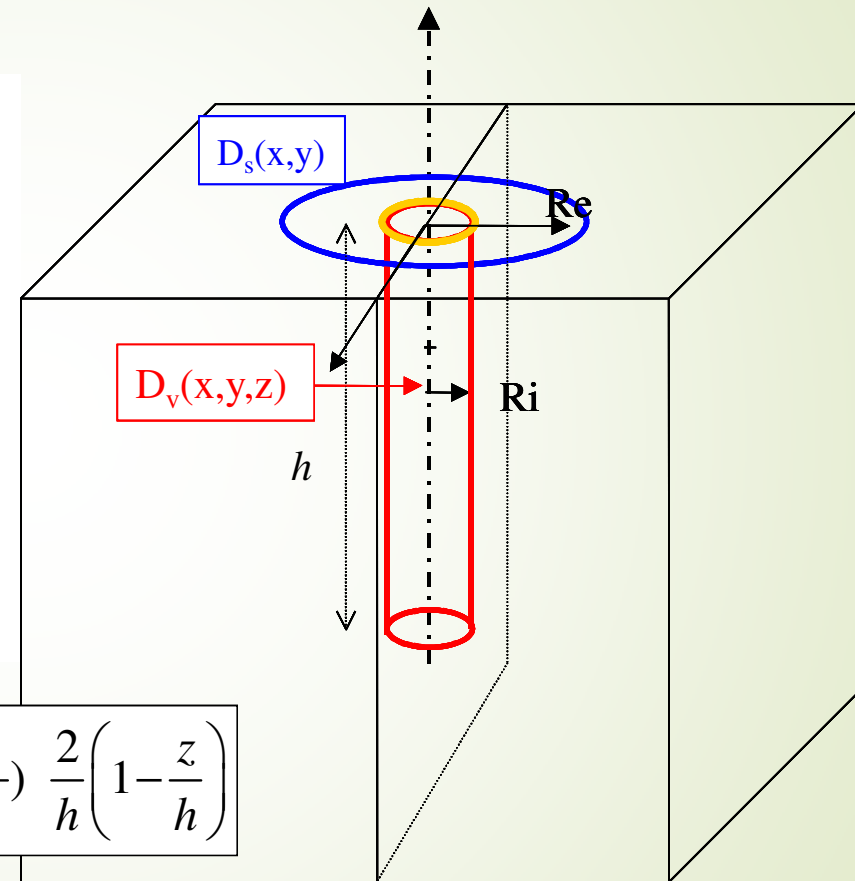
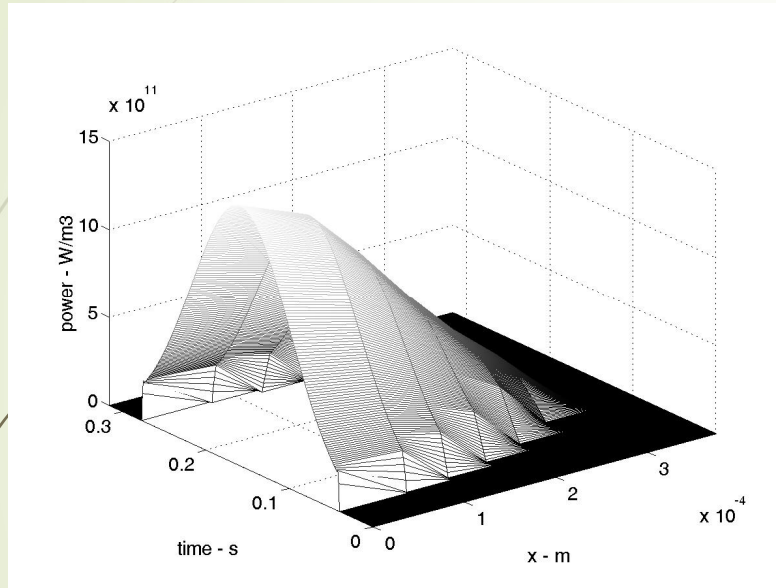
The Levenberg Marquardt method :

Sensitivity analysis



estimation with the iterative regularization method and with the conjugate gradient method

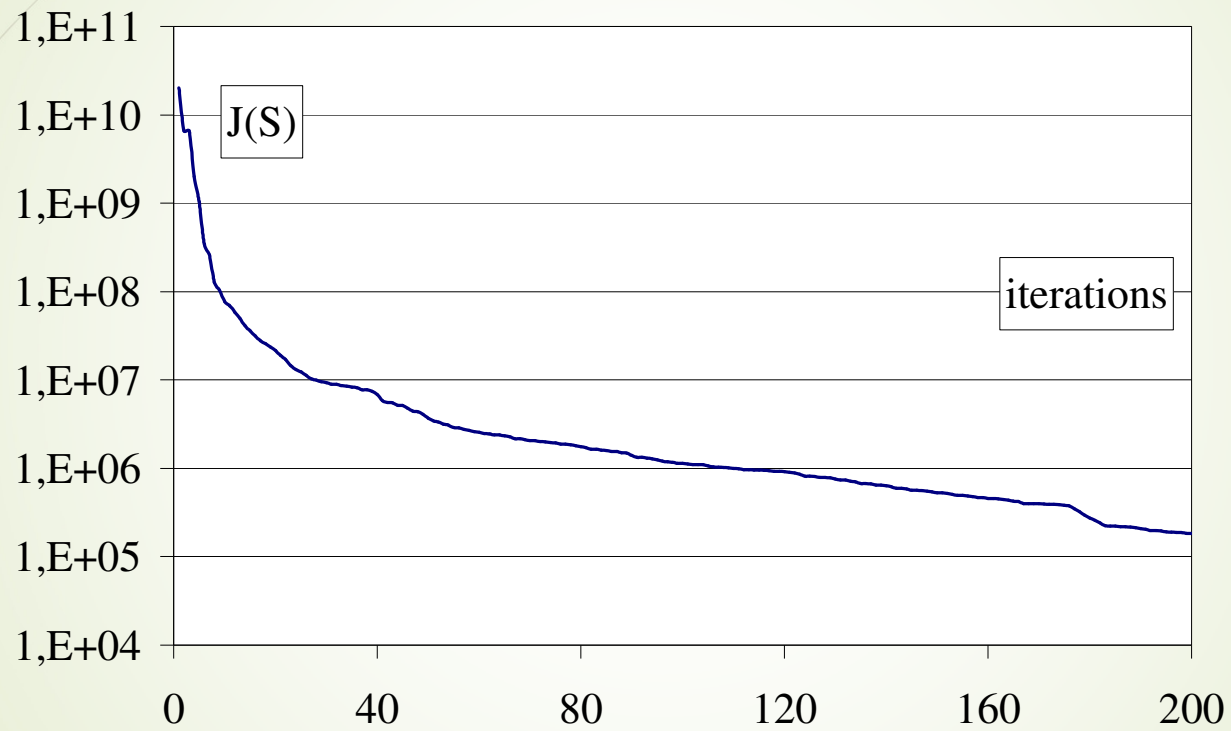
105



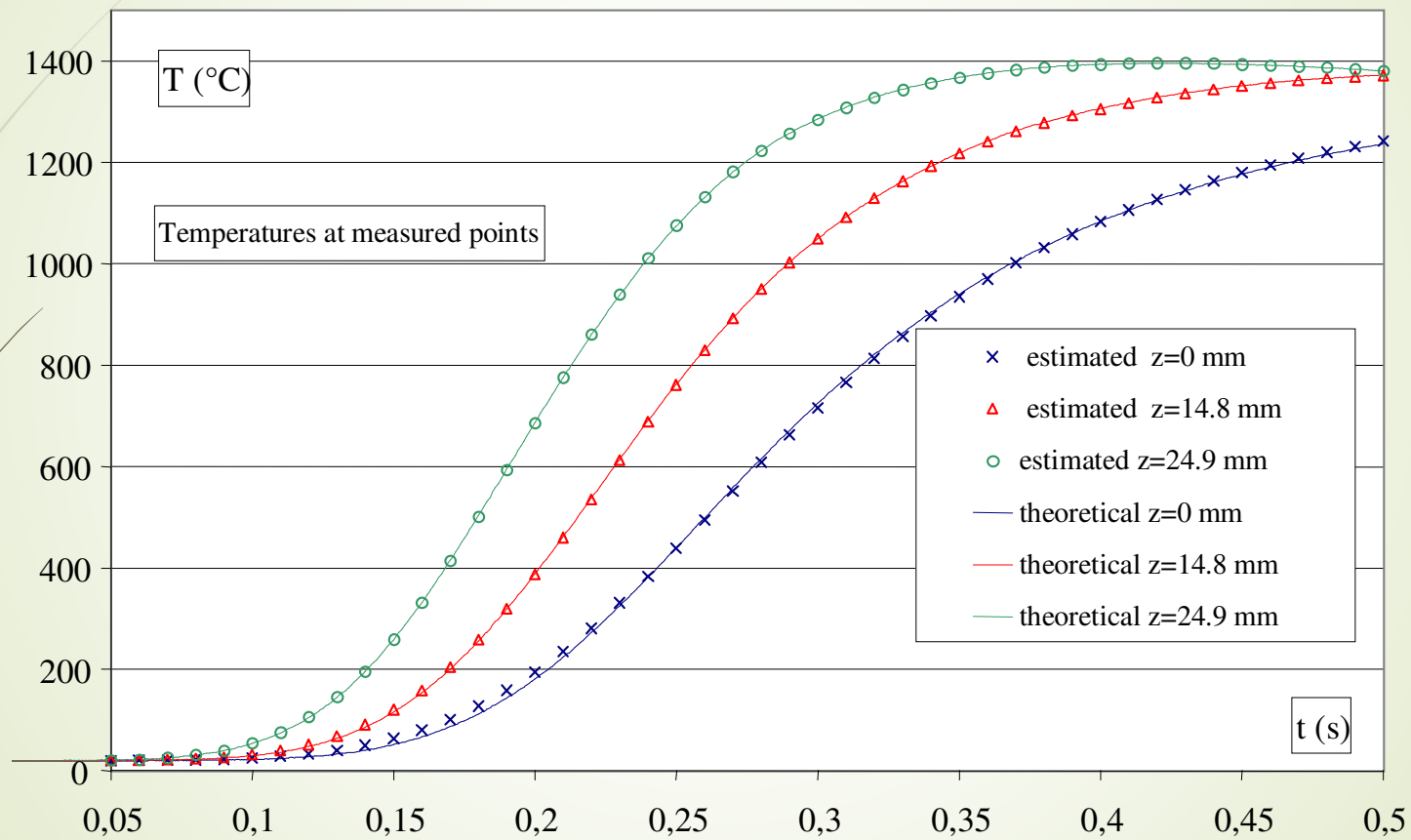
$$S(x, z, t) = \frac{\eta U I b}{2\pi\omega_0^2} \exp\left(-\frac{x^2 + (Vt - y_s)^2}{2\omega_0^2}\right) \frac{2}{h} \left(1 - \frac{z}{h}\right)$$

estimation with the iterative regularization method and with the conjugate gradient method

106

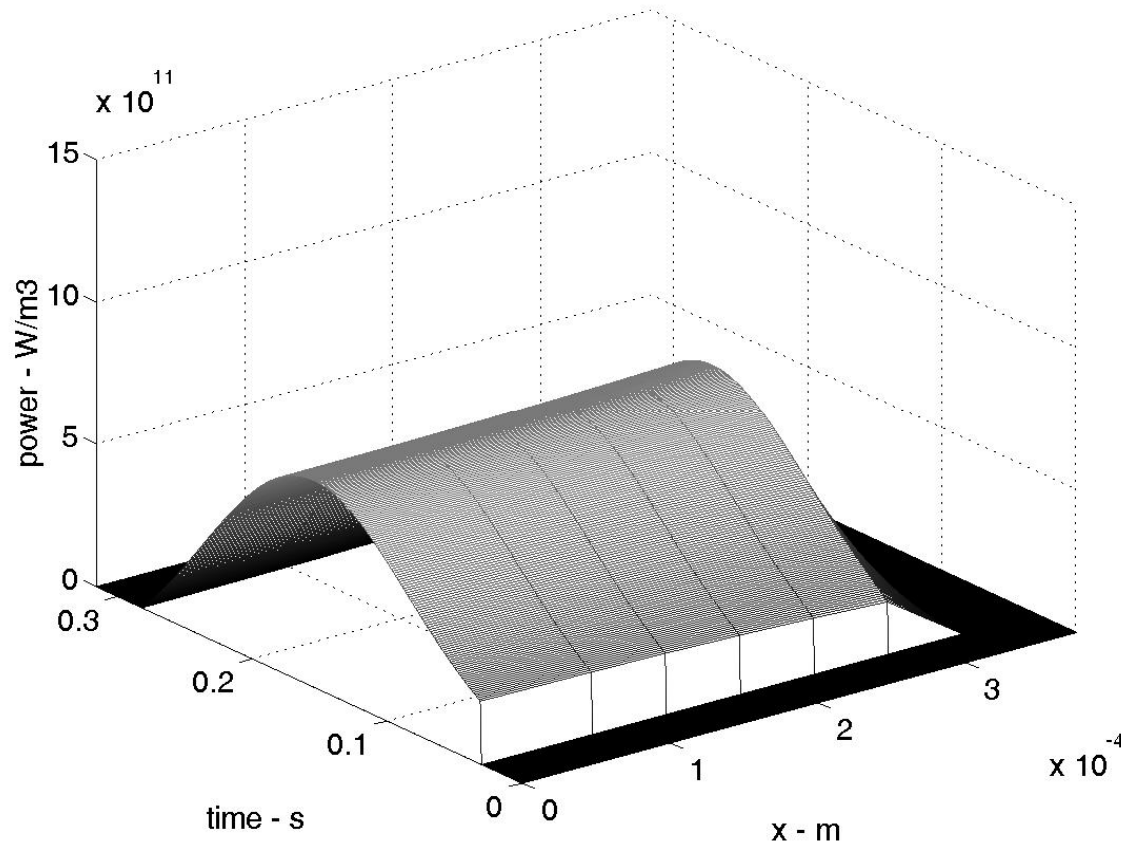


estimation with the iterative regularization method and with the conjugate gradient method



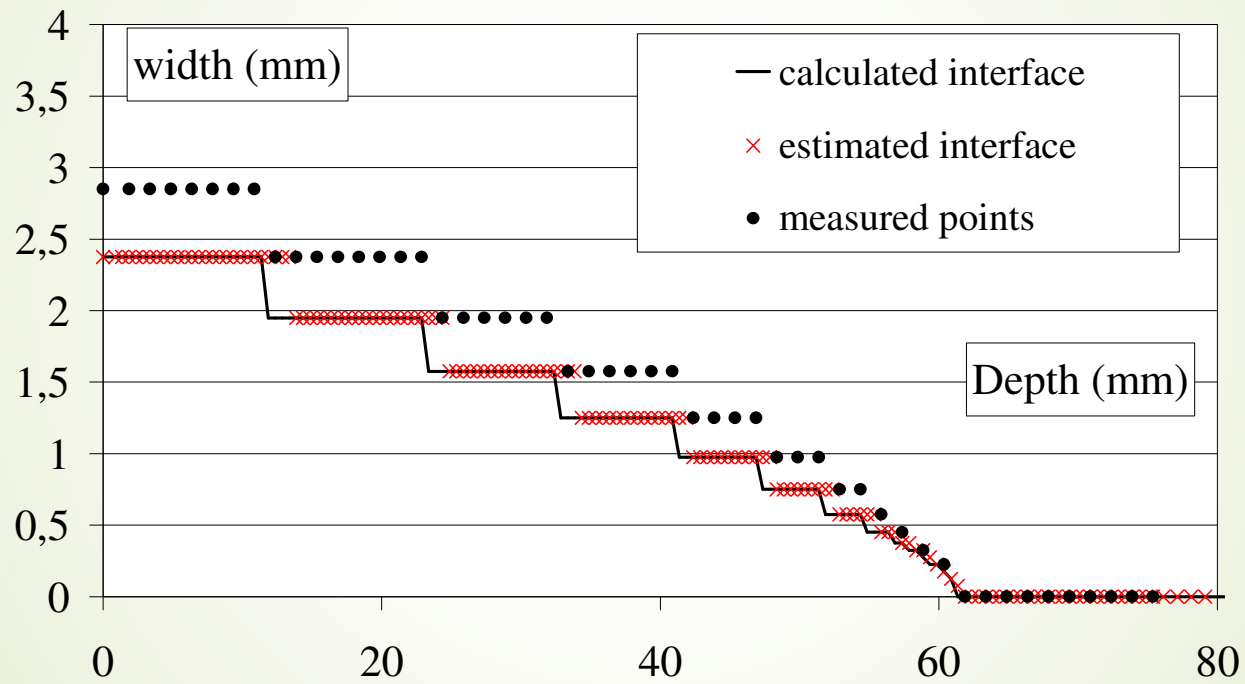
estimation with the iterative regularization method and with the conjugate gradient method

108



estimation with the iterative regularization method and with the conjugate gradient method

109



Conclusions for the theoretical estimation

110

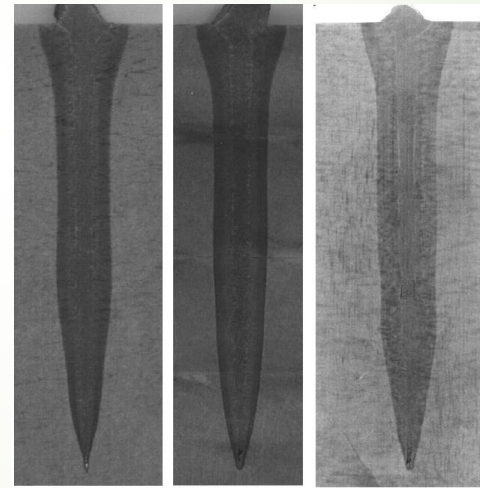
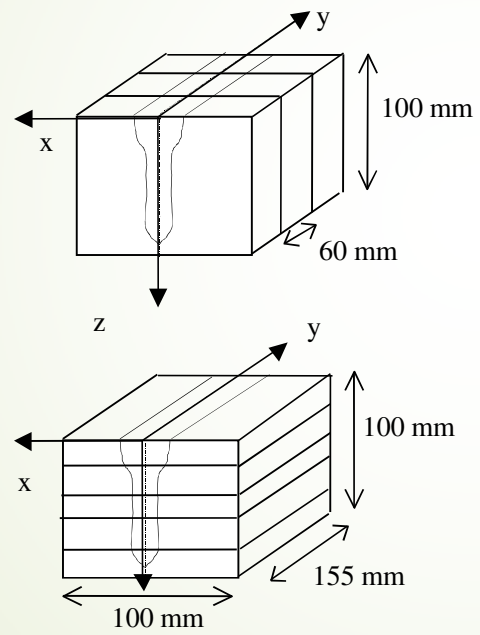
The distribution of the source according to the direction of advance of the beam and the direction of depth are well estimated in spite of a very small Fourier number.

The distribution according to the transverse direction cannot be estimated, but the sum of energy is well found.

The instrumentation

111

preliminary tests



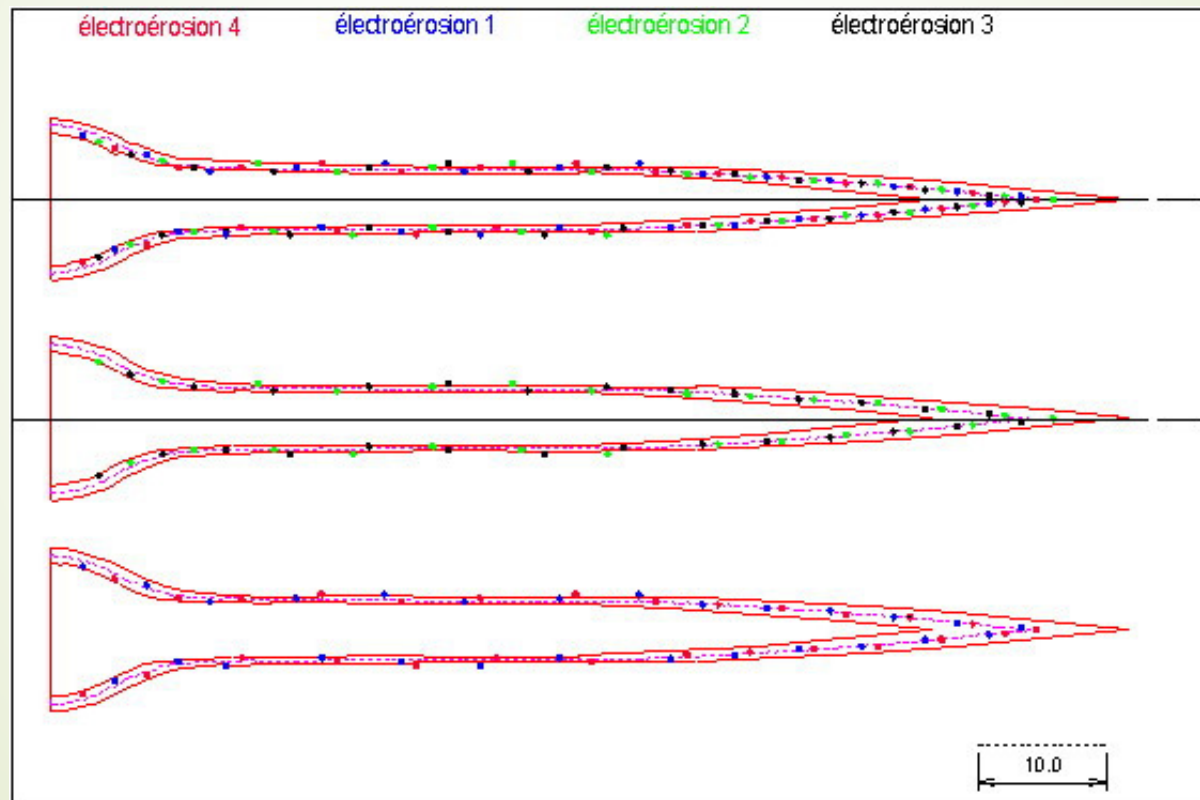
Informations with the preliminary tests

112

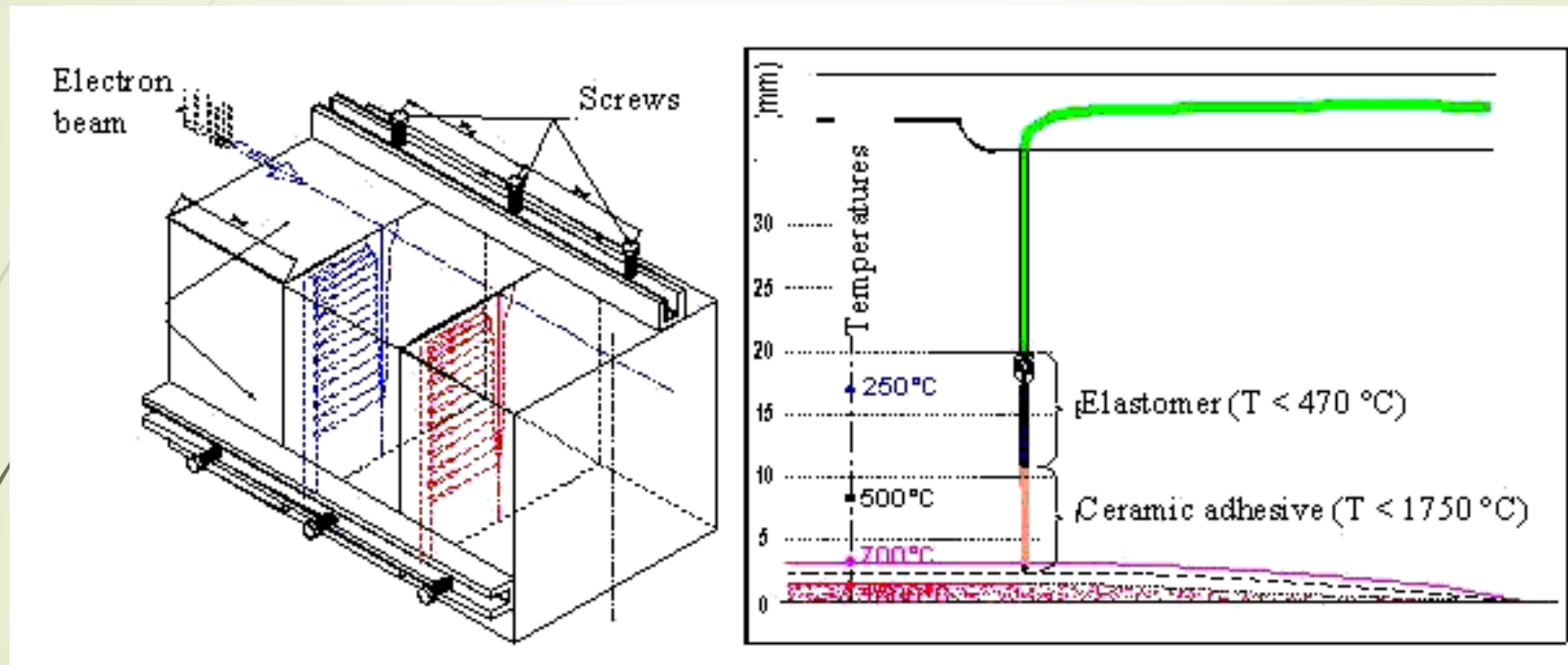
- a) We use thermocouples type K : diameter $50 \mu\text{m}$ with $T < 1267 \text{ }^\circ\text{C}$.
- b) The thermocouple installation is made starting from the shape of the reference welding on which we can raise the molten and heat affected zones, corresponding respectively to the isotherms $1500 \text{ }^\circ\text{C}$ and $723 \text{ }^\circ\text{C}$.
- c) We sought to position the thermocouples around this isotherm 1200°C ($\pm 0.3 \text{ mm}$).
- d) We chose to carry out two samples of 3 blocks having 2 interfaces equipped with thermocouples. Let us note that the interfaces red (23 thermocouples) and blue (24 thermocouples) are on the sample 1 and the interfaces black (23 thermocouples) and green (23 thermocouples) on the sample 2. We have 93 thermocouples in the heat affected zone.

The experiment

113

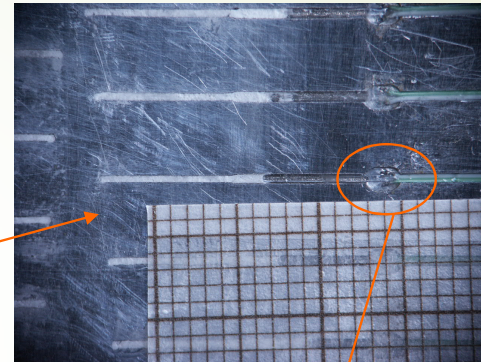
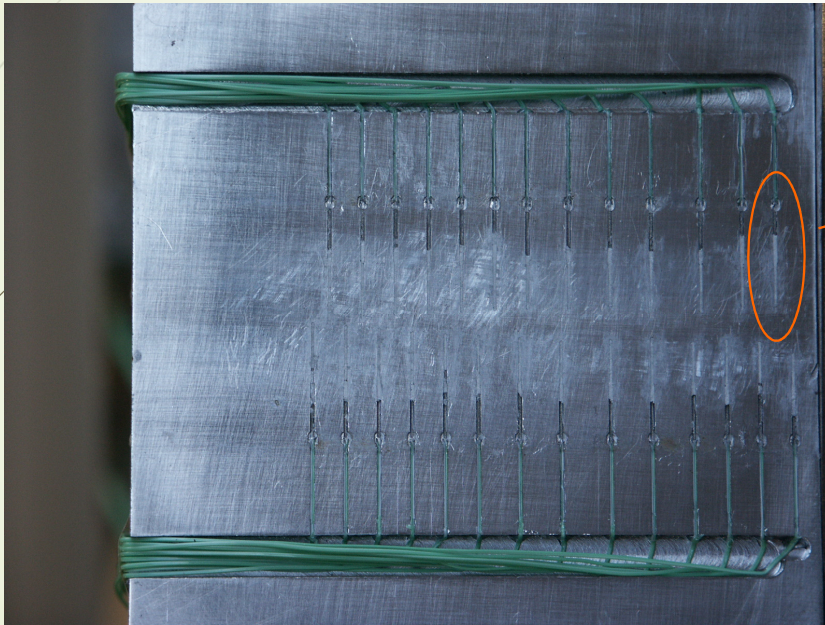


The experiment



The experiment

115



Welding of the samples

116

Welding was carried out on the site of the establishment of Indret of the Management of the Shipbuildings (D.C.N. Propulsion)

The maximum power of the electron beam is 100 KW for a vacuum chamber of 800 m³

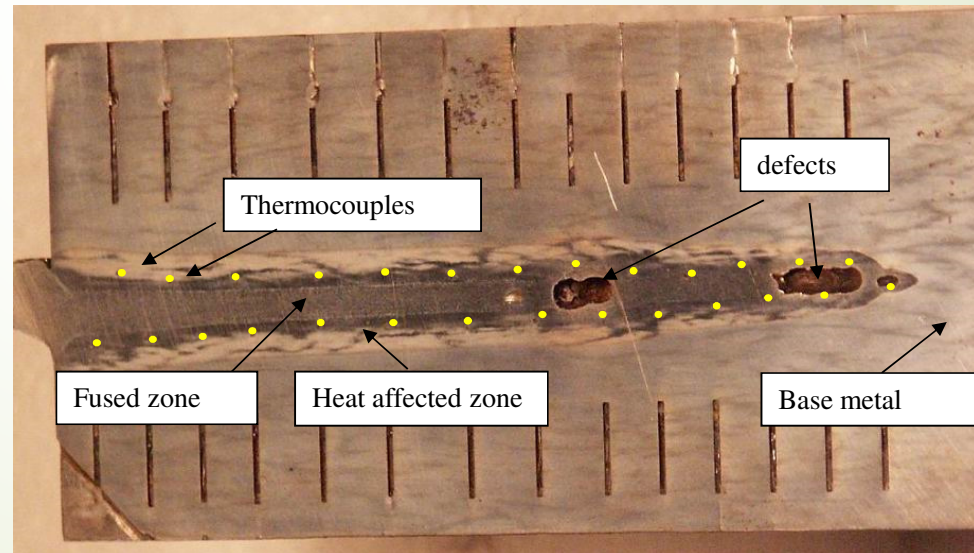
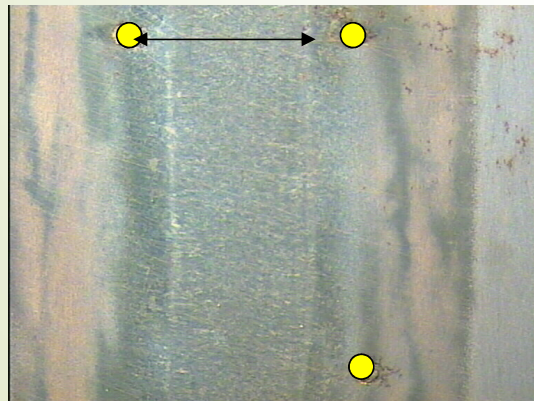
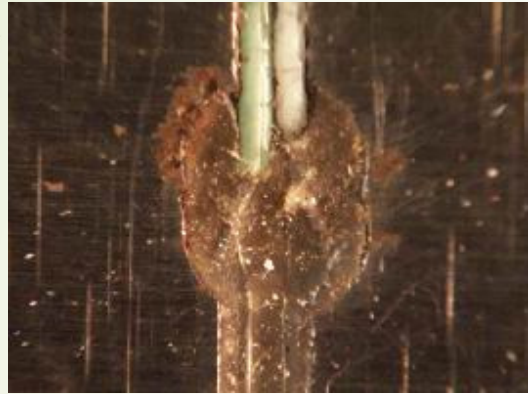
$U = 60 \text{ kV}$, $I_b = 0,29 \text{ A}$, $I_f = 2.46 \text{ A}$, $V = 2,5 \text{ mm/ s}$

After welding, 80% of the thermocouples gave exploitable information.

A checking of the technological choices was carried out by recutting the samples and by precisely determining the position of the thermocouples compared to the beam axis

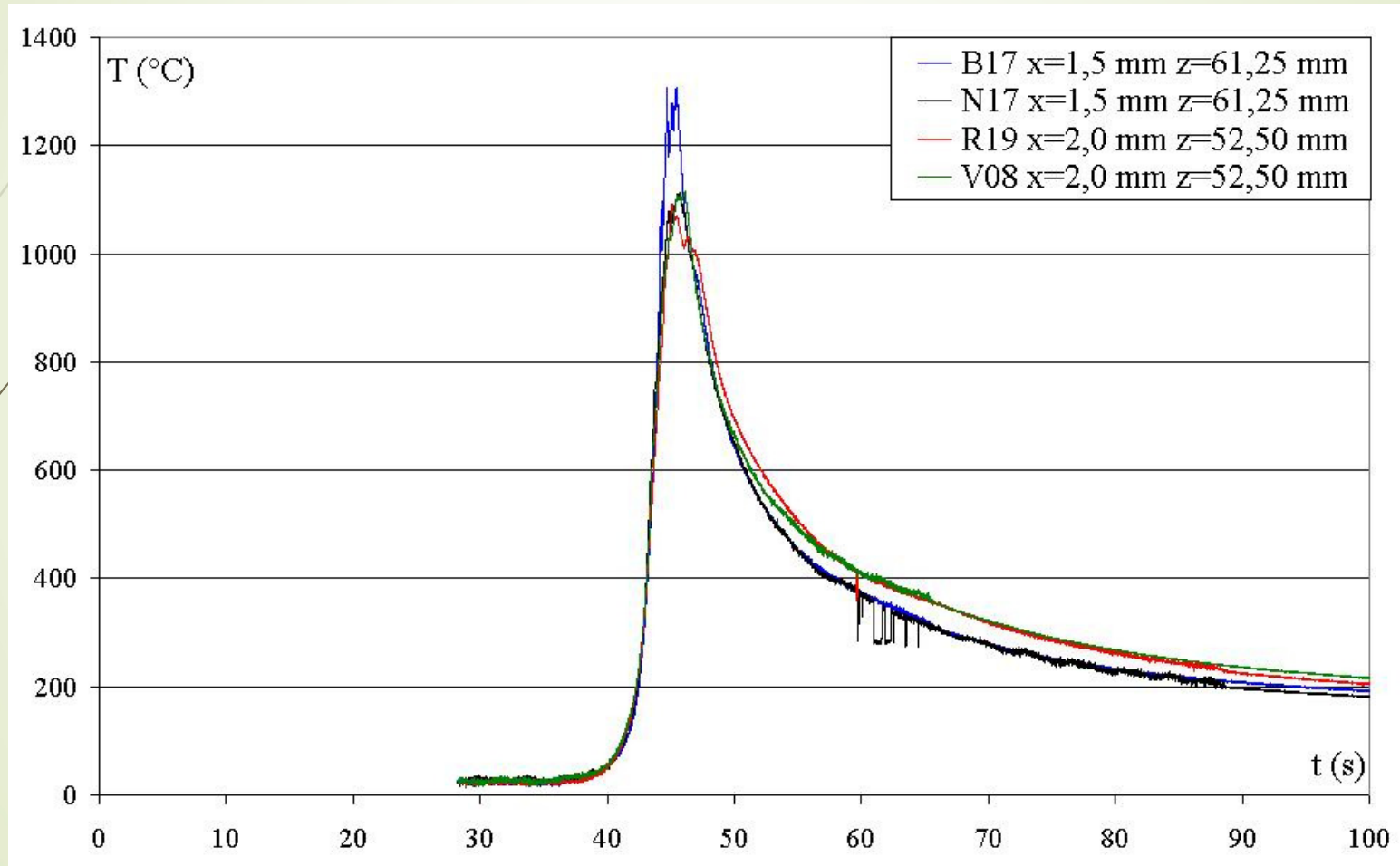
results

117

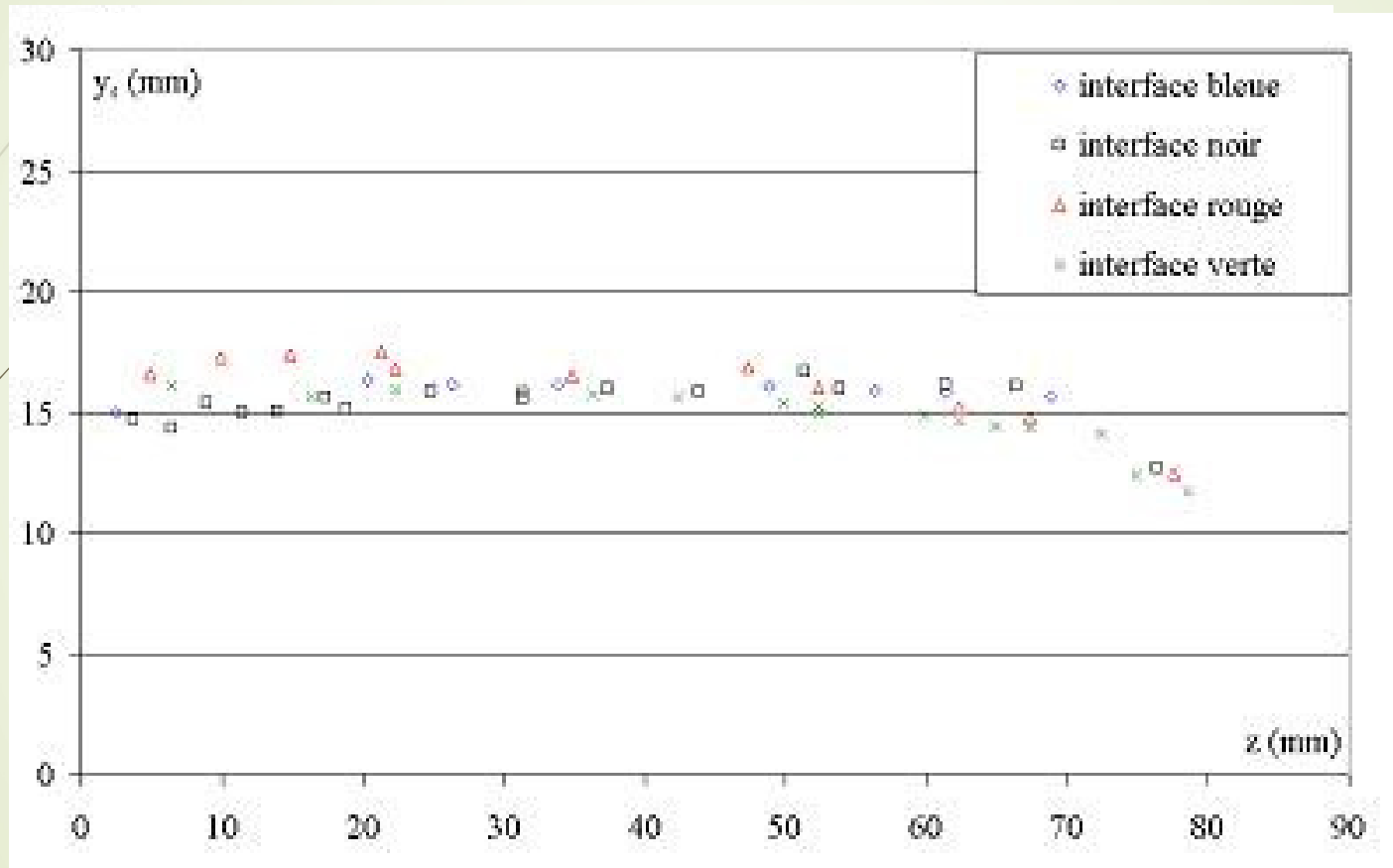


temporal synchronization of the 4 interfaces

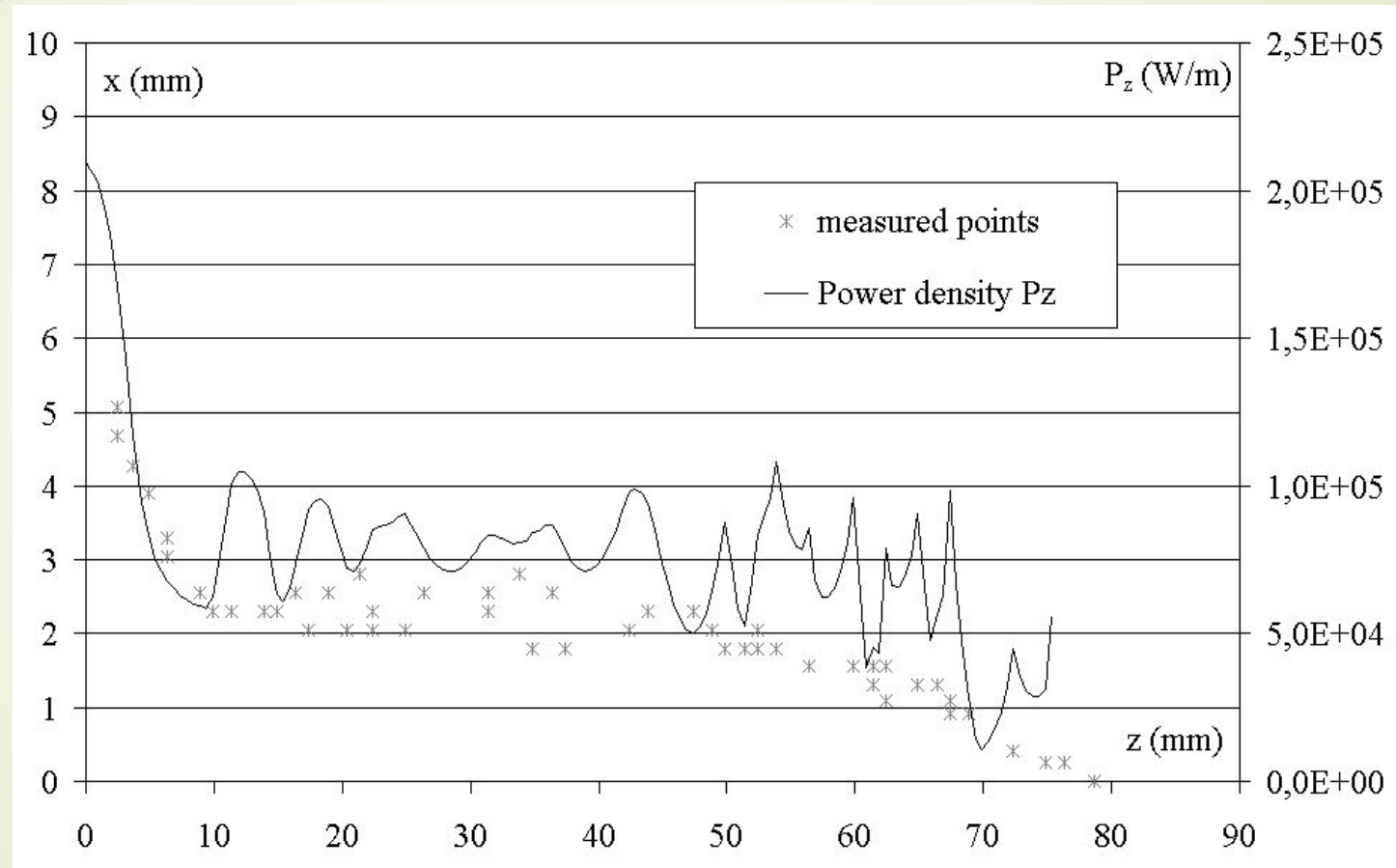
118



Results for 52 thermocouples taken out of the 4 interfaces
Levenberg Marquardt Method for $W_{FE}=0.000353$ ($\Phi=1\text{mm}$).

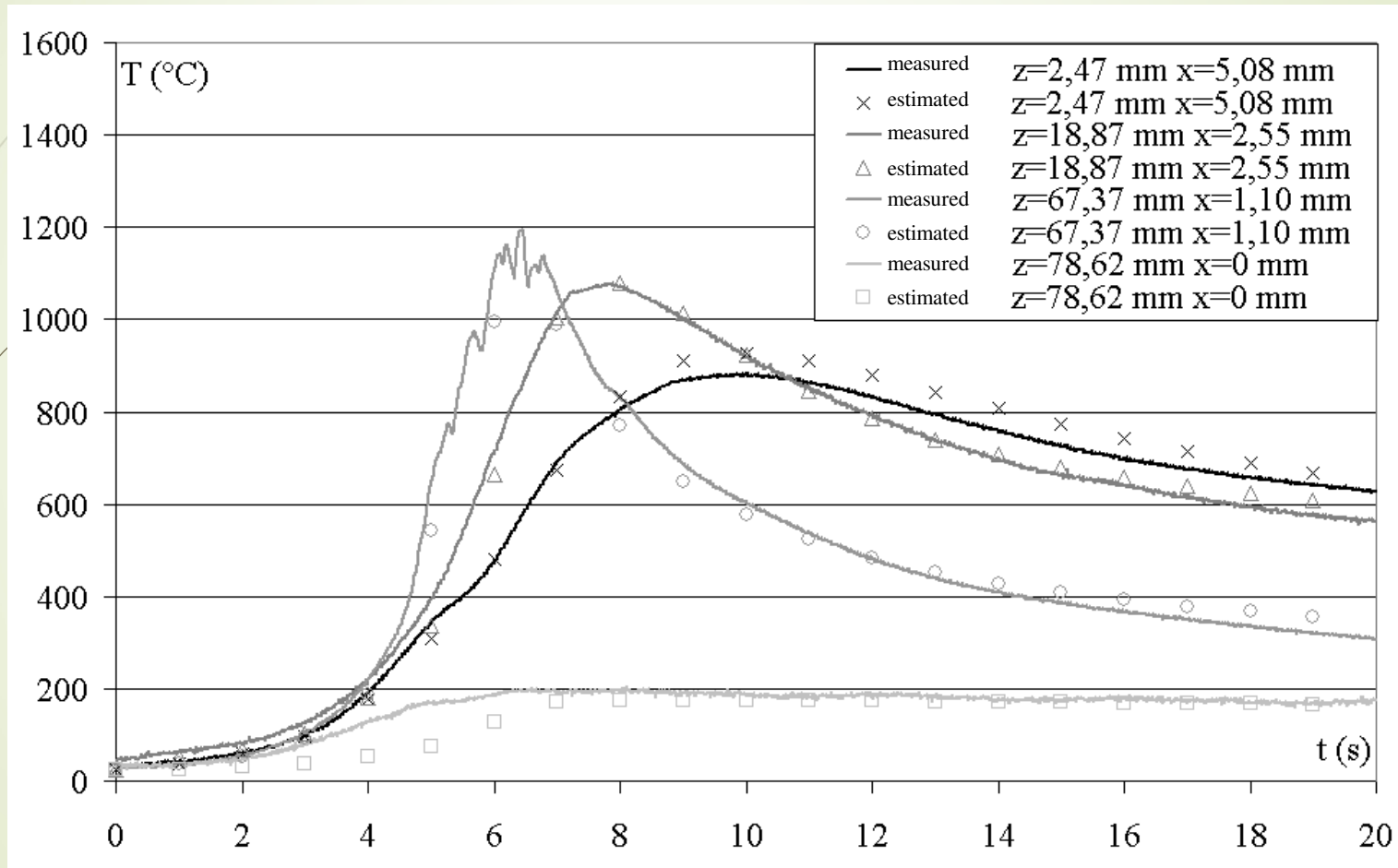


Results for 52 thermocouples taken out of the 4 interfaces
The iterative regularisation method

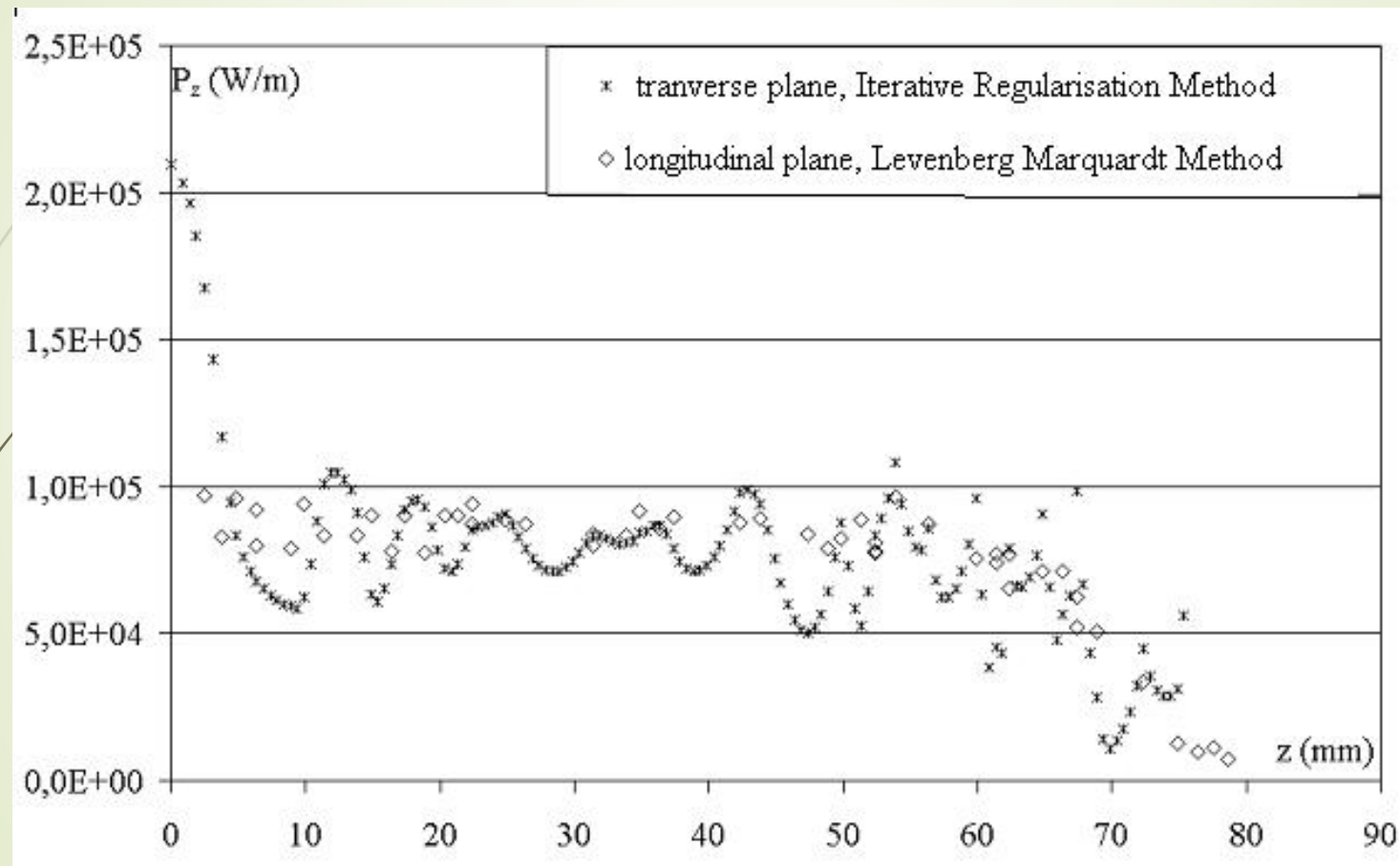


results for 52 thermocouples taken out of the 4 interfaces

121



results for 52 thermocouples taken out of the 4 interfaces comparison



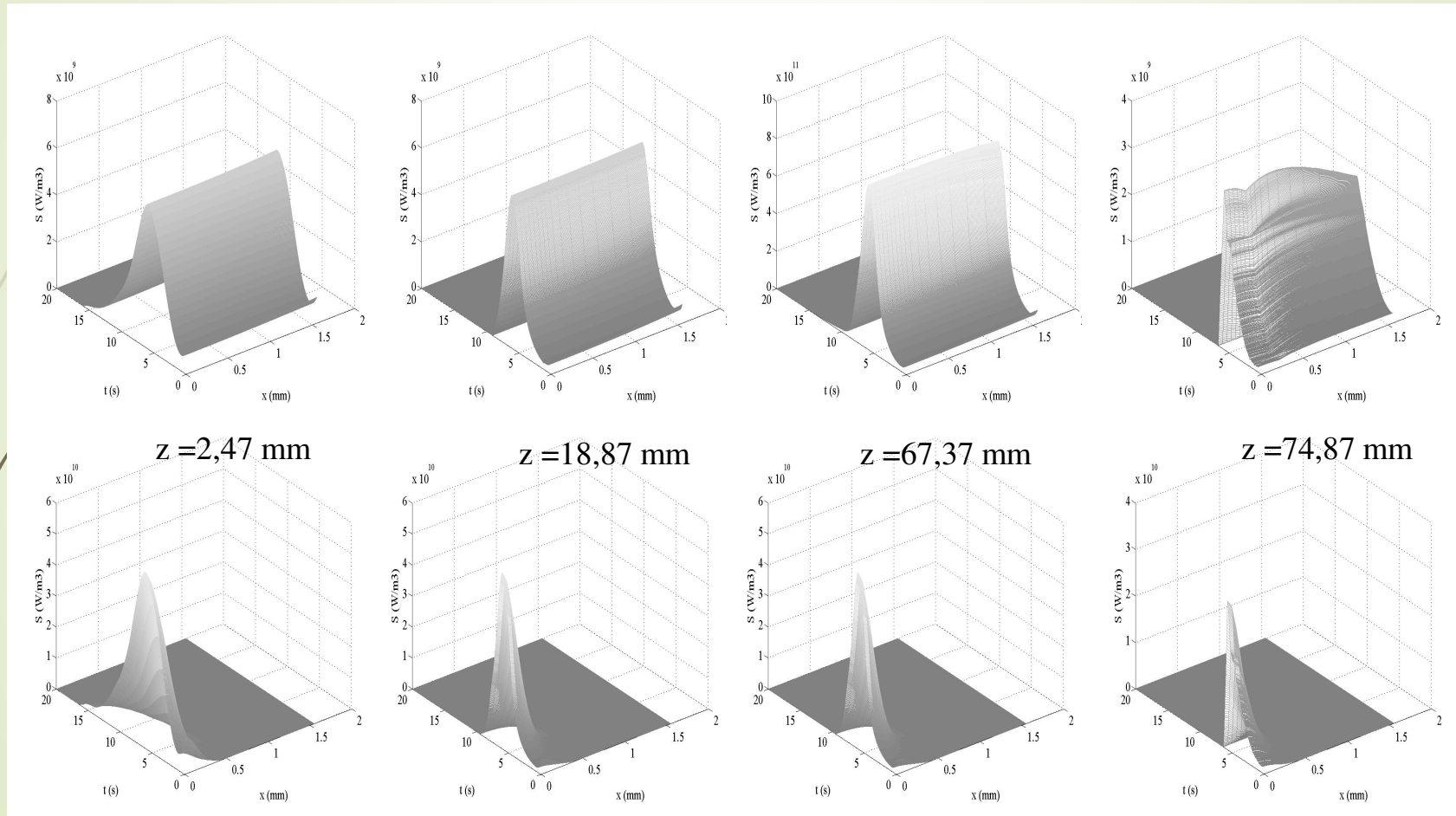
Definition of a optimal source

An optimal source was defined in order to set up a Gaussian distribution in the side direction where the estimate is not correct

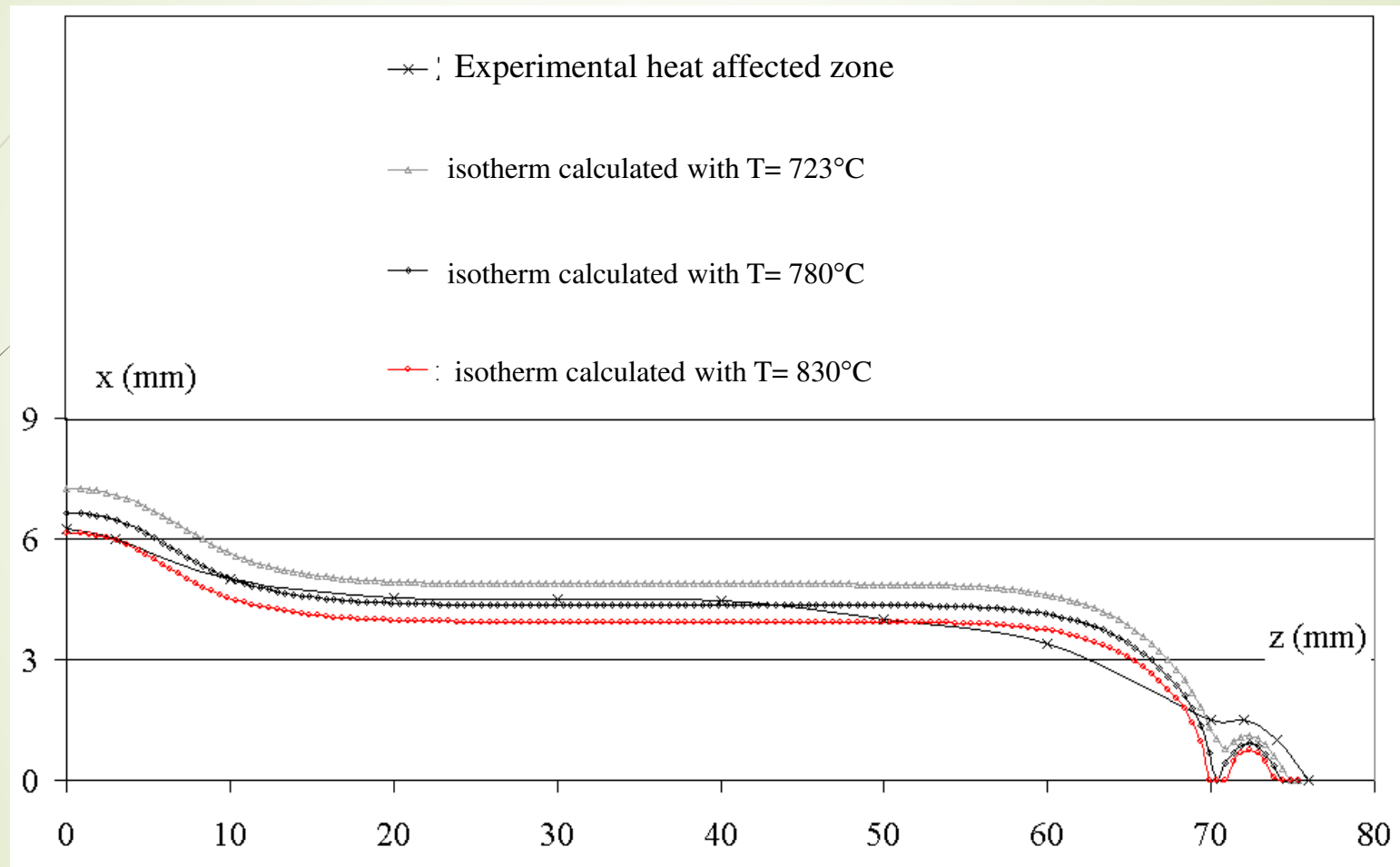
$$S'(x) = \frac{2 \iint S(x, z) dx dz}{\Delta H \sqrt{2\pi\omega_0}} \exp\left(-\frac{x^2}{2\omega_0^2}\right)$$

Comparison between the optimal and estimated sources

124

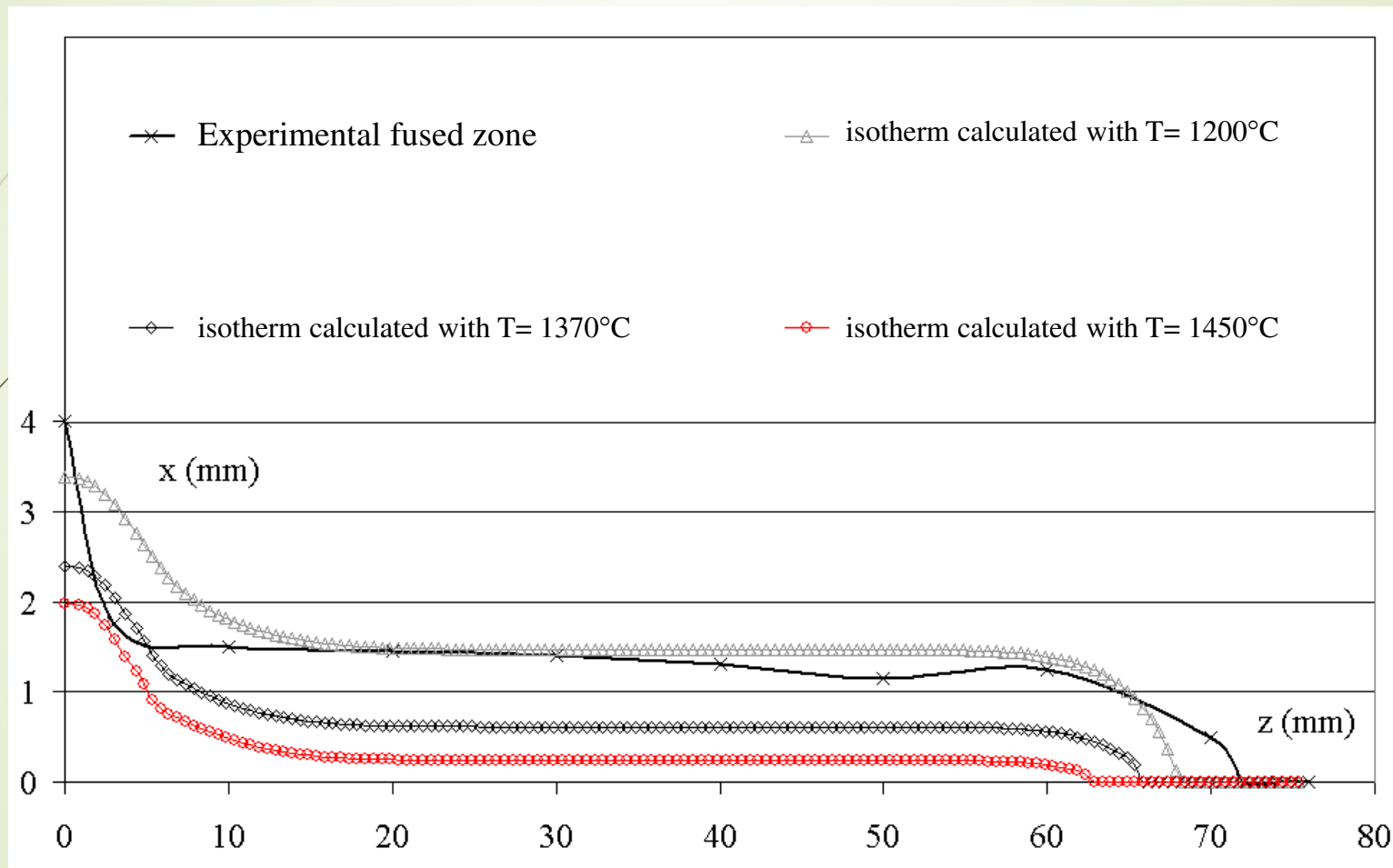


Comparison between the optimal and estimated sources



Comparison between the optimal and estimated sources

126



VI Conclusions

In this work, we have compared two methods for the estimation of the source term. (Iterative Regularization method and Levenberg Marquardt method)

A theoretical study has been realised

An experiment has been defined

The experimental estimation gives an optimal source. The heat affected zone limit is correct but the fused zone limit is not correct.



Thanks for your attention